UNIVERSITY OF GAZİANTEP
GRADUATE SCHOOL OF
NATURAL & APPLIED SCIENCES

EXERGY AND EXERGOECONMIC ANALYSIS OF GEOTHERMAL ASSISTED HIGH TEMPERATURE ELECTROLYSIS

M. Sc. THESIS
IN
MECHANICAL ENGINEERING

BY

ABDULKADİR AYANOĞLU
AUGUST 2010

Exergy and Exergoeconomic Analysis of Geothermal Assisted High Temperature Electrolysis

M.Sc. Thesis
in
Mechanical Engineering
University of Gaziantep

Supervisor
Prof. Dr. Mehmet KANOĞLU

by
Abdulkadir AYANOĞLU
August 2010

T.C.
UNIVERSITY OF GAZİANTEP
GRADUATE SCHOOL OF
NATURAL & APPLIED SCIENCES
MECHANICAL ENGINEERING DEPARTMENT

Name of the thesis: Exergy and Exergoeconmic Analysis of GeothermalAssisted High Temperature Electrolysis

Name of the student: Abdulkadir AYANOĞLU

Exam date: 04.08.2010

Approval of the Graduate School of Natural and Applied Sciences

Prof. Dr. Ramazan KOÇ
Director

I certify that this thesis satisfies all the requirements as a thesis for the degree of Master of Science.

Prof. Dr. L.Canan DÜLGER
Head of Department

This is to certify that we have read this thesis and that in our opinion it is fully adequate, in scope and quality, as a thesis for the degree of Master of Science.

Prof. Dr. Mehmet KANOĞLU
Supervisor

Examining Committee Members

Prof. Dr. M. Sait SÖYLEMEZ _____

Prof. Dr. Mehmet KANOĞLU _____

Assoc. Prof. Dr. Hüsamettin BULUT _____

ABSTRACT

EXERGY AND EXERGOECONOMIC ANALYSIS OF GEOTHERMAL ASSISTED HİGH TEMPERATURE ELECTROLYSIS

AYANOĞLU Abdulkadir

M.Sc. in Mechanical Engineering

Supervisor: Prof. Dr. Mehmet KANOĞLU

August 2010, 109 pages

In this thesis, energy, exergy, and exergoeconomic analysis of a geothermal assisted high temperature electrolysis process is performed. Energy and exergy analysis is applied to each component of the system for three environment (dead state) temperatures: standart environment temperature (25°C), summer temperature (11°C) and winter temperature (-1°C) at a given location. Energy and exergy performance parameters such as heat, power, exergy destruction, and exergy efficiencies are determined for three dead state temperatures. Heat exchanger network and high temperature electrolysis unit are primarily responsible for exergy destructions in the system. Cost analysis is applied to each component of the system. The cost functions of each stream in the plant are obtained using specific exergy costing (SPECO) method. Cost relations at the component level are related with certain exergoeconomic variables in the system. The capital investment cost, the operating and maintenance costs and the total cost of the system are found to be 422.21 €/kWh, 2.04 €/kWh and 424.25 €/kWh, respectively. The net electrical power input to the system is 122,129 kW for high temperature electrolysis. The specific unit exergetic costs of the power input to the system are 0.17 €/kWh, 0.20 €/kWh, and 0.24 €/kWh at 25°C, 11°C, and -1°C, respectively. Cost of hydrogen production is determined to be 1.6 €/kWh for 1 kg of hydrogen production. The cost of steam entering the system is obtained as 2.73 €/kWh.

Key words: Geothermal Energy, Hydrogen, High Temperature Electrolysis, Energy, Exergy, Exergoeconomic Analysis.

ÖZET

Jeotermal Destekli Yüksek Sıcaklık Elektrolizinin Ekserji ve Eksergoekonomik Analizi

AYANOĞLU Abdulkadir
Yüksek Lisans Tezi, Mak. Müh. Bölümü
Tez Yöneticisi: Prof. Dr. Mehmet KANOĞLU
Ağustos 2010, 109 sayfa

Bu çalışmada, jeotermal destekli yüksek sıcaklık elektrolizin enerji, ekserji ve eksergoekonomik analizi yapılmıştır. Sistemin her bir birleşeni için belli bir yer için standart çevre sıcaklığında (25°C), yaz sıcaklığında (11°C) ve kış sıcaklığında (-1°C) enerji ve ekserji analizleri yapılmıştır. Enerji ve ekserji parametrelerinden olan ısı, güç, ekserji yıkımı ve ekserji verimliliği üç ölü hal sıcaklığı için bulunmuştur. Isı eşanjörleri ile yüksek sıcaklık elektrolizi ünitesi ekserji yıkımının en fazla olduğu yerlerdir. Sistemdeki her bir bileşenin maliyet analizi yapılmıştır. Sistemdeki her akımın maliyet fonksiyonları, birim ekserji maliyetlendirme (SPECO) metodu geleneksel ekonomik metotlarla biraraya getirilerek hesaplanmıştır. Elde edilen maliyet değerleri ekserjiye bağlı tanımlanan ekonomik değişkenlerle ilişkilendirilmiştir. Sistemin ilk yatırım maliyeti, bakım ve onarım maliyeti ve toplam maliyeti sırasıyla 422.21 €/kWh, 2.04 €/kWh ve 424.25 €/kWh olarak hesaplanmıştır. Sistemdeki yüksek sıcaklık elektroliz için 122,129 kW elektrik enerjisi kullanılmıştır. Güç girişi için birim ekserji maliyeti 25°C ölü hal sıcaklığında 0.17 €/kWh, 11°C'de 0.20 €/kWh ve -1°C'de 0.24 €/kWh olarak hesaplanmıştır. Sistemden üretilen birim kütle hidrojenin maliyeti 1.6 €/kWh bulunmuştur. Sisteme giren buharın maliyeti 2.73 €/kWh olarak hesaplanmıştır.

Anahtar Kelimeler: Jeotermal Enerjisi, Hidrojen, Yüksek Sıcaklık Elektroliz, Enerji, Ekserji, Eksergoekonomik Analiz.

ACKNOWLEDGEMENTS

I would like to thank my supervisor Prof. Dr. Mehmet Kanoğlu for giving me the opportunity to do my dissertation in the area of thermoeconomy. Without his tireless interest and continuous guidance, the completion of this thesis would not have been possible.

I would like to thank Assist. Prof. Dr. Ayşegül ABUŞOĞLU for her positive criticism, suggestions and motivated supports. And finally, I would love to thank to my family for their endless supports.

CONTENTS

LIST OF FIGURES

Page

LIST OF TABLES

Page

LIST OF SYMBOLS

c	cost per unit of exergy (€/GJ)
$\dot{C}$	cost rate associated with exergy (€/h)
C	payment (€)
E	the amount of emission based on energy content (g/kWh)
$\dot{E}$	exergy rate (kW)
$\dot{E}_{heat}$	rate of exergy transfer by heat (kW)
h	enthalpy (kJ/kg)
i	rate of return (%)
$\dot{m}$	mass flow rate (kg/s)
P	present value of the payment (€)
$\dot{Q}$	rate of heat transfer (kW)
s	entropy (kJ/kg K)
T	temperature (K)
T_o	environment temperature (K)
T_{in}	inlet temperature (K)
T_{out}	outlet temperature (K)
w	specific work (kJ/kg)
$\dot{W}$	power (kW)
$y_{dest,k}$	component exergy destruction over total exergy input
$y^*_{dest,k}$	component exergy destruction over total exergy destruction
$\dot{Z}$	rate associated with the sum of capital investment and O&M (€/h)
$\dot{Z}^{CL}$	cost rate associated with capital investment (€/h)
$\dot{Z}^{OM}$	cost rate associated with operation and maintance (€/h)

Abbreviations

HTSE	High-temperature steam electrolysis
HT	High Temperature Heat Exchanger
MT	Medium Temperature Heat Exchanger
LT	Low Temperature Heat Exchanger
H_2O	Water
CRF	Capital Recovery Factor
EES	Engineering Equation Solver
EXC	Expenditure Costs
OMC	Operating and Maintenance Costs

Subscripts

eff	effective
L	levelized
k	any component
m	year
dest	destruction

Greek Letters

η	energy efficiency
ε	exergy efficiency
ψ	specific flow exergy (kJ/kg)
τ	total annual operating hours of system at full load (h)

CHAPTER 1

INTRODUCTION

1.1. Introduction

Energy is an important part of most aspects of daily life. The quality of life, and even its sustenance, depends on the availability of energy. Therefore, it is important to have a good understanding of the sources of energy, the conversion of energy from one form to another, and the ramifications of these conversions. Energy exists in numerous forms such as thermal, mechanical, electric, chemical, and nuclear [1].

The world's energy resources are limited. This caused many countries to re-examine their energy policies and take drastic measures in eliminating inefficiencies and waste. It has also sparked interest in the scientific community to take a closer look at the energy conversion devices and to develop new techniques to better utilize the existing limited resources. The first law of thermodynamics deals with the quantity of energy and asserts that energy cannot be created or destroyed. This law merely serves as a necessary tool for the bookkeeping of energy during a process and offers no challenges to the engineer. The second law, however, deals with the quality of energy. More specifically, it is concerned with the degradation of energy during a process, the entropy generation, and the lost opportunities to do work; and it offers plenty of room for improvement. The second law of thermodynamics has proved to be a very powerful tool in the optimization of complex thermodynamic systems [1].

The majority of energy produced in the world today is obtained from fossil fuels (i.e. coal, petroleum, natural gas), and nuclear energy. In addition, sustainable and environmentally friendly resources, such as hydroelectric and geothermal,

sunlight, wind, biogas, and wood, are also utilized [2]. With increasing awareness of the detrimental effects of the burning of fossil fuels on the environment, there has been an increasing interest worldwide in using clean and renewable energy sources. [3].

Renewable energy sources such as biomass, solar, wind, and hydropower have enormous potential to provide energy services in more sustainable ways, with zero or almost zero emissions of both air pollutants and greenhouse gases. Currently renewable energy sources supply approximately 20% of the world energy demand. A large percentage of that figure represents traditional biomass, mostly wood fuel used for cooking and heating, especially in rural areas of developing countries. New renewable energy sources (solar energy, wind energy, modern bio-energy, geothermal energy, and small hydropower) contribute about 1% of total primary energy. The limited contribution of renewables to total energy supply is due to their characteristics of being low-density, irregular sources and high cost. Substantial price reductions in the fast decades have brought some of these sources close to competing with fossil fuels, even at current low prices. Wind and solar energy, while still a small percentage of total energy consumption, are growing at a rate of 30% per year. Modern, distributed forms of biomass seem particularly promising for their potential to provide rural areas with clean, modern forms of energy based on the use of indigenous biomass resources that have traditionally been used inefficiently and in polluting ways. Depletion of fossil fuels and environmental considerations have led engineers and scientists to anticipate the need to develop a clean, renewable and sustainable energy system. [4]. Geothermal energy, hydropower, solar energy, wind power and biomass energy are the major renewable energy resources for world in the future.

Hydrogen is a very efficient and clean fuel. Hydrogen, produced from renewable energy (e.g., solar) sources, would result in a permanent energy system, which we would never have to change [5]. Hydrogen produced from water using renewable energy and technologies becomes a renewable or environmentally benign fuel. Hydrogen is widely believed to be world's next-generation fuel, because of its lower environmental impact and greenhouse gas emissions, in comparison to fossil fuels. Hydrogen demand is expected to increase very rapidly over the coming

decades. It has been suggested that hydrogen should replace petroleum products for fueling all forms of transportation (automobile, marine, air and rail) to reduce CO_2 emissions, limit dependence on imported petroleum, and prepare for time in which oil reserves would become exhausted. Besides that, the nuclear and chemical industries, automobile manufacturing industry, the aerospace industry, manufacturing of portable sources of power (such as mobiles phones, computers, everyday technology) and other industrial sectors are all showing great interest in development of hydrogen as a fuel. The interest in the use of hydrogen in all these industrial sectors is motivated by both the depletion of fossil fuel resources and the need of drastically reducing the carbon emissions that affect the climate [6].

Hydrogen produced through renewable energy sources, most commonly with a device which uses electricity to separate water into hydrogen and oxygen called an electrolyzer, is an emissions-free way to carry energy. Hydrogen is plentiful and can safely be harnessed for a variety of stationary and mobile applications [7].

There are several energy sources that can be used for hydrogen production, such as renewables, nuclear and fossil fuels. One of these alternatives is geothermal energy which can be used for hydrogen production through electrolysis or high temperature electrolysis.

Geothermal energy, one of the most promising among renewable energy sources, has proven to be sustainable, clean, and safe. Geothermal energy provides a clean, renewable energy source that could dramatically improve our environment, economy and energy security. Geothermal energy generates far less (almost none) air emissions than fossil fuels and decreases the reliance on imported energy. Today, in most ways, geothermal energy has come of age; the technology has improved, the economics has become more appealing, and substantial progress has been achieved in reducing environmental impacts. Geothermal energy provides an affordable, clean method of generating electricity and providing thermal energy. Two challenges for geothermal energy are that resources are difficult to locate and tend to be found in rural areas. The fact that they are found in remote areas constrains generation and direct use development. It is difficult to transmit heat energy or electricity to the population centers where people will use it. [8]. Then using geothermal energy for

hydrogen production becomes a viable alternative for getting the most out of geothermal power.

1.2 Thesis Structure

In this thesis we analyze a geothermal assisted high temperature electrolysis system thermodynamically and thermoeconomically by means of energy, exergy, and and exergetic cost accounting methods. The outline of the study with respect to chapters is as follows:

Chapter 1 gives general information about energy, renewable energy, hydrogen energy and the rational using geothermal energy for hydrogen production.

Chapter 2 presents a detailed literature survey about renewable energy, geothermal energy, hydrogen energy, electrolysis, and high temperature electrolysis. Previous work on using geothermal energy for hydrogen production and the current status of geothermal assisted high temperature electrolysis are provided.

In Chapter 3, general formulations of thermodynamic analysis including both energy and exergy methods are given. Also, general principles, terminology, and formulation of thermoeconomic analysis, which is also called exergoeconomic analysis are presented. The formulations given in this chapter are applicable to geothermal assisted high temperature electrolysis.

In Chapter 4, thermodynamic analysis of geothermal assisted high temperature electrolysis process is performed using both energy and exergy analysis. The calculations are performed and the results are obtained. Exergy efficiencies and destructions of major components and the overall system are obtained.

In Chapter 5, exergoeconomic analysis of geothermal assisted high temperature electrolysis system is performed. Cost data is obtained and specific exergy cost method (SPECO) is used. The results would indicate the sites for losses based on economic results. The results of the analyses can be used to develop and assess measures to improve the process and reduce product costs.

In Chapter 6, the overall discussion for the results is provided and main conclusions from the study are drawn. The results of the energy, exergy and exergoeconomic analyses can be used to develop and assess measures to improve the process step, and to reduce product costs.

CHAPTER 2

LITERATURE SURVEY

2.1 Introduction

Renewable energy is energy which comes from natural resources such as sunlight, wind, and geothermal heat, which are naturally replenished. In 2006, about 18% of global energy consumption came from renewables with 13% coming from traditional biomass which is mainly used for heating, and 3% from hydroelectricity. The share of other renewable (wind, solar, geothermal) increases dramatically [9]. Among these sources geothermal energy provides a clean, renewable energy that could improve our environment, economy and energy security. Geothermal energy generates less air emissions than fossil fuels and decreases the reliance on imported energy. Today, in most ways, geothermal energy has come of age; the technology has improved, the economics has become more appealing, and substantial progress has been achieved in reducing environmental impacts.

Renewables on the other hand are desired energy sources for hydrogen production due to their diversity, regionality, abundance, and potential for sustainability. That being asserted, there are many challenges to producing hydrogen from renewables and perhaps the major one is reducing the cost to be competitive with gasoline and diesel fuels [10]. The geothermal based hydrogen production is another suitable alternative that uses renewable energy of the geothermal water/steam to produce hydrogen using a high temperature electrolyses process.

Hydrogen is colorless, highly flammable, light in weight, low melting point, low boiling point and much lighter than air [11]. Current hydrogen production sources are 48% natural gas, 30% oil, 18% coal, and 4% electrolysis [12]. Currently more than 80% of the world's energy supply comes from fossil fuels. The ongoing growth in fossil fuel consumption suggests that global carbon dioxide emissions are still rising [13]. Veziroglu et. al. [14] suggested that the solution to these global problems would require replacement of existing fossil fuel systems by hydrogen energy systems. Therefore, hydrogen energy systems appear to be one of the most effective solutions, and can play a significant role in providing better environment and sustainability [15]. Hydrogen has the highest specific energy content of all conventional fuels and is the most abundant element in the universe [16]. Hydrogen is considered in many countries as an important alternative energy indicator and a bridge to a sustainable energy future. The promise of hydrogen as an energy carrier that can provide pollution-free, carbon-free power and fuels for buildings, industry, and transport makes it a potentially critical player in our energy future [17].

2.2 Geothermal Energy

Geothermal energy is generated from heat stored in the earth, or the collection of absorbed heat derived from underground [18]. Geothermal energy source can be used for direct electricity production and/or for heating and cooling applications. Three main type usages of geothermal energy sources are high temperature, medium temperature and low temperature. High temperature fields which are 200-350ºC, are suitable for electricty production, and for low and high temperature electrolyses.

Erdogdu [19] presented not only a review of the potential and utilization of the geothermal energy in Turkey but also provided some guidelines for policy makers. Geothermal energy, renewable energy and exergy analysis were the most frequently used keywords appearing in geothermal energy publications, as rewiewed by Celiktas et al. [20]. Fridleifsson [21] presented a paper for describing the status of geothermal energy development in the world. He compared the status of the renewable energy resources. Barbier [22] made a brief discussion on training of specialists, geothermal literature, on-line information, and geothermal associations.

Renewable energy sources such as geothermal energy, biomass energy, solar energy, wind power and hydropower are the major resources available in Turkey. Although the geothermal industry is highly developed in Turkey, excellent geothermal sources still remain undeveloped since cost for a new natural gas plant is just half of a new geothermal plant [23].

Turkey has an important place among the richest countries (the first in Europe, seventh in the world) in geothermal potential. Around 1000 hot and mineralized natural self flowing springs exist in Turkey. The geothermal resources in Turkey can be classified into three groups: low temperature fields (<70°C), moderate temperature fields (70–150°C), and high temperature fields (more than 170°C). Although they exist all over the country, most of them lie in the Western, North-Western, and Middle Anatolia. The temperature limit is accepted to be 20°C for balneological purposes. With the exception this, there are 170 geothermal fields with a temperature over 35°C in Turkey. Aydın-Germencik (232°C), Denizli-Kızıldere (242°C), Çanakkale-Tuzla (173°C), and Aydın-Salavatlı (171°C) fields those are suitable for electricity generation. Depending on the use of new technologies, the Manisa-Salihli-Caferbeyli (155°C), Kütahya-Simav (162°C), Izmir-Seferihisar (153°C), Dikili (130°C), and Denizli-Gölemezli (under search) fields [23].

Turkey's geothermal power generation plants are:

1. Kızıldere-Denizli was commissioned in 1984, has 17.8 MWe capacity at maximum temperature 243°C
2. Dora-I Salavatlı-Aydın was commissioned in 2006, has 7.35 MWe capacity at maximum temperature 172°C
3. Bereket Energy-Denizli was commissioned in 2007, has 7.5 MWe capacity at maximum temperature 145°C
4. Gürmat-Germencik-Aydın was commissioned in 2009, has 47.4 MWe capacity at maximum temperature 232°C
5. Tuzla-Çanakkale was commissioned in 2009, has 7.5 MWe capacity at maximum temperature 171°C
6. Dora-II Salavatlı-Aydın was commissioned in 2010, has 9.7 MWe capacity at maximum temperature 174°C [24].

2.3 Hydrogen Production by Solar Energy

Solar radiation accounts for most of the available renewable energy on earth [25]. Pregger et al. [26] studied the increasing industrial hydrogen demand in various countries. Nakamura [27] analyzed possibilities of producing hydrogen from water utilizing solar heat at high temperatures. Shabani et al. [28] classified the solar hydrogen production systems based on the energy input mode. Classification of solar hydrogen production using solar energy can be classified mainly into four types: photovoltaic, solar thermal energy, photo electrolysis and biophotolysis .

Steinfeld [29] analyzed a two step thermochemical cycle for hydrogen production from water using solar energy. Zedtwitz et al. [30] studied three different methods which produced hydrogen via solar thermal decarbonisation of fossil fuels. Zini et al. [31] studied twelve case-studies on hydrogen production systems from direct sunlight.

Ford et al. [32] utilizated solar energy for hydrogen production. Liua et al. [33] reported two months operation data of China's first solar-hydrogen system. A discussion of prospects of solar thermal hydrogen production in terms of technological and economic potentials and their possible role for a future hydrogen supply were done by refs. [34-35].

Cherigui et al. [36] studied the development of solar energy system for hydrogen production. Almogren et al. [37] studied a model for solar-hydrogen energy system for Saudi Arabia. Padina et al. [38] designed and simulated a new solar hydrogen production system via high-temperature electrolyser. An industrial-scale solar-hydrogen demonstration program at Neunburg vorm Wald, Germany was started in 1986 by a joint venture company Solar-Wasserstoff-Bayern GmbH (SWB) with the aim to demonstrate solar-hydrogen energy cycle without any carbon dioxide release [39].

The solar-photovoltaic electrolysis process seems to be the most practical if a renewable energy source is to be used [40]. Bolton [41] selected four solar hydrogen

systems to show sufficient promise for further research and development: (1) photovoltaic cells plus an electrolyzer; (2) photoelectrochemical cells with one or more semiconductor electrodes; (3) photobiological systems; and (4) photodegradation systems. Several recommendations have been made for future work in this area.

Zini et al. [42] presented and discussed twelve case-studies on systems that generate, store and use hydrogen from photovoltaic energy. It included solar photovoltaic (PV) source for hydrogen generation, and storage and fuel cell for generating power [43-44]. A simplified solar photovoltaic (PV) model was developed to optimize thermal and economical performance of domestic photovoltaic-electrolyzer systems and production of hydrogen [45-46].

Gibson et al. [47] investigated a model for the factors that affect the efficiency of solar hydrogen generation and to design a more efficient and cost effective solar powered PV-electrolysis system. Valenciaga et al. [48] studied a complete control scheme to efficiently manage the operation of an autonomous wind based hydrogen production system. Honnery et al. [49] examined that wind turbines are grouped to form arrays that are linked to local hydrogen generation and transmission networks.

Greiner et al. [50] presented a method for the assessment of wind–hydrogen energy systems. Clu´a et al. [51] dealt with the control of a hydrogen production system supplied by wind power and assisted by the grid. Sopian et al. [52] described the performance of an integrated PV wind hydrogen energy production system.

Xuan [53] discussed the relevant research on biomass to produce hydrogen by pyrolysis and gasification. Hulteberg et al. [54] integrated a system which was designed and combined the two processes for the production of hydrogen: i) gasification of biomass and ii) electrolysis of water. Holladay et al. [55] reviewed the technologies related to hydrogen production from both fossil and renewable biomass resources.

Zhao et al. [56] developed an efficient method for hydrogen production from biomass. In literature, some potential biomass-based hydrogen production methods were discussed under two main categories: i) thermo-chemical (gasification, pyrolysis and SCW), ii) bio-chemical conversions (fermentation, photosynthesis, and biological water gas shift reaction). One of the most common biomass resources, oil palm shell was used for producing hydrogen by gasification process [57-58].

2.4 Geothermal Energy Use in Hydrogen Production via High Temperature Electrolysis (HTE) Process

High temperature electrolysis (HTE) is based on the technology of solid oxide fuel cells (SOFCs). In order to achieve competitive efficiencies, there have been an increased interest in intermediate temperature SOFCs which typically operate between 823 and 1073 K. The HTE uses a combination of thermal energy and electricity to split water in an electrolyzer similar to a solid oxide fuel cell (SOFC). The SOFC can make the electrode over potential decrease and the mobility of the oxygen anion increase. These are advantages for increasing the hydrogen production efficiency [59-63].

HTE pocess can reach an efficiency of 94%. High Temperature Electrolysis is a promising method because its most parts consist of environmentally sound and common materials. Toshiba has been developing HTE technology which has been selected three hydrogen production technologies according to the heat source temperature, as presented by Ozaki et al. [64].

Balta et al. [65] studied, geothermal-based hydrogen production methods, their technologies, and application possibilities in detail. A high-temperature electrolysis (HTE) process coupled with and powered by a geothermal source is considered for a case study, and its thermodynamic analysis through energy and exergy is conducted for performance evaluation purposes. Their study may be divided into two groups, namely: (i) reviewing and evaluating geothermal based hydrogen production methods and their current status and applications, and (ii) energetic and exergetic analyses of an HTE process coupled with a geothermal source for possible hydrogen production.

Sigurvinsson et al. [66] implemented a method in a software tool which performs the optimisation using genetic algorithms. The first application of the method was done by taking into account the prices of electricity and geothermal heat in the Icelandic context. They stated that even with a geothermal temperature as low as 230ºC, the HTE could compete with alkaline electrolysis. It appeared from the results of the optimization that HTE can function with geothermal heat, at geothermal temperatures above 200°C.

The Jules Verne project, a collaboration between France and Iceland, aimed at studying and then validating the possibilities of producing hydrogen with HTE coupled with a geothermal source. The production of hydrogen by HTE appears to be very promising mainly in the Icelandic geothermal context. One key to the HTE efficiency was the recuperation of heat at the outlet of the electrolyser by heat exchangers. The needed heat exchangers were under testing for medium and low temperatures, but for over 850ºC, they still need further development [67].

The performance of electrolysis processes can be improved by functioning at HTE. This leads to a reduction in energy consumption but requires some of the energy necessary for the dissociation of water to be in the form of thermal energy, and the ability to recover some of the heat contained in the outlet products of the electrolysis. Heat would be obtained by coupling the process either to a high-temperature reactor or to a geothermal source. A techno-economic optimisation of the upper heat exchanger network in the HTE process was conducted. It was also noted that the cost of the input heat can be increased by 10% when coupling the system to a HTR, whereas it was more than doubled in the geothermal case [68]. Han [69] studied at a model for the geothermal plant that was set with an inlet temperature of 200 °C via electrolysis to produce hydrogen.

Water electrolysis might become a competitive hydrogen production method in the future, with the decline of global fossil fuel reserves, the ever growing availability of electricity from other renewable energy resources and the technology improvement of water electrolysis itself [70]. A mathematical model for an advanced alkaline electrolyzer has been developed. The model is based on a combination of

fundamental thermodynamics, heat transfer theory, and empirical electrochemical relationships [71]. Herranz presented a work that deals with the development of a system to control and monitor the operating parameters of an alkaline electrolyzer and a metal hydride storage system that allow for a continuous hydrogen production [72].

2.4 Energy and Exergy Analysis of Hydrogen Production from Geothermal Energy

Energy and exergy efficiencies are considered by many to be useful for the assessment of energy conversion and other systems and for efficiency improvement. Energy and exergy-based efficiencies were used in the analysis of power cycles such as vapor and gas power cycles, cogeneration cycles and geothermal power cycles [73].

Ni et al. [74] investigated energy and exergy analysis for thermodynamic–electrochemical characteristics of hydrogen production by a solid oxide steam electrolyzer (SOSE) plant. This study provided a better understanding of the energy and exergy flows in SOSE hydrogen production and demonstrated the importance of exergy analysis for identifying and quantifying the exergy destruction. They also conducted energy and exergy analysis to investigate the thermodynamic-electrochemical characteristics of hydrogen production by a PEM electrolyser plant and found that the energy and exergy efficienciencies of the system were the same and were influenced by the operating temperatures, current density and the thickness of PEM electrolyte.

Balta et al. [65] analyzed a geothermal based hydrogen production system in terms of energy and exergy efficiencies and reported that the efficiency varies with the geothermal inlet temperature. This process involved high temperature steam electrolysis (HTSE) coupled with geothermal source.

Exergy characterizes the thermodynamic quality of a given quantity of energy [75]. Exergetic efficiency compares the actual performance of a process/system to the ideal one and exergy destruction quantifies the losses that hinder the

performance. Exergy analysis is a very powerful tool for energy systems, particularly when it is combined with exergoeconomic (i.e., thermoeconomic). Thermoeconomic, as an exergy-aided cost-reduction method, provides important information for the design of cost effective energy-conversion plants. The exergy costing principle is used to assign monetary values to all material and energy streams within a plant as well as to the exergy destruction within each plant component. The design evaluation and optimization is based on the trade-offs between exergy destruction (or exergetic efficiency) and investment cost for the most important plant components. Thermoeconomic provides the designer with information about the cost formation process, the interactions among thermodynamics and economics and the interactions among plant components. This information is very valuable for improving the design of energy-conversion plants [76-79].

2.6 Conclusions

It is clear that there are a number of studies on using renewable energy sources for hydrogen production. A limited number of studies are found on using geothermal energy for hydrogen production. However, there is no study in open literature on exergoeconomic analysis of hydrogen production by geothermal energy. In this study, thermodynamic and exergoeconomic analysis of hydrogen production by geothermal energy via high-temperature electrolysis (HTE) process will be performed.

CHAPTER 3

THERMODYNAMIC AND THERMOECONOMIC ANALYSIS

3.1 Introduction

Energy is the most fundamental term in thermodynamics and energy engineering. Energy analysis is often one of the most significant parts of engineering analysis. Energy can be stored within a system in various macroscopic forms, it can be transformed from one form to another, and it can be transferred between systems. The total amount of energy is conserved in all transformations and transfers. Energy balances are widely used in the design and analysis of energy conversion systems. Although energy balances can determine energy supply requirements in the form of material streams, heat, and shaft work, they do not provide sufficient information on how efficiently energy is used.

Exergy is the theoretical maximum of useful work (shaft work or electrical work) obtainable from a thermal system as this is brought into thermodynamic equilibrium with the reference environment while heat transfer occurs with this environment only. Alternatively, exergy is the theoretical minimum of work (shaft work or electrical work) required to form a quantity of matter from substances present in the environment and to bring the matter to a specified state. Hence, exergy is a measure of the departure of the state of the system from the state of the reference environment. The processes in all real energy conversion systems are irreversible and a part of the exergy supplied to the total system is destroyed. Only in a reversible process does the exergy remain constant [1].

The second law of thermodynamics complements and enhances an energy balance by enabling calculation of both the true thermodynamic value of an energy carrier, and the real thermodynamic inefficiencies in processes or systems. The concept of exergy is extremely useful for this purpose. The real inefficiencies of a system are exergy destruction, occurring within the system boundaries, and exergy losses, which are exergy transfers out of the system that are not further used in the overall installation. Some of the common causes for exergy destruction include chemical reaction, heat transfer across a finite temperature difference, fluid friction, flow throttling, and mixing of dissimilar fluids.

Thermoeconomics (i.e. exergoeconomics) is, in its widest possible sense, the science of natural resources saving that connects physics and economics by means of the second law of thermodynamics. It is the branch of engineering that combines exergy analysis and economic principles to provide system designer or operator with information not available through conventional energy analysis and economic evaluations but crucial to the design and operation of a cost-effective system [80]. Thermoeconomics assesses the cost of consumed resources, money and system irreversibilities in terms of the overall production process. They help to point out how resources may be used more effectively in order to save them. Money costs express the economic effect of inefficiencies and are used to improve the cost effectiveness of production processes. Assessing the cost of the flow streams and processes in a plant helps to understand the process of cost formation, from the input resources to the final products.

In this chapter we present general formulations of thermodynamic and thermoeconomic analyses including energy and exergy methods. The formulations are applicable to hydrogen production with high temperature electrolysis from geothermal energy sources.

3.2 Energy Analysis

Energy conservation is expressed by energy balances and together with corresponding mass balances they are widely used in the modeling and analysis of energy conversion systems.

3.2.1 Mass Balance

The conservation of mass principle can be expressed as the net mass transfer to or from a system during a process is equal to the net change (increase or decrease) in the total mass of the system during that process [1]. In the rate form it is expressed as

$$\sum \dot{m}_{\mathrm{i}} - \sum \dot{m}_{\mathrm{e}} = \frac{dm_{\mathrm{system}}}{dt} \tag{3.1}$$

where *i* and *e* refer to inlet and exit states of the any control volume, respectively. During a steady flow process, the total amount of mass contained within a control volume does not change with time (m_{CV} = constant). Then the conservation of mass principle requires that the total amount of mass entering a control volume equal the total amount of mass leaving it. For a general steady-flow system with multiple inlets and exits, the conservation of mass principle can be expressed in the rate form as

$$\sum \dot{m}_{\mathrm{i}} = \sum \dot{m}_{\mathrm{e}} \tag{3.2}$$

3.2.2 Energy Balance

Based on experimental observations, the first law of thermodynamics states that energy can be neither created nor destroyed; it can only change forms. Therefore, every bit of energy should be accounted for during a process [1,81,82]. The conservation of energy principle may be expressed as follows: The net change (increase or decrease) in the total energy of the system during a process is equal to the difference between the total energy leaving the system during that process. Energy balance for any system undergoing any kind of process can be expressed more compactly in the rate form as [1]

$$\dot{E}_{\mathrm{in}} - \dot{E}_{\mathrm{out}} = \Delta \dot{E}_{\mathrm{system}} \tag{3.3}$$

During a steady-flow process, the total energy content of a control volume remains constant (E_{CV} = constant), and thus the change in the total energy is zero.

Therefore, the amount of energy entering a control volume in all forms (by heat, work, and mass) must be equal to the amount of energy leaving it. Then the rate form of the general energy balance reduces for a steady-flow process to

$$\dot{E}_{\text{in}} = \dot{E}_{\text{out}} \tag{3.4}$$

Noting that energy can be transferred by heat, work, and mass only, the energy balance above for a general steady-flow system can also be written more explicitly as

$$\dot{Q}_{\text{in}} + \dot{W}_{\text{in}} + \sum \dot{m}_{\text{i}} \left(h_{\text{i}} + \frac{V_{\text{i}}^2}{2} + g z_{\text{i}} \right) = \dot{Q}_{\text{out}} + \dot{W}_{\text{out}} + \sum \dot{m}_{\text{e}} \left(h_{\text{e}} + \frac{V_{\text{e}}^2}{2} + g z_{\text{e}} \right) \tag{3.5}$$

where h_{i}, h_{e}, V_{i}, V_{e}, z_{i}, z_{e} represent enthalpy, velocity, and elevation of mass entering and leaving the control volume, respectively.

3.3 Exergy Analysis

For the evaluation and improvement of thermal systems, it is essential to understand the sources of thermodynamic inefficiencies and the interactions among system components. All real energy conversion processes are irreversible due to dissipative effects such as chemical reaction, heat transfer through a finite temperature difference, mixing of matter at different compositions or states, unrestrained expansion, and friction. Exergy balances assist in calculating the exergy destruction within system components. Thus, the thermodynamic inefficiencies and the processes that cause them are identified. Only a part of the thermodynamic inefficiencies can be avoided by using the best currently available technology. Improvement efforts should be centered on avoidable inefficiencies. Dimensionless variables can be used for performance evaluations. Appropriately defined exergetic efficiency unambiguously characterizes the performance of a system from the thermodynamic viewpoint.

3.3.1 Reference Environment and Exergy Components

The environment, which appears in the definition of exergy, is a large equilibrium system in which the state variables (T_0, p_0) and the chemical potential of the chemical components contained in it remain constant when in a thermodynamic process heat and materials are exchanged between another system and the environment. This environment is called exergy-reference environment or thermodynamic environment. The temperature T_0 and pressure p_0 of the environment are often taken as standard-state values, such as 298.15 K and 1.013 bar. However, these properties may be specified differently depending on the application. For example, T_0 and p_0 may be taken as the actual or average ambient temperature and pressure, respectively, for the time and location at which the system under consideration operates or is designed to operate. For example, if the system uses air, T_0 would be specified as the average air temperature. If both air and water from the natural surroundings are used, T_0 would usually be specified as the lower of the temperatures for air and water when the installation operates above the ambient temperature [1,82,83].

Although the intensive properties of the environment are assumed to remain constant, the extensive properties can change as a result of interactions with other systems. It is important that no chemical reactions can take place between the environmental chemical components. The exergy of the environment is equal to zero. The environment is part of the surroundings of any thermal system.

In the absence of nuclear, magnetic, electrical, and surface tension effects, the total exergy of a system (E_{sys}) can be divided into four components: Physical exergy $E_{\text{sys}}^{\text{PH}}$, kinetic exergy E^{KN}, potential exergy E^{PT}, and chemical exergy E^{CH}. Then the total exergy of a system is given by

$$E_{\text{sys}} = E_{\text{sys}}^{\text{PH}} + E^{\text{KN}} + E^{\text{PT}} + E^{\text{CH}} \tag{3.6}$$

The subscript *sys* distinguishes the total exergy and physical exergy of a system from other exergy quantities, including transfers associated with streams of matter. The total specific exergy on a mass basis e_{sys} is

$$e_{\mathrm{sys}} = e_{\mathrm{sys}}^{\mathrm{PH}} + e^{\mathrm{KN}} + e^{\mathrm{PT}} + e^{\mathrm{CH}} \tag{3.7}$$

The physical exergy associated with a thermodynamic system is given by

$$E_{\mathrm{sys}}^{\mathrm{PH}} = (U - U_0) + p_0(V - V_0) - T_0(S - S_0) \tag{3.8}$$

where U, V and S represent the internal energy, volume and entropy of the system, respectively. The subscript 0 denotes the state of the same system at the temperature T_0 and pressure p_0 of the environment. The rate of physical exergy $\dot{E}^{\mathrm{PH}}$ associated with a material stream is

$$\dot{E}^{\mathrm{PH}} = (H - H_0) - T_0(S - S_0) \tag{3.9}$$

where H and S denote the enthalpy and entropy, respectively. The subscript 0 denotes property values at the temperature T_0 and pressure p_0 of the environment. The physical exergy of a system consists of thermal exergy $\dot{E}^{\mathrm{T}}$ (due to system temperature) and mechanical exergy $\dot{E}^{\mathrm{M}}$ (due to system pressure):

$$\dot{E}^{\mathrm{PH}} = \dot{E}^{\mathrm{T}} + \dot{E}^{\mathrm{M}} \tag{3.10}$$

An unambiguous calculation of the specific thermal and specific mechanical exergy is possible only for ideal gases and incompressible liquids:

$$e^{\mathrm{T}} = \int_{T_0, p_0}^{T_0, p} c\left(1 - \frac{T}{T_0}\right)\mathrm{d}T \tag{3.11}$$

$$e^{\mathrm{M}} = \int_{T_0, p_0}^{T_0, p} v \, \mathrm{d}p \tag{3.12}$$

where v denotes specific volume. For any fluid, the specific thermal exergy of a stream at temperature T and pressure p is expressed as

$$e^{\mathrm{T}} = e^{\mathrm{PH}}(T, p) - e^{\mathrm{PH}}(T_0, p) \tag{3.13}$$

The mechanical exergy is determined from

$$E^{\mathrm{M}} = E^{\mathrm{PH}} - E^{\mathrm{T}} \tag{3.14}$$

Kinetic and potential exergies are equal to kinetic and potential energies, respectively.

$$E^{\mathrm{KN}} = \frac{1}{2} m \vec{v}^2 \tag{3.15}$$

$$E^{\mathrm{PT}} = mgz \tag{3.16}$$

Here $\vec{v}$ and z denote velocity and elevation relative to coordinates in the environment $(\vec{v}_0 = 0, z_0 = 0)$. Equations 3.15 and 3.16 can be used in conjunction with both systems and material streams. The exergy associated with shaft work, flow of electricity, kinetic energy, or potential energy is equal to the energy amount of each of these quantities.

Chemical exergy is the theoretical maximum useful work obtainable as the system at temperature T and pressure p is brought into chemical equilibrium with the reference environment while heat transfer occurs only with this environment. Thus, for calculating the chemical exergy, not only the temperature T_0 and pressure p_0 but also the chemical composition of the environment $x_{\mathrm{i}}^{\mathrm{e}}$ have to be specified. By

definition, the exergy of the reference environment is equal to zero and there is no possibility of developing work from interactions between parts of the environment.

The standard molar chemical exergy $e_{\text{sub}}^{\text{CH}}$ of any substance consisting of its elements can be determined using the change in the specific Gibbs function $\Delta\overline{g}$ for the formation of this substance from the reaction of chemical elements present in the environment:

$$e_{\text{sub}}^{\text{CH}}(T_0, p_0) = \overline{g}_{\text{sub}}(T_0, p_0) - \sum_{\text{i}=1}^{\text{M}} v_{\text{i}} \left[e_{\text{i}}^{\text{CH}}(T_0, p_0) - \overline{g}_{\text{i}}(T_0, p_0) \right] \tag{3.17}$$

where $\overline{g}_{\text{i}}$, v_{i} and e_{i}^{CH} denote, for the *i*-th chemical element, the Gibbs function at T_0 and p_0, the stoichiometric coefficient in the reaction, and the standard chemical exergy, respectively. The chemical exergy of a gas *i,* having the mole fraction x_{i}^{e} in the environmental gas phase is [80,83]

$$e_{\text{i}}^{\text{ch}} = -\overline{R} T_0 \ln x_{\text{i}}^{\text{e}} \tag{3.18}$$

The chemical exergy of an ideal mixture of *N* ideal gases is given by

$$e_{\text{M,ig}}^{\text{ch}} = \sum_{i=1}^{N} x_{\text{i}} e_{\text{i}}^{\text{ch}} + \overline{R} T_0 \sum_{i=1}^{N} x_{\text{i}} \ln x_{\text{i}} \tag{3.19}$$

where T_0 is the environmental temperature, e_{i}^{ch} is the standart molar chemical exergy of the i-th substance and x_{i} is the mole fraction of the k-th substance in the system at T_0. For the chemical exergy calculations of liquids, the chemical exergy can be obtained if the activity coefficients γ_{k} are known such as

$$e_{\text{M,l}}^{\text{ch}} = \sum_{i=1}^{N} x_{\text{i}} e_{\text{i}}^{\text{ch}} + \overline{R} T_0 \sum_{i=1}^{N} x_{\text{i}} \ln(\gamma_{\text{k}} x_{\text{i}}) \tag{3.20}$$

The standard chemical exergy of a substance not present in the environment can be calculated by considering a reversible reaction of the substance with other substances for which the standard chemical exergies are known. For energy conversion processes, calculation of the exergy of fossil fuels is particularly important. The chemical exergy of a fossil fuel $e_{\mathrm{f}}^{\mathrm{ch}}$ on a molar basis can be derived from exergy, energy, and entropy balances for the reversible reaction:

$$e_f^{ch} = -\left(\Delta\bar{h}_R - T_0\Delta\bar{s}_R\right) + \Delta e^{ch} = -\Delta\bar{g}_R + \Delta e^{ch} \tag{3.21}$$

with $\Delta\bar{h}_{\mathrm{R}} = \sum_i \nu_{\mathrm{i}}\bar{h}_{\mathrm{i}} = -\bar{h}_{\mathrm{f}} + \sum_k \nu_{\mathrm{k}}\bar{h}_{\mathrm{k}} = -HHV$

$$\Delta\bar{s}_{\mathrm{R}} = \sum_i \nu_{\mathrm{i}}\bar{s}_{\mathrm{i}} = -\bar{s}_{\mathrm{f}} + \sum_k \nu_{\mathrm{k}}\bar{s}_{\mathrm{k}}$$

$$\Delta\bar{g}_{\mathrm{R}} = \Delta\bar{h}_{\mathrm{R}} - T_0\Delta\bar{s}_{\mathrm{R}}$$

$$\Delta e^{\mathrm{ch}} = \sum_k \nu_{\mathrm{k}} e_{\mathrm{k}}^{\mathrm{ch}}$$

where i and k denote O_2, CO_2, H_2O. $\Delta\bar{h}_{\mathrm{R}}$, $\Delta\bar{s}_{\mathrm{R}}$, and $\Delta\bar{g}_{\mathrm{R}}$ denote the molar enthalpy, entropy and Gibbs function, respectively of the reversible combustion reaction of the fuel with oxygen. HHV is the molar higher heating value of the fuel and ν_{k} is the stoichiometric coefficient of the k-th substance in this reaction. For some fuels such as coal and oil, the enthalpy and entropy values of the fuel must be estimated using available approaches before the chemical exergy can be calculated. The higher heating value is the primary contributor to the chemical exergy of a fossil fuel. The molar chemical exergy of a fossil fuel may be estimated with the aid of its molar higher heating value as

$$\frac{e_{\mathrm{f}}^{\mathrm{ch}}}{HHV} \approx \begin{cases} 0.95 - 0.985 & \text{for gaseous fuels except } \mathrm{H_2} \text{ and } \mathrm{CH_4} \\ 0.98 - 1.0 & \text{for liquid fuels} \\ 1.0 - 1.04 & \text{for solid fuels} \end{cases}$$

For hydrogen and methane this ratio is 0.83 and 0.94, respectively.

3.3.2 Exergy Balance, Exergy Destruction, and Exergy Loss

All thermodynamic processes are governed by the laws of conservation of mass and energy. These conservation laws state that mass and energy can neither be created nor destroyed in a process. Exergy, however, is not conserved but is destroyed by irreversible processes within a system. Consequently, an exergy balance must contain a destruction term, which vanishes only in a reversible process. Furthermore, exergy is lost, in general, when a material or energy stream is rejected to the environment.

The exergy destruction represents the exergy destroyed $\dot{E}_{\mathrm{D}}$ due to irreversibilities (entropy generation) within a system. The irreversibilities are caused by chemical reaction, heat transfer through a finite temperature difference, mixing of matter, and unrestrained expansion and friction. The exergy destruction is calculated with the aid of either (a) an exergy balance formulated for the system being considered, or (b) the entropy generation, $\dot{S}_{\mathrm{gen}}$, within the system (calculated from an entropy balance) and the relationship [80,84]

$$\dot{E}_{\mathrm{D}} = T_0 \dot{S}_{\mathrm{gen}} \tag{3.22}$$

The former way is recommended when a comprehensive exergetic evaluation is conducted. The exergy destruction in the overall system is equal to the sum of the exergy destruction in all system components:

$$\dot{E}_{\mathrm{D,total}} = \sum_{\mathrm{k}=1}^{\mathrm{n_k}} \dot{E}_{\mathrm{D,k}} \tag{3.23}$$

The rate of exergy destruction in the *k*th component of a system is given by

$$\dot{E}_{\mathrm{D,k}} = \dot{E}_{\mathrm{F,k}} - \dot{E}_{\mathrm{P,k}} - \dot{E}_{\mathrm{L,k}} \tag{3.24}$$

where, $\dot{E}_{F,k}$ and $\dot{E}_{P,k}$ are the so-called exergetic fuel and exergetic product, respectively, and $\dot{E}_{L,k}$ represents the exergy rate loss in the *k*th component, which is usually zero when the component boundaries are at T_0. For an overall system, $\dot{E}_{L,\text{total}}$ includes the exergy flow rates of all non-useful streams rejected by this system to the surroundings.

The total exergy destruction value is also obtained from the exergy balance written for the overall system

$$\dot{E}_{D,\text{total}} = \dot{E}_{F,\text{total}} - \dot{E}_{P,\text{total}} - \dot{E}_{L,\text{total}} \tag{3.25}$$

A useful splitting of the total exergy destruction within a component is between avoidable and unavoidable exergy destruction. Unavoidable $\dot{E}_{D,k}^{UN}$ is that part of exergy destruction within one component that cannot be eliminated even if the best available technology in the near future. The avoidable exergy destruction rate $\dot{E}_{D,k}^{AV}$ is the difference between the total and the unavoidable exergy destruction rate [83].

$$\dot{E}_D = \dot{E}_{D,k}^{AV} + \dot{E}_{D,k}^{UN} \tag{3.26}$$

It is apparent that all efforts to improve the thermodynamic efficiency of a component or system should focus on avoidable exergy destruction.

An exergy transfer across the boundary of a control volume system can be associated with either a material stream or an energy transfer by work or heat. By taking the positive direction of heat transfer to be to the system and the positive direction of work transfer to be from the system, the general form of the exergy balance for a control volume involving multiple inlet and outlet streams of matter and energy can be expressed as

$$\frac{dE_{CV}}{dt} = \sum\left(1-\frac{T_0}{T_k}\right)\dot{Q}_k - \left(\dot{W} - P_0\frac{dV_{CV}}{dt}\right) + \sum\dot{E}_i - \sum\dot{E}_e - \dot{E}_D \tag{3.27}$$

where $\dot{E}_{\mathrm{i}}$ and $\dot{E}_{\mathrm{e}}$ are the total exergy transfer rates at the inlet and outlet, respectively for the total, physical, chemical, kinetic, and potential exergy associated with mass transfers. The term $\dot{Q}_{\mathrm{k}}$ represents the rate of heat transfer at the location on the boundary where the temperature is T_{k}. The associated rate of exergy transfer $\dot{E}_{\mathrm{q,k}}$ is given by

$$\dot{E}_{\mathrm{q,k}} = \left(1 - \frac{T_0}{T_{\mathrm{k}}}\right)\dot{Q}_{\mathrm{k}} \tag{3.28}$$

For $T_{\mathrm{k}} > T_0$, the exergy rate $\dot{E}_{\mathrm{q,k}}$ associated with heat transfer is always smaller than the heat transfer rate $\dot{Q}_{\mathrm{k}}$. In applications below the temperature of the environment, $T_{\mathrm{k}} < T_0$, and $\dot{E}_{\mathrm{q,k}}$ and $\dot{Q}_{\mathrm{k}}$ have opposite signs: When energy is supplied to the system, exergy is removed from it and vice versa. For steady-flow systems, $\frac{dE_{\mathrm{CV}}}{dt} = 0$, and Equation 3.27 becomes

$$0 = \sum\left(1 - \frac{T_0}{T_{\mathrm{k}}}\right)\dot{Q}_{\mathrm{k}} - \left(\dot{W} - P_0\frac{dV_{\mathrm{CV}}}{dt}\right) + \sum\dot{E}_{\mathrm{i}} - \sum\dot{E}_{\mathrm{e}} - \dot{E}_{\mathrm{D}} \tag{3.29}$$

3.3.3 Exergetic Efficiency

Dimensionless criteria are used for performance evaluations. Appropriately defined exergetic efficiency unambiguously characterizes the performance of a system or system component from the thermodynamic view point. The exergetic efficiency should also be used to compare the performance of similar components operating under similar conditions. For the comparison of dissimilar components the exergy destruction ratio may be used.

The exergetic efficiency of the *k*th component ε_{k} is defined as the ratio between product and fuel. The exergy rates of product $\dot{E}_{\mathrm{P,k}}$ and the fuel $\dot{E}_{\mathrm{F,k}}$ are

defined by considering the desired result produced by the component, and the exergetic resources expended to generate this result, respectively:

$$\varepsilon_{\mathrm{k}} = \frac{\dot{E}_{\mathrm{P,k}}}{\dot{E}_{\mathrm{F,k}}} = 1 - \frac{\dot{E}_{\mathrm{D,k}} + \dot{E}_{\mathrm{L,k}}}{\dot{E}_{\mathrm{F,k}}} \tag{3.30}$$

The definition of exergetic efficiency must be meaningful from both the thermodynamic and the economic view points. General guidelines for defining exergetic efficiencies can be found in the literature [1,80,83-89]. A distinction between (a) physical and chemical exergy, or (b) thermal, mechanical and chemical exergy, or (c) thermal mechanical, reactive and non-reactive exergy may allow the definitions of more rational exergetic efficiencies for some components.

For the comparison of dissimilar components operating in the same system, modified exergetic efficiency can be defined based on the avoidable and unavoidable exergy destruction concept:

$$\varepsilon_{\mathrm{k}}^{*} = \frac{\dot{E}_{\mathrm{P,k}}}{\dot{E}_{\mathrm{F,k}} - \dot{E}_{\mathrm{D,k}}^{\mathrm{UN}}} = 1 - \frac{\dot{E}_{\mathrm{D,k}}^{\mathrm{AV}} + \dot{E}_{\mathrm{L,k}}}{\dot{E}_{\mathrm{F,k}} - \dot{E}_{\mathrm{D,k}}^{\mathrm{UN}}} \tag{3.31}$$

3.3.4 Exergy Destruction Ratio and Exergy Loss Ratio

In addition to the exergy destruction $\dot{E}_{\mathrm{D,k}}$ and the exergetic efficiencies ε_{k}, the exergy destruction ratio $y_{\mathrm{D,k}}$ is used in the thermodynamic evaluation of a component. This ratio compares the exergy destruction in the *k*th component with the total fuel exergy supplied $\dot{E}_{\mathrm{F,total}}$ to the overall system:

$$y_{\mathrm{D,k}} = \frac{\dot{E}_{\mathrm{D,k}}}{\dot{E}_{\mathrm{F,total}}} \tag{3.32}$$

Alternatively, the exergy destruction rate of the *k*th component can be compared to the total exergy destruction rate $\dot{E}_{\mathrm{D,total}}$:

$$y^{*}_{D,k} = \frac{\dot{E}_{D,k}}{\dot{E}_{D,total}} \tag{3.33}$$

The exergy loss ratio is defined similarly to Equation 3.32, by comparing the exergy loss to the total fuel exergy supplied to the overall system

$$y_{L,total} = \frac{\dot{E}_{L,total}}{\dot{E}_{F,total}} \tag{3.34}$$

The difference between the exergy destruction ratio and the exergetic efficiency is that in the former the exergy destruction within a component is related to the fuel exergy supplied to the overall system, whereas the latter refers the same exergy destruction to the fuel exergy supplied to the component. The exergy destruction ratio expresses the percentage of the decrease of the exergetic efficiency for the overall system caused by the exergy destruction in the *k*th system component:

$$\varepsilon_{total} = \frac{\dot{E}_{P,total}}{\dot{E}_{F,total}} = 1 - \frac{\dot{E}_{D,total} + \dot{E}_{L,total}}{\dot{E}_{F,total}} = 1 - y_{D,total} - y_{L,total} \tag{3.35}$$

Since in almost every case no exergy loss is defined at the component level, the exergy loss ratio is defined only for the overall system.

3.4 Economic Analysis

The successful completion of a thermal design project requires estimation of the major costs involved in the project [e.g. total capital investment, fuel costs, operating and maintenance (O & M) expenses, and cost of the final products] considering various assumptions and predictions referring to the economic, technological, and legal environments, and using techniques from engineering economics [80].

One of the most important factors affecting the selection of a design option for a thermal system is the cost of the final products. The cost of an item is the amount of money paid to acquire or produce it. The market price of an item is, in

general, affected not only by the production cost of the item and the desired profit but also by other factors such as demand, supply, competition, regulation and subsidies.

The total cost of an item consists of fixed costs and variable costs. The term "fixed costs" identifies those costs that do not depend strongly on the production rate. Costs for depreciation, taxes on facilities, insurance, maintenance, and rent belong to this category. "Variable costs" are those costs that vary more or less directly with the volume of output. These include the costs for materials, labor, fuel, and electric power [90].

Good cost estimation is a key factor in successfully completing a design project. Cost estimates should be made during all stages of design to provide a basis for decision making at each stage. Each company has its own preferred approach for conducting an economic analysis and calculating the cost of main products (i.e. unit price of electricity and steam).

3.4.1 Time Value of Money

Decisions about capital expenditures generally require consideration of the earning power of money. A euro in hand today is worth more than a euro received one year from now because the euro in hand now can be invested for the year. Thus, as the cost evaluation of a project requires comparisons of money transactions at various points in time, we need methods that will enable us to account for the value of money over time.

Future Value: If "*P*" euros (present value) are deposited in an account earning "*i*" percent interest per time period and the interest is compounded at the end of each of "*n*" time periods, the account will grow to a future value, "*F*"

$$F = P(1+i)^{n} \tag{3.36}$$

Interest is the compensation paid for the use of borrowed money. The interest rate is usually stated as a percentage; in equations, however, it is expressed as a decimal

(e.g., 0.07 instead of 7%). Instead of the term interest rate, we will use the terms rate of return for an investment made and annual cost of money for borrowed capital [91].

Compounding Frequency: In engineering economy, the unit of time is usually taken as the year. If compounding occurs "*p*" times per year ($p \geq 1$) for a total number of "*n*" years ($n \geq 1$), and "*i*" is the annual rate of return, Equation 3.36 becomes

$$F = P\left(1+\frac{i}{p}\right)^{\mathrm{np}} \tag{3.37}$$

Here the product "np" is the number of periods and "*i/p*" is the rate of return per period. In this case, the annual rate of return "*i*" is known as the nominal rate of return. The effective rate of return is the annual rate of return that would yield the same results if compounding were done once a year instead of "*p*" times per year. The effective rate of return, which is higher than the nominal rate of return, is obtained by eliminating *F/P* from Equations 3.36 and 3.37 as

$$i_{\mathrm{eff}} = \left(1+\frac{i}{p}\right)^{\mathrm{p}} - 1 \tag{3.38}$$

If continuous compounding of money ($p \to \infty$) is used, the future value is calculated from

$$F = Pe^{\mathrm{in}} \tag{3.39}$$

It is apparent that in the case of continuous compounding the effective rate of return becomes

$$i_{\mathrm{eff}} = e^{\mathrm{i}} - 1 \tag{3.40}$$

In Equations 3.39 and 3.40, "*i*" is the nominal annual rate of return and "*n*" is the total number of years. If the time is less than one year, the simple interest formula can be used to calculate the future value:

$$F = P(1 + ni_{\text{eff}}) \tag{3.41}$$

where "*n*" is now a fraction of a year and "i_{eff}" is the annual effective rate of return. Equations 3.37 and 3.39 can be expressed in the same form as Equation 3.36:

$$F = P(1 + i_{\text{eff}})^{\text{n}} \tag{3.42}$$

The term $(1 + i_{\text{eff}})^{\text{n}}$, referred to as the single – payment compound amount factor (SPCAF).

Unless otherwise indicated, the terms interest, rate of return, and annual cost of money refer to their effective values. Also, to simplify calculations, when the cost of money is calculated for one or more years plus a fractional part of a year, Equation 3.42 is applied with a non-integer exponent [90].

Present Value: When evaluating projects, we often need to know the present value of funds that we will spend or receive at some definite periods in the future. The present value (or present worth) of a future amount is the amount that if deposited at a given rate of return and compounded would yield the actual amount received at a future date. From Equation 3.42 we see that a given future amount *F* has a present value *P*:

$$P = F\frac{1}{(1 + i_{\text{eff}})^{\text{n}}} \tag{3.43}$$

The term $1/(1 + i_{\text{eff}})^{\text{n}}$, called the single – payment present – worth factor or the single – payment discount factor (SPDF). Since the difference between the future value and the present value is often called discount, in this case the term i_{eff} is called the effective discount rate.

Annuities: An annuity is a series of equal amount money transactions occurring at equal time intervals (periods). Usually, the time period corresponds to one year. Money transactions of this type can be used, for instance to pay off a debt or accumulate a desired amount of capital. Annuities are used in this study to calculate the levelized costs of the final product, fuel, and so forth. An annuity term is the time from the beginning of the first time interval to the end of the last time interval.

If A euros are deposited at the end of each period in an account earning i_{eff} percent per period (effective rate of return per period), the future sum F (amount of the annuity or future value of the annuity) acquired at the end of the n$^{\text{th}}$ period is

$$F = A\frac{(1+i_{\text{eff}})^{\text{n}}-1}{i_{\text{eff}}} \tag{3.44}$$

The term $\left[(1+i_{\text{eff}})^{\text{n}}-1\right]/i_{\text{eff}}$ is called the uniform – series compound – amount factor (USCAF), and the reciprocal term of it is called the uniform – series sinking fund factor (USSFF). By combining Equations 3.43 and 3.44, we obtain

$$\frac{P}{A} = \frac{(1+i_{eff})^{\text{n}}-1}{i_{eff}(1+i_{eff})^{\text{n}}} \tag{3.45}$$

The expression on the right side of this equation is called the uniform – series present – worth factor (USPWF). The reciprocal of this factor is the capital recovery factor (CRF):

$$\text{CRF} = \frac{A}{P} = \frac{i_{\text{eff}}(1+i_{\text{eff}})^{n}}{(1+i_{\text{eff}})^{n}-1} \tag{3.46}$$

The CRF is used to determine the equal amounts A of a series of n money transactions, the present value of which is P.

Capitalized Cost: An asset (e.g., a piece of equipment) of fixed – capital cost C_{FC} will have a finite economic life of n years. The economic life (or book life) of an asset is the best estimate of the length of time that the asset can be used. The salvage value of an asset is the estimated economic worth of the asset at the end of its economic life.

Engineers often want to determine the total cost of an asset under conditions permitting perpetual replacement of the asset without considering inflation. The so-called capitalized cost C_K is defined in engineering economics as the first cost of the asset plus the present value of the indefinite annuity that corresponds to the perpetual replacement of the asset every *n* year. Assuming that the renewal cost of the asset remains constant (no inflation) at $C_{FC} - S$, and that both the useful life of the asset and the rate of return remain constant, the present value of the indefinite annuity is calculated from Equation 3.43 as [80]

$$(C_K - C_{FC}) = (C_K - S)/(1 + i_{eff})^n \tag{3.47}$$

That is, the capitalized cost C_K is in excess of the fixed – capital cost C_{FC} by an amount which, when compounded at an effective rate of return i_{eff} for *n* years, will have a future value of C_K minus the salvage value *S* of the asset. Solving the last equation for C_K, we obtain the capitalized cost as

$$C_K = \left[C_{FC} - \frac{S}{(1 + i_{eff})^n} \right] \left[\frac{(1 + i_{eff})^n}{(1 + i_{eff})^n - 1} \right] \tag{3.48}$$

The second factor in square brackets on the right side of the equation is called the capitalized – cost factor (CCF). The capitalized – cost factor is equal to the capital – recovery factor of an ordinary annuity (Equation 3.47) divided by the effective rate of return.

The use of the term capitalized cost is more meaningful in accounting than in engineering economics where the term merely characterizes a special case of present

– value calculation referring to an infinite project life. However, because the term capitalized cost is encountered very often in the literature of both engineering economics and accounting, it is important to be familiar with the different meanings that may be attached to it [80,91].

3.4.2 Inflation, Escalation, and Levelization

Inflation: General price inflation is the rise in price levels associated with an increase in available currency and credit without a proportional increase in available goods and services of equal quality [80]. The consumer price index, which is tabulated by the government, is composite prices index that measures general inflation.

When inflation occurs, costs change every year. Cost changes in past years are considered using appropriate cost indices. For future years a varying annual inflation rate can be used, but such a rate always represents a prediction. For simplicity we assume a constant average annual inflation rate (r_i) for future years.

Escalation: The real escalation rate of expenditure is the annual rate of expenditure change caused by factors such as resource depletion, increased demand, and technological advances [92]. The first two factors lead to a positive real escalation rate whereas the third factor results in a negative rate. The real escalation rate (r_r) is independent and exclusive of inflation.

The nominal (or apparent) escalation rate (r_n) is the total annual rate of change in cost and includes the effects of both real escalation rate and inflation:

$$(1+r_n)=(1+r_r)(1+r_i) \tag{3.49}$$

To simplify calculations, we assume that all costs except fuel costs and the values of by-products change annually with the constant average inflation rate r_i; that is, we take $r_r = 0$. Since fuel costs are expected over a long period of future years to increase on the average faster than the predicted inflation rate, a positive real

escalation rate for fuel costs may be appropriate for the economic analysis of thermal systems.

Levelization: Cost escalation applied to an expenditure (e.g., fuel costs or O&M costs) over n-year period results in a non-uniform cost schedule in which the expenditure at any year is equal to the previous year expenditure multiplied by $\left(1+r_{\mathrm{n}}\right)$, where r_{n} is the constant rate of change, the nominal escalation rate. The constant – escalation levelization factor (CELF) is used to express the relationship between the value of expenditure at the beginning of the first year $\left(P_0\right)$ and an equivalent annuity (A), which is now called a levelized value. The levelization factor depends on both the effective annual cost – of – money rate, or discount rate i_{eff} and the nominal escalation rate r_{n}:

$$\frac{A}{P_0} = \mathrm{CELF} = \frac{k\left(1-k^{\mathrm{n}}\right)}{1-k}\mathrm{CRF} \tag{3.50}$$

where

$$k = \frac{1+r_{\mathrm{n}}}{1+i_{\mathrm{eff}}} \tag{3.51}$$

and the variables CRF and r_{n} are determined from Equations 3.46 and 3.49, respectively. Equation 3.50 assumes that all transactions are made at the end of their respective years and $\left(P_0\right)$ is the cost at the beginning of the first year.

The concept of levelization is general and is defined as the use of time – value – of – money arithmetic to convert a series of varying quantities to a financially equivalent constant quantity (annuity) over a specified time interval. We will apply the concept of levelization to calculate the levelized fuel and O&M costs, the levelized total revenue requirements and the levelized total cost of the main product of a thermal system [80].

In the economic analysis of the thermal systems, the annual values of carrying charges, fuel costs, raw water costs, and operating and maintenance (O&M) expenses supplied to the overall system are the necessary input data. However these cost components may vary significantly within the economic life. Therefore, levelized annual values for all cost components should be used in the economic analysis and evaluations of the overall system. The levelized cost is given by [93]

$$A = \mathrm{CRF}\sum_{\mathrm{m}=1}^{\mathrm{n}} P_{\mathrm{m}} = \frac{i_{\mathrm{eff}}\left(1+i_{\mathrm{eff}}\right)^{\mathrm{n}}}{\left(1+i_{\mathrm{eff}}\right)^{\mathrm{n}}-1}\sum_{\mathrm{m}=1}^{\mathrm{n}} P_{\mathrm{m}} \tag{3.52}$$

where

$$P_{\mathrm{m}} = C_{\mathrm{m}}\frac{1}{\left(1+i_{\mathrm{eff}}\right)^{\mathrm{m}}} \tag{3.53}$$

The cost rate associated with the capital and O&M expenses for the *k*th component of a thermal system is

$$\dot{Z}_{\mathrm{k}} = \frac{\mathrm{CC_L}}{\tau}\frac{\mathrm{PEC_k}}{\sum_{\mathrm{k}}\mathrm{PEC_k}} + \frac{\mathrm{OMC_L}}{\tau}\frac{\mathrm{PEC_k}}{\sum_{\mathrm{k}}\mathrm{PEC_k}} \tag{3.54}$$

The first term in the nominator of the right hand side of the equation gives $\dot{Z}_{\mathrm{k}}^{\mathrm{CI}}$, and the second term gives $\dot{Z}_{\mathrm{k}}^{\mathrm{OM}}$. The levelized cost rate of the expenditure (fuel, raw water) supplied to the overall system is

$$\dot{\mathrm{C}}_{\mathrm{EX}} = \frac{\mathrm{EXC_L}}{\tau} \tag{3.55}$$

3.5 Thermoeconomic Analysis

Cost accounting in a company is concerned primarily with (a) determining the actual cost of products or services, (b) providing a rational basis for pricing goods and services, (c) providing a means for allocating and controlling expenditures, and

(d) providing information on which operating decisions may be based and evaluated [80]. This frequently calls for the use of cost balances. In a conventional economic analysis, a cost balance is usually formulated the overall system operating at steady state

$$\dot{C}_{\mathrm{P,TOT}} = \dot{C}_{\mathrm{F,TOT}} + \dot{Z}^{\mathrm{CI}}_{\mathrm{TOT}} + \dot{Z}^{\mathrm{OM}}_{\mathrm{TOT}} \tag{3.56}$$

The cost balance expresses that the cost rate associated with the product of the system $\dot{C}_{\mathrm{P}}$ equals the total rate of expenditures made to generate the product, namely the fuel cost rate $\dot{C}_{\mathrm{F}}$ and the cost rates associated with capital investment $\dot{Z}^{\mathrm{CI}}$ and operating and maintenance $\dot{Z}^{\mathrm{OM}}$. When referring to a single stream associated with a fuel or product, the expression fuel stream or product stream is used. The rates $\dot{Z}^{\mathrm{CI}}$ and $\dot{Z}^{\mathrm{OM}}$ are calculated by dividing the annual contributions of capital investment and the annual operating and maintenance (O&M) costs, respectively, by the number of time units (usually hours or seconds) of system operation per year. The sum of these two variables is denoted by $\dot{Z}$

$$\dot{Z} = \dot{Z}^{\mathrm{CI}} + \dot{Z}^{\mathrm{OM}} \tag{3.57}$$

3.5.1 Exergy Costing

Cost may be defined as the amount of resources needed to obtain a functional product. On one hand, resources take a general meaning. On the other hand, cost is associated with the purpose of production. It is associated neither with price nor with the resources that could be saved if the production process were less efficient or more conventional one [94]. Cost is an emergent property. It cannot be measured as a physical magnitude of a flow stream as temperature or pressure; it depends on the system structure and appears as an outcome of the system analysis. Therefore, it needs precise rules for calculating it from physical data. Cost is a property that cannot be found in the product itself [80,95].

In thermoeconomics, the words history, degradation, exergy, quality, cost, resource, consumption, purpose and causality are related to one another. In the cost

formation process, it is essential to analytically search for the locations and physical mechanisms that make up a specific productive flow [96]. The resources are used to provide physico-chemical qualities to the intermediate products until a finished product is obtained. The main problem to be solved using exergy is how to measure and homogenize the accounting of these qualities.

Since exergy measures the true thermodynamic value of the effects associated with heat, work and mass interactions through systems, it is meaningful to use exergy as a basis for assigning costs in thermal systems. Indeed, thermoeconomics rests on the notion that exergy is the only rational basis for assigning costs to the interactions that a thermal system experiences with its surroundings and to the sources of inefficiencies within it. This approach is referred as "exergy costing".

In exergy costing a cost is associated with each exergy stream. Thus for entering and exiting streams of matter with associated rates of exergy transfer, power and the exergy transfer rate associated with heat transfer may be written, respectively as

$$\dot{C}_{\mathrm{i}} = c_{\mathrm{i}}\dot{E}_{\mathrm{i}} = c_{\mathrm{i}}(\dot{m}_{\mathrm{i}}e_{\mathrm{i}}) \tag{3.58}$$

$$\dot{C}_{\mathrm{e}} = c_{\mathrm{e}}\dot{E}_{\mathrm{e}} = c_{\mathrm{e}}(\dot{m}_{\mathrm{e}}e_{\mathrm{e}}) \tag{3.59}$$

$$\dot{C}_{\mathrm{w}} = c_{\mathrm{w}}\dot{W} \tag{3.60}$$

$$\dot{C}_{\mathrm{q}} = c_{\mathrm{q}}\dot{E}_{\mathrm{q}} \tag{3.61}$$

where c_{i}, c_{e}, c_{w}, and c_{q} denote average costs per unit of exergy of material stream at inlet and exit, power and heat respectively and $\dot{C}_{\mathrm{i}}$, $\dot{C}_{\mathrm{e}}$, $\dot{C}_{\mathrm{w}}$ and $\dot{C}_{\mathrm{q}}$ are the corresponding cost rates, $\dot{E}_{\mathrm{i}}$ and $\dot{E}_{\mathrm{e}}$ are exergy transfers for entering and exiting streams of matter, $\dot{W}$ is power, and $\dot{E}_{\mathrm{q}}$ is the exergy transfer rate associated with heat transfer.

Accordingly, for a component receiving heat transfer and generating power, we may write [80,97,98]

$$\sum_{\mathrm{e}} \left(c_{\mathrm{e}} \dot{E}_{\mathrm{e}}\right)_{\mathrm{k}} + c_{\mathrm{w,k}} \dot{W}_{\mathrm{k}} = c_{\mathrm{q,k}} \dot{E}_{\mathrm{q,k}} + \sum_{\mathrm{i}} \left(c_{\mathrm{i}} \dot{E}_{\mathrm{i}}\right)_{\mathrm{k}} + \dot{Z}_{\mathrm{k}} \tag{3.62}$$

This equation simply states that the total cost of the exiting exergy streams equals the total expenditure to obtain them: the cost of the entering exergy streams plus the capital and other costs. Note that when a component receives power (as in a compressor or a pump) the second term of the left hand side would move with its positive sign to the right side of this expression. Cost balances are generally written so that all terms are positive.

The exergy rates exiting and entering the k^{th} component are calculated using exergy relations in previous sections of this chapter. The term $\dot{Z}_{\mathrm{k}}$ may be obtained by first calculating the capital investment and operating and maintenance (O&M) costs associated with the k^{th} component and then computing the levelized values of these costs per unit of time (year, hour, or second) of system operation. Based on these costs the general equation for the cost rate $\left(\dot{Z}_{\mathrm{i}}\right)$ in €/s associated with capital investment and the maintenance costs for the k^{th} component is

$$\dot{Z}_{\mathrm{k}} = \frac{Z_{\mathrm{k}} (CRF) \varphi}{(N \times 3600)} \tag{3.63}$$

where Z_{k} is the purchase cost of the k^{th} component (€), CRF is the annual capital recovery factor; N is the number of hours of plant operation per year, and φ is the maintenance factor.

When two or more products, by-products and residues are produced simultaneously, how costs can be allocated? Indeed, the main problem of allocating costs has been to find a function that adequately characterizes every one of the internal flows in a system and distributes cost proportionally. This function needs to be universal, sensitive and additive. That is, it needs to have an objective value for

every possible material manifestations and it needs to vary when these manifestations do so and each internal flow property needs to be represented additively. There is a wide international consensus that the best function, at least for energy systems, is exergy, which can contain in its own analytical structure of the flow history [94,99].

3.5.2 Aggregation Level for Applying Exergy Costing

For calculating approximate average costs, we can stop our analysis by disaggregating our system at not very detailed level since the level at which the cost balances are formulated affects the results of a thermoeconomic analysis. Cumulative exergy consumption analysis does not go into process details but focuses on the overall exergy consumption.

Accordingly, in thermal design, it is recommended that the lowest possible aggregation level be used [80,96,99,100]. This level is usually represented by the individual components (compressors, turbines, heat exchangers etc.). Even in cases where the available information is insufficient for applying exergy costing at the component level, it is generally preferable to make appropriate assumptions that enable exergy costing to be applied at the component level than to consider only groups of components [80].

3.6 Thermoeconomic Variables for Component Evaluation

The following quantities, known as thermoeconomic variables, play a central role in the thermoeconomic evaluation and optimization of thermal systems:

- the average unit cost of fuel, $c_{\mathrm{F,k}}$ (i.e. $c_{\mathrm{F,k}} = \dfrac{\dot{C}_{\mathrm{F,k}}}{\dot{E}_{\mathrm{F,k}}}$)
- the average unit cost of product, $c_{\mathrm{P,k}}$ (i.e. $c_{\mathrm{P,k}} = \dfrac{\dot{C}_{\mathrm{P,k}}}{\dot{E}_{\mathrm{P,k}}}$)
- the cost rate of exergy destruction, $\dot{C}_{\mathrm{D,k}}$
- the relative cost difference, r_{k}
- the exergoeconomic factor, f_{k}

In this chapter, three of these variables are discussed: $\dot{C}_{D,k}$, r_k, and f_k while all five thermoeconomic variables are applied to the thermoeconomic analysis and evaluation of geothermal assisted high temperature electrolysis system (see Chapter 5).

3.6.1 Cost of Exergy Destruction

In the cost balance formulas (i.e. Equations 3.56 and 3.62), there is no cost term directly associated with exergy destruction. Accordingly, the cost associated with the exergy destruction in a component or process is a hidden cost, but very important one, that can be revealed only through thermoeconomic analysis. Using the specific exergetic costs associated with fuel, product, and exergy loss for the *k*th component, the cost rate balance can be written as

$$c_{P,k}\dot{E}_{P,k} = c_{F,k}\dot{E}_{F,k} - \dot{C}_{L,k} + \dot{Z}_k \tag{3.64}$$

Using Equation 3.20, in order to eliminate $\dot{E}_{F,k}$, we obtain

$$c_{P,k}\dot{E}_{P,k} = c_{F,k}\dot{E}_{P,k} + \left(c_{F,k}\dot{E}_{L,k} - \dot{C}_{L,k}\right) + \dot{Z}_k + c_{F,k}\dot{E}_{D,k} \tag{3.65}$$

or to eliminate $\dot{E}_{P,k}$, we obtain

$$c_{P,k}\dot{E}_{P,k} = c_{F,k}\dot{E}_{F,k} + \left(c_{P,k}\dot{E}_{L,k} - \dot{C}_{L,k}\right) + \dot{Z}_k + c_{P,k}\dot{E}_{D,k} \tag{3.66}$$

In both Equations 3.65 and 3.66, the last term on the right hand side involves the rate of exergy destruction. Assuming that the product, $\dot{E}_{P,k}$ is fixed and that the unit cost of fuel, $c_{F,k}$ of the *k*th component is independent of the exergy destruction, the cost of exergy destruction can be expressed as

$$\dot{C}_{D,k} = c_{F,k}\dot{E}_{D,k} \tag{3.67}$$

As the fuel rate $\dot{E}_{F,k}$ must account for the fixed product rate $\dot{E}_{P,k}$, and the rate of exergy destruction rate $\dot{E}_{D,k}$, we may interpret $\dot{C}_{D,k}$ in Equation 3.67 as the cost rate of the additional fuel that must be supplied to the *k*th component.

Alternatively, assuming that the fuel $\dot{E}_{F,k}$ is fixed and that the unit cost of product $c_{P,k}$ of the *k*th component is independent of exergy destruction, we can define the cost of exergy destruction by the last term of Equation 3.66 as

$$\dot{C}_{D,k} = c_{P,k}\dot{E}_{D,k} \tag{3.68}$$

When exergy of fuel $\dot{E}_{F,k}$ is fixed, the exergy destruction $\dot{E}_{D,k}$ reduces to the product of the *k*th component $\dot{E}_{P,k}$, and therefore Equation 3.68 can be interpreted as the monetary loss associated with the loss of product.

3.6.2 Relative Cost Difference

The relative cost difference r_k for the *k*th component is defined as

$$r_k = \frac{c_{P,k} - c_{F,k}}{c_{F,k}} \tag{3.69}$$

The variable expresses the relative increase in the average cost per exergy unit between fuel and product of the component. The relative cost difference is a useful variable for evaluating and optimizing a system component. In an iterative cost optimization of a system, if the cost of fuel of a major component changes from one iteration to the next, the objective of the cost optimization of the component should be to minimize the relative cost difference instead of minimizing the cost per exergy unit of the product with this component.

If Equation 3.35 is rewritten for revealing the real cost sources associated with the *k*th component, using Equations 3.57 and 3.65 and taking $\dot{C}_{\mathrm{L,k}} = 0$, we obtain

$$r_{\mathrm{k}} = \frac{c_{\mathrm{F,k}}\left(\dot{E}_{\mathrm{D,k}} + \dot{E}_{\mathrm{L,k}}\right) + \left(\dot{Z}_{\mathrm{k}}^{\mathrm{CI}} + \dot{Z}_{\mathrm{k}}^{\mathrm{OM}}\right)}{c_{\mathrm{F,k}}\dot{E}_{\mathrm{P,k}}} \tag{3.70}$$

Using the exergetic efficiency of the *k*th component, and using Equation 3.26, Equation 3.70 may be written as

$$r_{\mathrm{k}} = \frac{1-\varepsilon_{\mathrm{k}}}{\varepsilon_{\mathrm{k}}} + \frac{\dot{Z}_{\mathrm{k}}^{\mathrm{CI}} + \dot{Z}_{\mathrm{k}}^{\mathrm{OM}}}{c_{\mathrm{F,k}}\dot{E}_{\mathrm{P,k}}} \tag{3.71}$$

3.6.3 Exergoeconomic Factor

As Equations 3.70 and 3.71 indicate, the cost sources in a component may be grouped into two categories. The first consists of non-exergy related costs (capital investment, and operating and maintenance expenses), while the second category consists of exergy destruction and exergy loss. In evaluating the performance of a component, we want to know the relative significance of each category. This is provided by the exergoeconomic factor, f_{k} defined for the *k*th component as

$$f_{\mathrm{k}} = \frac{\dot{Z}_{\mathrm{k}}}{\dot{Z}_{\mathrm{k}} + c_{\mathrm{F,k}}\left(\dot{E}_{\mathrm{D,k}} + \dot{E}_{\mathrm{L,k}}\right)} \tag{3.72}$$

The total cost rate causing the increase in the unit cost from fuel to product is given by the denominator in Equation 3.72. Accordingly, the exergoeconomic factor expresses as a ratio the contribution of the non-exergy related cost to total cost increase. A low value of the exergoeconomic factor calculated for a major component suggests that cost savings in the entire system might be achieved by improving the component efficiency (reducing the exergy destruction) even if the capital investment for this component will increase. On the other hand, a high value

of this factor suggests a decrease in the investment costs of this component at the expense of its exergetic efficiency.

3.7 The Specific Exergy Costing (SPECO) Method

The costs associated with each material and energy stream in a system are calculated with the aid of (a) cost balances written for each system component, and (b) auxiliary costing equations. Assuming that the costs of the exergy streams entering a component known, a cost balance is not sufficient to determine the costs of the exiting exergy streams when the number of exiting streams is larger than one. In this case, auxiliary costing equations must be formulated for the component being considered, the number of these equations being equal to the number of exiting streams minus one [91,98,99].

Different approaches for formulating efficiencies and auxiliary costing equations have been suggested in the literature. These approaches can be divided into two groups: (1) The exergoeconomic accounting methods [80,93,95,101-109] aim at the costing of product streams, the evaluation of components and systems, and the iterative optimization of energy systems; (2) The Lagrangian-based approaches [110-118] aim in optimizing the overall system and the calculation of marginal costs. In literature only total exergy values were used and the auxiliary costing equations were formulated explicitly by using assumptions derived from experience, postulates, or the purpose of the system being analyzed.

A different approach, based on the LIFO (Last In First Out) accounting principle, was presented in refs. [119,120]. In this approach, fuels, products, and costs are defined systematically registering exergy and cost additions and removals from each material and energy stream. In this way, “local average costs” are obtained since the cost per exergy unit of the exergy used in a component is evaluated at the cost at which the removed exergy units were supplied by upstream components. An automatic criterion to generate the auxiliary costing equations based on this principle can be achieved by using computer implementation and an algebraic formulation [121]. In this study, the name SPECO, specific exergy costing method, was given to

this approach because of the need of using specific exergies and costs for registering all additions and removals of exergy and cost.

The basic principles of the SPECO approach were then directly applied to exergy streams instead of material and energy streams [99]. It was demonstrated that these principles are sufficient for systematically defining fuel and product of the components and for formulating the auxiliary costing equations used to calculate either average costs (AVCO approach) or local average costs (LIFO approach).

Lagrangian-based approaches, on the other side, employ mathematical techniques to arrive at costs. It can be easily demonstrated that the same cost balances and auxiliary equations used in accounting methods can be obtained through partial derivatives in the Lagrangian-based approaches.

The SPECO method consists of the following three steps:

Step 1- identification of exergy streams: Initially, a decision must be made with respect to whether the analysis of the components should be conducted using total exergy or separate forms of the total exergy of a material stream (e.g. thermal, mechanical, and chemical exergies). Considering separate exergy forms improves the accuracy of the results. However, this improvement is often marginal and not necessary for extracting the main conclusions from the exergoeconomic evaluation.

Step 2- definition of fuel and product: The product is defined to be equal to the sum of all the exergy values to be considered at the outlet (including the exergy of energy streams generated in the component) plus all the exergy increases between inlet and outlet (i.e. the exergy additions to the respective material streams) that are in accord with the purpose of the component. Similarly, the fuel is defined to be equal to all the exergy values to be considered at the inlet (including the exergy streams supplied to the component) plus all the exergy decreases between inlet and outlet (i.e. the exergy removals form the respective material streams) minus all the exergy increases (between inlet and outlet) that are not in accord with the purpose of the component.

Step 3- cost equations: Exergoeconomics rests on the notion that exergy is the only rational basis for assigning costs to the interactions a thermal system experiences with its surroundings and to the sources of inefficiencies within it [80]. All the equations given in section 3.6 are used throughout the analysis at this step.

3.7.1 The $\dot{F}$ and $\dot{P}$ Principles

The $\dot{F}$ (fuel) principle refers to the removal of exergy from an exergy stream within the component being considered, when for this stream, the exergy difference between inlet and outlet is considered in the definition of the fuel. The $\dot{F}$ principle states that the total cost associated with this removal of exergy must be equal to the cost at which the removed exergy has supplied to the same stream in the upstream components.

The $\dot{P}$ (product) principle refers to the supply of exergy to an exergy stream within the component being considered. The $\dot{P}$ principle states that each exergy unit is supplied to any stream associated with the products at the same average cost c_p. This cost is calculated from the cost balance and the equations obtained by $\dot{F}$ principle. Aggregation level influences accuracy of the results, so it should be set at a lower level [80].

3.8 Conclusions

In this chapter, we provided general principles, terminology, and formulation of thermodynamic and thermoeconomic analyses. The procedure and formulation are applicable to all energy systems including hydrogen production with high temperature analysis from geothermal energy source. Detailed formulations considering the operation of the entire system and components will be provided in Chapters 4 and 5.

CHAPTER 4

THERMODYNAMIC ANALYSIS

4.1 Introduction

The use of energy as a measure for identifying and measuring the benefits of energy systems can be misleading and confusing. Exergy can be used to assess and improve energy systems, and can help better understand the benefits of the system by providing more useful and meaningful information than energy provides. Exergy clearly identifies efficiency improvements and reductions in thermodynamic losses attributable to more sustainable technologies [122].

For each state of the high temperature electrolysis system (HTSE), energy and exergy values, exergy efficiency, and exergy destruction are calculated and tabulated. For high temperature electrolysis, the Gibbs free energy and the standard chemical exergy of compounds are calculated. Parametric studies are performed.

In this chapter, energy and exery analyses of geothermal assisted HTSE is conducted using the methodologies described in earlier chapters. The results are obtained and discussed.

4.2 Description of Geothermal Assisted High Temperature Steam Electrolysis System

The schematic of geothermal assisted high temperature electrolysis system is shown in Fig. 4.1. For this system the usable temperature of the geothermal source a

the Nesjavellir Site in Iceland is considered. The source is approximately at 230 C and 15 bar. This is relatively low and the vaporisationand heating of the water for the electrolyser needs to be carried out in several stages.

- The water vapor at a temperature of 230 C heated in three types heat exchangers (High Temperature Heat Exchanger [HT], Medium Temperature Heat Exchanger [MT], and Low Temperature Heat Exchanger [LT]). The water vapor enters at states 1 and 5 and exits at states 4 and 8. Then, they are combined at state 9 and exit the electrolyser up to a temperature of 950 C.

- In the electrolyser, the electric power is not only used for splitting the water molecules into hydrogen and oxygen but also for heating the gas from the inlet to the outlet. The temperature of the oxygen ($T_{in,O2}$=950 C) and hydrogen ($T_{in,H2}$=950 C) are the same at the outlet. Since we are limiting ourselves to exothermal or isothermal conditions: $T_{in,O2} = T_{in,H2} = T_{in,elec}$.

- Hydrogen enters the heat exchangers at state 10 and exits at state 15, with $T_{out,H2} > T_{in,H2O}$.

- Oxygen enters the heat exchangers at state 16 and exits at state 21, with $T_{out,O2} > T_{in,H2O}$.

Before getting into energy and exergy analyses, the following assumptions are made:

- The values for the reference environment (dead state) temperature (T_0) for winter is -1 C and for summer is 11 C and pressure (P_0) is 100 kPa.

- All processes are considered steady-state and steady-flow with negligible potential and kinetic energy effects in an adiabatic form [123].

The results of energy and exergy analysis are given in Tables 4.1, 4.2, and 4.3 for three different dead state temperatures: 25 C, -1 C, and 11 C.

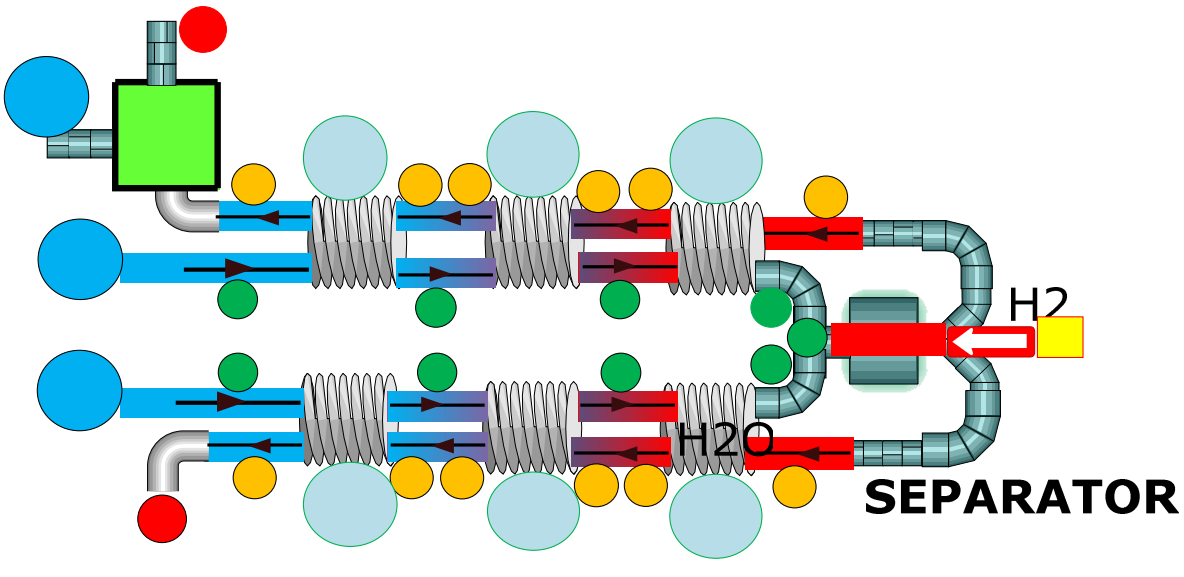

Figure 4.1 The schematic of geothermal assisted high temperature electrolysis system (Modified from 42)

HT: High Temperature Heat Exchanger, MT: Medium Temperature Heat Exchanger, LT: Low Temperature Heat Exchanger, HTE: Electrolyser Unit, Seperator

Table 4.1 System data, thermodynamic properties, and exergies in the system with respect to state points in Figure 4.1 for 25 °C.

State no	Substance	T (K)	P (kPa)	$\dot{m}$ (kg/s)	h (kJ/kg)	s (kJ/kg.K)	$\dot{E}x$ (kW)	$\dot{E}$ (kW)
0	H_2O	298	100	-	104.8	0.3669	-	-
0'	H_2	298	100	-	0	64.82	-	-
0''	O_2	298	100	-	0	6.407	-	-
1	H_2O	503	1500	9.95	2874	6.613	9035	28,596
2	H_2O	753	1500	9.95	3429	7.513	11,886	34,119
3	H_2O	978	1500	9.95	3932	8.096	15,163	39,123
4	H_2O	1185	1500	9.95	4421	8.549	18,685	43,989
5	H_2O	503	1500	3.48	2874	6.613	3158	10,001
6	H_2O	693	1500	3.48	3299	7.332	3894	11,481
7	H_2O	983	1500	3.48	3944	8.108	5332	13725
8	H_2O	1185	1500	3.48	4421	8.559	6535	15,385
9	H_2O	1185	1500	13.43	4421	8.559	15,221	59,374
10	H_2	1223	10,000	1.0	13,653	66.51	13,144	13,653
11	H_2	987	10,000	1.0	10,056	63.24	10,527	10.05
12	H_2	987	2000	1.0	10,056	69.88	8548	10.05
13	H_2	782	2000	1.0	7016	66.43	6536	7016
14	H_2	782	7000	1.0	7016	61.27	8074	7016
15	H_2	577	7000	1.0	4030	56.84	6408	4030
10'	H_2O	1223	10,000	4.43	4486	7.731	9688	19,873
11'	H_2O	987	10,000	4.43	3903	7.202	7801	17,290
12'	H_2O	987	2000	4.43	3950	7.982	6982	17,499
13'	H_2O	782	2000	4.43	3488	7.457	5626	15,452
14'	H_2O	782	7000	4.43	3432	6.826	6211	15,204
15'	H_2O	577	7000	4.43	2854	5.958	4798	11,447
16	O_2	1223	10,000	8.0	955.3	6.634	7104	7642
17	O_2	987	10,000	8.0	725.9	6.428	5760	5807
18	O_2	987	2000	8.0	725.9	6.816	4832	5807
19	O_2	782	2000	8.0	406.6	6.474	3096	3252
20	O_2	782	7000	8.0	406.6	6.149	3864	3252
21	O_2	569	7000	8.0	258.2	5.917	3132	2066

Table 4.2 System data, thermodynamic properties, and exergies in the system with respect to state points in Figure 4.1 for 11 °C.

State no	Substance	T (K)	P (kPa)	$\dot{m}$ (kg/s)	h (kJ/kg)	s (kJ/kg.K)	$\dot{E}x$ (kW)	$\dot{E}$ (kW)
0	H_2O	284	100	-	45.64	0.1635	-	-
0'	H_2	284	100	-	-	64.13	-	-
0"	O_2	284	100	-	-	6.366	-	-
1	H_2O	503	1500	9.95	2875	6.616	9471	27,313
2	H_2O	753	1500	9.95	3430	7.514	12,317	32,582
3	H_2O	978	1500	9.95	3932	8.097	15,517	37,357
4	H_2O	1185	1500	9.95	4422	8.551	18,943	42,006
5	H_2O	503	1500	3.48	2875	6.616	3469	10,005
6	H_2O	693	1500	3.48	3299	7.334	4237	11,482
7	H_2O	983	1500	3.48	3944	8.109	5713	13,724
8	H_2O	1185	1500	3.48	4422	8.551	6939	15,388
9	H_2O	1185	1500	13.43	4422	8.551	26,780	59,384
10	H_2	1223	1000	1.0	13,651	66,5	12,997	13,651
11	H_2	987	1000	1.0	10.054	63,24	10,308	10.054
12	H_2	987	2000	1.0	10.054	69,87	8243	10.054
13	H_2	782	2000	1.0	7014	66,42	6363	7014
14	H_2	782	7000	1.0	7014	61,26	7830	7014
15	H_2	577	7000	1.0	4030	56,83	6103	4030
10'	H_2O	1223	1000	4.43	4487	7,733	10,151	19,877
11'	H_2O	987	1000	4.43	3904	7,204	8234	17,294
12'	H_2O	987	2000	4.43	3950	7,983	7458	17,499
13'	H_2O	782	2000	4.43	3488	7,459	6070	15,451
14'	H_2O	782	7000	4.43	3433	6,828	6621	15,207
15'	H_2O	577	7000	4.43	2856	5,962	5155	12,652
16	O_2	1223	1000	8.0	955.2	6.637	7025	7641
17	O_2	987	1000	8.0	695.3	6,401	5482	5562
18	O_2	987	2000	8.0	695.3	6,819	4532	5562
19	O_2	782	2000	8.0	476.3	6,571	3345	3810
20	O_2	782	7000	8.0	476.3	6,245	4084	3810
21	O_2	569	7000	8.0	258.1	5,92	3078	2065

Table 4.3 System data, thermodynamic properties, and exergies in the system with respect to state points in Figure 4.1 for -1 °C.

State no	Substance	T (K)	P (kPa)	$\dot{m}$ (kg/s)	h (kJ/kg)	s (kJ/kg.K)	$\dot{E}x$ (kW)	$\dot{E}$ (kW)
0	H_2O	272	100	-	-335.2	-1.229	-	-
0'	H_2	272	100	-	-	63.53	-	-
0"	O_2	272	100	-	-	6.326	-	-
1	H_2O	503	1500	9.95	2875	6.616	10,711	28607
2	H_2O	753	1500	9.95	3430	7.514	13,798	34,126
3	H_2O	978	1500	9.95	3932	8.097	17,220	39,126
4	H_2O	1185	1500	9.95	4422	8.551	20,863	43,996
5	H_2O	503	1500	3.48	2875	6.616	3746	10,005
6	H_2O	693	1500	3.48	3299	7.334	4543	11,482
7	H_2O	983	1500	3.48	3944	8.109	6052	13,724
8	H_2O	1185	1500	3.48	4422	8.551	7297	15,388
9	H_2O	1185	1500	13.43	4422	8.551	28,159	59,384
10	H_2	1223	10,00	1.0	13,651	6.637	12,841	13,651
11	H_2	987	10,00	1.0	10.054	6.401	10,133	10.054
12	H_2	987	2000	1.0	10.054	6.819	8328	10.054
13	H_2	782	2000	1.0	7014	6.571	6226	7014
14	H_2	782	7000	1.0	7014	6.245	7632	7014
15	H_2	577	7000	1.0	4030	5.92	5851	4030
10'	H_2O	1223	10,00	4.43	4487	7.733	10,641	19,877
11'	H_2O	987	10,00	4.43	3904	7.204	8617	17,294
12'	H_2O	987	2000	4.43	3950	7.983	7883	17,499
13'	H_2O	782	2000	4.43	3488	7.459	6467	15,451
14'	H_2O	782	7000	4.43	3433	6.828	6984	15,207
15'	H_2O	577	7000	4.43	2856	5.962	5473	12652
16	O_2	1223	10,00	8.0	955.2	6.637	6964	7641
17	O_2	987	10,00	8.0	695.3	6.401	5399	5562
18	O_2	987	2000	8.0	695.3	6.819	4489	5562
19	O_2	782	2000	8.0	476.3	6.571	3278	3810
20	O_2	782	7000	8.0	476.3	6.245	3986	3810
21	O_2	569	7000	8.0	258.1	5.92	2948	2065

4.3 Energy and Exergy Relations for System Components

Energy and exergy relations for the components of the plant were provided in Chapter 3. The relations are based on general formulations provided in Chapter 3 and include mass, energy, and exergy balances as well as exergy destructions and exergy efficiencies. State numbers refer to Fig. 4.1.

In the study of Sigurvinsson et al. [123] counter current heat exchangers were used, while the inlet temperature of the electrolyses was kept as 950 C. The temperatures in the geothermal case ranged from 200 to 950 C. The heat exchangers were classified into three groups according to the ranges of the temperatures since this temperature range cannot be covered with one type of heat exchangers.

Therefore

- Low temperature (LT): stainless heat exchanger, $T < 600$□C and 7 MPa.
- Medium temperature (MT): nickel based heat exchanger, 600 □C < T < 850□C and 7 MPa.
- High temperature (HT): ceramic based heat exchanger, $T > 850$ □C and 10–50 MPa.

The heat exchanger suggested for the > 850 °C temperature level is still being tested and further detail will be available soon. However it could also be possible to operate the electrolyser at lower than 850°C temperatures using existing technology.

Low Temperature Heat Exchanger 1 (LT-1)

$$\dot{m}_1 = \dot{m}_2 \tag{4.1}$$

$$\dot{m}_{10} = \dot{m}_{14} = m_{15} \tag{4.2}$$

$$\dot{m}_{14'} = m_{15'} \tag{4.3}$$

$$\dot{m}_1(h_1 - h_2) = m_{10}(h_{15} - h_{14}) + \dot{m}_{10'}(h_{15'} - h_{14'}) \tag{4.4}$$

$$\dot{E}_{HE,Dest,HT-1} = \dot{m}_1(\psi_1 - \psi_2) - \dot{m}_{10}(\psi_{15} - \psi_{14}) - \dot{m}_{10'}(\psi_{15'} - \psi_{14'}) \tag{4.5}$$

$$\psi_1 - \psi_2 = (h_1 - h_2) - T_0(s_1 - s_2) \tag{4.6}$$

$$\psi_{15} - \psi_{14} = (h_{15} - h_{14}) - T_0(s_{15} - s_{14}) \tag{4.7}$$

$$\psi_{15'} - \psi_{14'} = (h_{15'} - h_{14'}) - T_0(s_{15'} - s_{14'}) \tag{4.8}$$

$$\varepsilon_{LT-1} = \frac{\dot{m}_{10}(\psi_{15} - \psi_{14}) + \dot{m}_{10'}(\psi_{15'} - \psi_{14'})}{\dot{m}_1(\psi_1 - \psi_2)} \tag{4.9}$$

Medium Temperature Heat Exchanger 1 (MT-1)

$$\dot{m}_1 = \dot{m}_2 = \dot{m}_3 \tag{4.10}$$

$$\dot{m}_{10} = \dot{m}_{12} = m_{13} \tag{4.11}$$

$$\dot{m}_{10'} = m_{12'} = m_{13'} \tag{4.12}$$

$$\dot{m}_1(h_2 - h_3) = m_{10}(h_{13} - h_{12}) + \dot{m}_{10'}(h_{13'} - h_{12'}) \tag{4.13}$$

$$\dot{E}_{HE,Dest,MT-1} = \dot{m}_1(\psi_2 - \psi_3) - \dot{m}_{10}(\psi_{13} - \psi_{12}) - \dot{m}_{10'}(\psi_{13'} - \psi_{12'}) \tag{4.14}$$

$$\psi_2 - \psi_3 = (h_2 - h_3) - T_0(s_2 - s_3) \tag{4.15}$$

$$\psi_{13} - \psi_{12} = (h_{13} - h_{12}) - T_0(s_{13} - s_{12}) \tag{4.16}$$

$$\psi_{13'} - \psi_{12'} = (h_{13'} - h_{12'}) - T_0(s_{13'} - s_{12'}) \tag{4.17}$$

$$\varepsilon_{MT-1} = \frac{\dot{m}_{10}(\psi_{13} - \psi_{12}) + \dot{m}_{10'}(\psi_{13'} - \psi_{12'})}{\dot{m}_1(\psi_2 - \psi_3)} \tag{4.18}$$

High Temperature Heat Exchanger 1(HT-1)

$$\dot{m}_1 = \dot{m}_3 = \dot{m}_4 \tag{4.19}$$

$$\dot{m}_{10} = \dot{m}_{11} \tag{4.20}$$

$$\dot{m}_{10'} = m_{11'} \tag{4.21}$$

$$\dot{m}_1(h_3 - h_4) = m_{10}(h_{11} - h_{10}) + \dot{m}_{10'}(h_{11'} - h_{10'}) \tag{4.22}$$

$$\dot{E}_{HE,Dest,HT-1} = \dot{m}_1(\psi_3 - \psi_4) - \dot{m}_{10}(\psi_{11} - \psi_{10}) - \dot{m}_{10'}(\psi_{11'} - \psi_{10'}) \tag{4.23}$$

$$\psi_3 - \psi_4 = (h_3 - h_4) - T_0(s_3 - s_4) \tag{4.24}$$

$$\psi_{10} - \psi_{11} = (h_{10} - h_{11}) - T_0(s_{10} - s_{11}) \tag{4.25}$$

$$\psi_{10'} - \psi_{11'} = (h_{10'} - h_{11'}) - T_0(s_{10'} - s_{11'}) \tag{4.26}$$

$$\varepsilon_{HT-1} = \frac{\dot{m}_{10}(\psi_{11} - \psi_{10}) + \dot{m}_{10'}(\psi_{11'} - \psi_{02'})}{\dot{m}_1(\psi_3 - \psi_4)} \tag{4.27}$$

Low Temperature Heat Exchanger 2 (LT-2)

$$\dot{m}_5 = \dot{m}_6 \tag{4.28}$$

$$\dot{m}_{16} = \dot{m}_{20} = \dot{m}_{21} \tag{4.29}$$

$$\dot{m}_5(h_5 - h_6) = m_{16}(h_{21} - h_{20}) \tag{4.30}$$

$$\dot{E}_{HE,Dest,LT-2} = \dot{m}_5(\psi_5 - \psi_6) - \dot{m}_{16}(\psi_{21} - \psi_{20}) \tag{4.31}$$

$$\psi_5 - \psi_6 = (h_5 - h_6) - T_0(s_5 - s_6) \tag{4.32}$$

$$\psi_{21} - \psi_{20} = (h_{21} - h_{20}) - T_0(s_{21} - s_{20}) \tag{4.33}$$

$$\varepsilon_{LT-2} = \frac{\dot{m}_{16}(\psi_{21} - \psi_{20})}{\dot{m}_5(\psi_5 - \psi_6)} \tag{4.34}$$

Medium Temperature Heat Exchanger 2 (MT-2)

$$\dot{m}_5 = \dot{m}_6 = \dot{m}_7 \tag{4.35}$$

$$\dot{m}_{16} = \dot{m}_{18} = \dot{m}_{19} \tag{4.36}$$

$$\dot{m}_5(h_6 - h_7) = m_{19}(h_{19} - h_{18}) \tag{4.37}$$

$$\dot{E}_{HE,Dest,MT-2} = \dot{m}_5(\psi_6 - \psi_7) - \dot{m}_{16}(\psi_{19} - \psi_{18}) \tag{4.38}$$

$$\psi_6 - \psi_7 = (h_6 - h_7) - T_0(s_6 - s_7) \tag{4.39}$$

$$\psi_{19} - \psi_{18} = (h_{19} - h_{18}) - T_0(s_{19} - s_{18}) \tag{4.40}$$

$$\varepsilon_{MT-2} = \frac{\dot{m}_{16}(\psi_{19} - \psi_{18})}{\dot{m}_5(\psi_6 - \psi_7)} \tag{4.41}$$

High Temperature Heat Exchanger 2 (HT-2)

$$\dot{m}_{16} = \dot{m}_{17} \tag{4.42}$$

$$\dot{m}_5 = \dot{m}_7 = \dot{m}_8 \tag{4.43}$$

$$\dot{m}_5(h_7 - h_8) = m_{16}(h_{17} - h_{16}) \tag{4.44}$$

$$\dot{E}_{HE,Dest,HT-2} = \dot{m}_5(\psi_7 - \psi_8) - \dot{m}_{16}(\psi_{17} - \psi_{16}) \tag{4.45}$$

$$\psi_7 - \psi_8 = (h_7 - h_8) - T_0(s_7 - s_8) \tag{4.46}$$

$$\psi_{17} - \psi_{16} = (h_{17} - h_{16}) - T_0(s_{17} - s_{16}) \tag{4.47}$$

$$\varepsilon_{MT-2} = \frac{\dot{m}_{16}(\psi_{17} - \psi_{16})}{\dot{m}_5(\psi_7 - \psi_6)} \tag{4.48}$$

4.4 Analysis of High-Temperature Steam Electrolysis

High-temperature steam electrolysis (HTSE) is still considered in the early developmental stage. The HTSE offers a promising method for highly efficient hydrogen production. From the thermodynamic viewpoint of water decomposition, it is more advantageous to electrolyse water at high temperature (800-1000°C) because the energy is supplied in mixed form of electricity and heat. The steam to be dissociated enters on the cathode side. After the steam has been divided into hydrogen gas and oxygen ions, the oxygen ions are transported through the ceramic material to the anode where they discharge and form oxygen gas. The most common ceramic material is zirconia, ZrO_2 [124].

There are three possible operating modes for HTE depending on the energy balance at the electrolyser level: endothermal, isothermal and exothermal.

4.4.1 Endothermal of High-Temperature Steam Electrolysis

The temperature of the steam decreases from the input of the electrolyser to the output. This corresponds to the best energy efficiency but worst production cost because an endothermal electrolyser is much more expensive than an exothermal one.

4.4.2 Isothermal of High-Temperature Steam Electrolysis

The temperature of the steam is the same at the input as at the output. The energy efficiency is better than in the exothermal case but the electrolyser cost still outweighs better efficiency.

4.4.3 Exothermal of High-Temperature Steam Electrolysis

The temperature of the steam increases from the input of the electrolyser to the output. This corresponds to the worst energy efficiency but best production cost because an exothermal electrolyser investment cost is the lowest of the three possibilities. The exothermal mode is best suited for the geothermal context since the input temperature is only 230 C.

The reaction of steam electrolysis is given by:

$$H_2O \rightarrow H_2 + (½)O_2 \tag{4.49}$$

Anode: $2OH^-_{(aq)} \rightarrow (½)O_2 + H_2O_{(liq)} + 2e^- \tag{4.50}$

Cathede: $H_2O + 2e^- \rightarrow H_{2(g)} + 2OH^-_{(aq)} \tag{4.51}$

Standard thermodynamic parameters such as $\Delta H(T)$, $\Delta G(T)$, and $\Delta S(T)$ are functions of temperature. Therefore, the standard thermodynamic parameters at different temperatures can be calculated according to Kirchhoff's equation, entropy equation and the relation between ΔG and Nernst potential. The entropy equation and the Gibbs function. These equations are given by [125-127].

$$\Delta H = \Delta G + T\Delta S \tag{4.52}$$

$$\Delta H(T) = -H_{H_2O}(T) + H_{H_2}(T) + ½H_{O_2}(T) \tag{4.53}$$

$$\Delta S(T) = -S_{H_2O(liq)}(T) + S_{H_2}(T) + (½)S_{O_2}(T) \tag{4.54}$$

$$\Delta G(T) = -G_{H_2O(liq)} + G_{H_2}(T) + (½)G_{O_2}(T) \tag{4.55}$$

Minimum work for electrolysis is the change in the Gibbs function:

$$W_{\min,el} = \Delta G \tag{4.56}$$

The efficieny of HTE range between 64% to 94% [128]. We take an efficiency of 80% in the following relation

$$\eta = \frac{w_{\min}}{w_{act}} \tag{4.57}$$

and determine the minimum work as $w_{\min} = 97{,}703$ kJ/kg H_2O since from Equations 4.52 to 4.54, actual work equals to 122,129 kJ/kg H_2O.

The advantage of high temperature electrolysis is that some of the energy required comes from heat. This decreases electricity demand. The effect of electrolysis temperature on electricity and heat demand is shown in Fig. 4.2. As the electrolysis temperature increases electricty demand decreases and heat demand increases. As a

result of beter efficiency of high temperature electrolysis total energy demand also decreases.

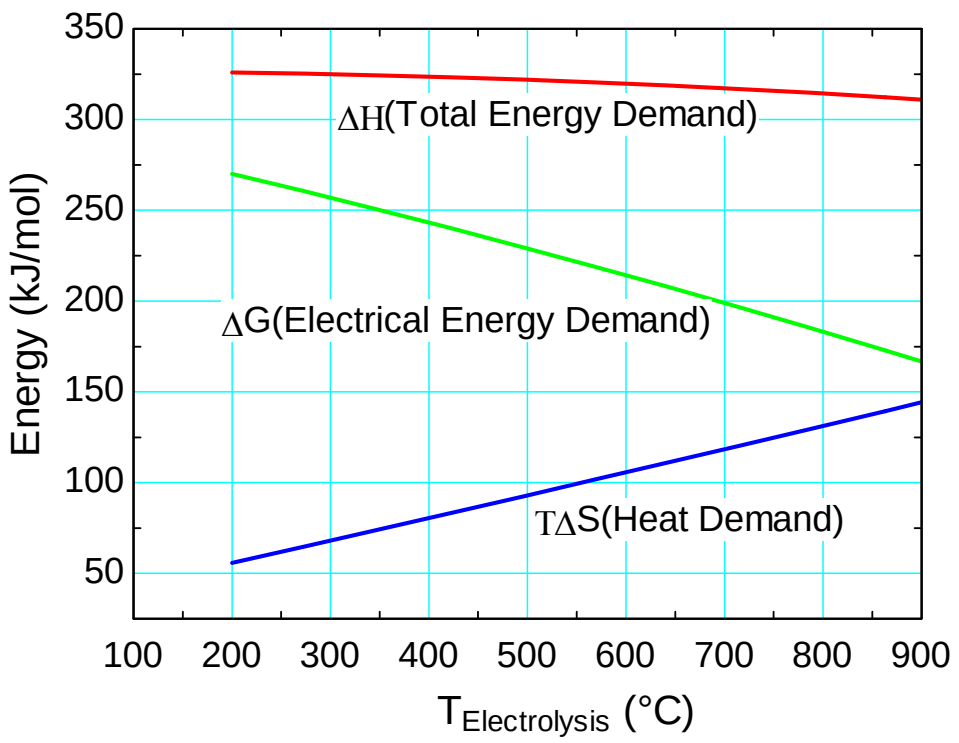

Figure 4.2 Energy demand for high temperature electrolysis.

Fig. 4.3 gives the relationship between hydrogen production cost and electrolysis temperature. At 900 °C, cost of hydrogen per kg is 1.6 €/kg. As the electrolysis temperature increases, cost of hydrogen production decreases. The trend is almost linear.

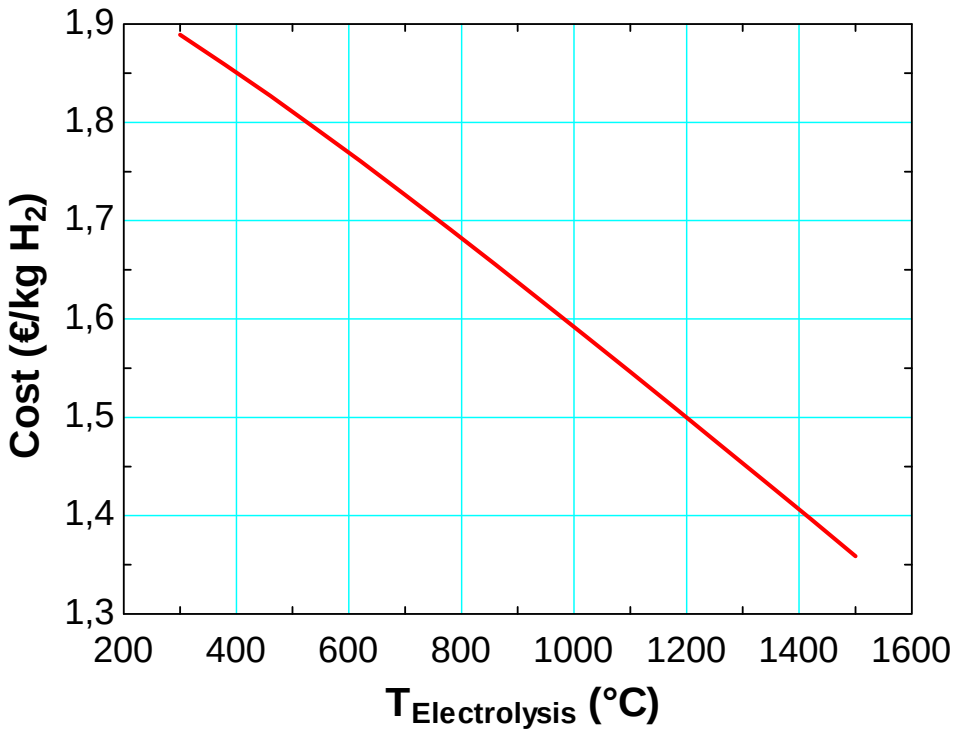

Figure 4.3 Effect of electrolysis temperature on hydrogen production cost.

4.5 Results of Thermodynamic Analysis

The usable temperature of the geothermal source is approximately 230 °C at 15 bar. The temperature, pressure, and mass flow rate data for water, hydrogen and oxygen are given in Table 4.1, Table 4.2 and Table 4.3 according to their state numbers specified in Figure 4.1. The specific physical exergy and energy rates are calculated for each state, as presented in Table 4.1 through Table 4.3. In this study, the reference state is taken to be 25□C for the reference enviroment, 11□C for summer and -1□C for winter at a pressure of 100 kPa. The thermodynamic properties of water, hydrogen and oxygen are obtained using the Engineering Equation Solver (EES) program. Note that state 0 indicates the restricted dead state for the water, hydrogen and oxygen.

The chemical exergy is associated with the departure of the chemical composition of a system from that of the environment. For the simplicity, the chemical exergy considered in the analysis is rather a standard chemical exergy, based on the standard values of the dead state temperature of 25□C and pressure of 100 kPa. Generally, these values are in a good agreement with the calculated chemical exergy, relative to alternative specifications of the environment. In the analyses, the values of

the chemical exergies of the reactants and products for electrolyser are taken from References [125-127].

Using energy and exergy formulations and using state data given in Tables 4.1 through 4.3, calculations are performed. Energetic and exergetic analysis results of the major components of the system are given in Tables 4.4 through Table 4.6 at three different dead state temperatures. The results include heat transfer, work, fuel exergy, product exergy, exergy destruction terms and exergy efficiency.

The results in Tables 4.4 through 4.6 indicate that heat exchangers operate at relatively high exergy efficiencies and that most exergy destructions in the cycle are due to heat exchanger network.

Exergy destructions as a function of second-law efficiency (exergy efficiency) for three dead state temperatures are given in Figures 4.4 through 4.9 for the heat exchangers of the system. It is clear that as the exergy efficiency increases the exergy destruction decreases. As the dead state temperature increases from -1°C to 11°C and 25°C, exergy destructions decrease. This indicates that the system performs better at higher dead state temperatures.

Table 4.4 Energetic and exergetic analyses results for components of the system at 25 °C.

	$\dot{Q}$ (kW)	$\dot{W}$ (kW)	$\dot{E}_F$ (kW)	$\dot{E}_P$ (kW)	$\dot{E}_D$ (kW)	y^* (%)	y (%)	ε (%)
LT-1	5523	0	23320	23092	228	10.55	0.08	92.6
MT-1	5004	0	27416	27325	91	4.21	0.03	97.3
HT-1	4866	0	37995	36743	982	44.46	0.37	73.77
LT-2	1480	0	7025	6911	114	5.27	0.04	85.87
MT-2	2244	0	8726	8428	298	13.79	0.11	82.83
HT-2	1660	0	12436	12295	141	6.52	0.05	89.5
HTSE	0	122,129	147,350	147,044	306	14.16	0.11	-

Table 4.5 Energetic and exergetic analyses results for components of the system at 11 °C.

	$\dot{Q}$ (kW)	$\dot{W}$ (kW)	$\dot{E}_F$ (kW)	$\dot{E}_P$ (kW)	$\dot{E}_D$ (kW)	y^* (%)	y (%)	ε (%)
LT-1	5269	0	23922	23575	347	8.63	0.12	89.13
MT-1	4775	0	28018	27950	68	1.69	0.02	95.3
HT-1	4649	0	38665	37485	1180	29.34	0.43	74.12
LT-2	1477	0	7553	7364	192	4.77	0.07	76.34
MT-2	2242	0	8769	8480	289	7.18	0.10	80.42
HT-2	1664	0	12738	12421	317	7.88	0.11	79.45
HTSE	0	122,129	148,909	147,281	1628	40.48	0.60	-

Table 4.6 Energetic and exergetic analyses results for components of the system at -1 °C.

	$\dot{Q}$ (kW)	$\dot{W}$ (kW)	$\dot{E}_F$ (kW)	$\dot{E}_P$ (kW)	$\dot{E}_D$ (kW)	y^* (%)	y (%)	ε (%)
LT-1	5519	0	25327	25122	205	4.11	0.07	93.77
MT-1	5000	0	28593	28497	96	1.92	0.03	97.27
HT-1	4870	0	40624	39613	1011	20.28	0.36	78.27
LT-2	1477	0	7732	7491	241	4.83	0.08	76.78
MT-2	2242	0	9032	8734	298	5.98	0.10	80.25
HT-2	1664	0	13016	12696	320	6.42	0.11	79.55
HTSE	0	122,129	150,288	147,476	2812	56.24	1.00	-

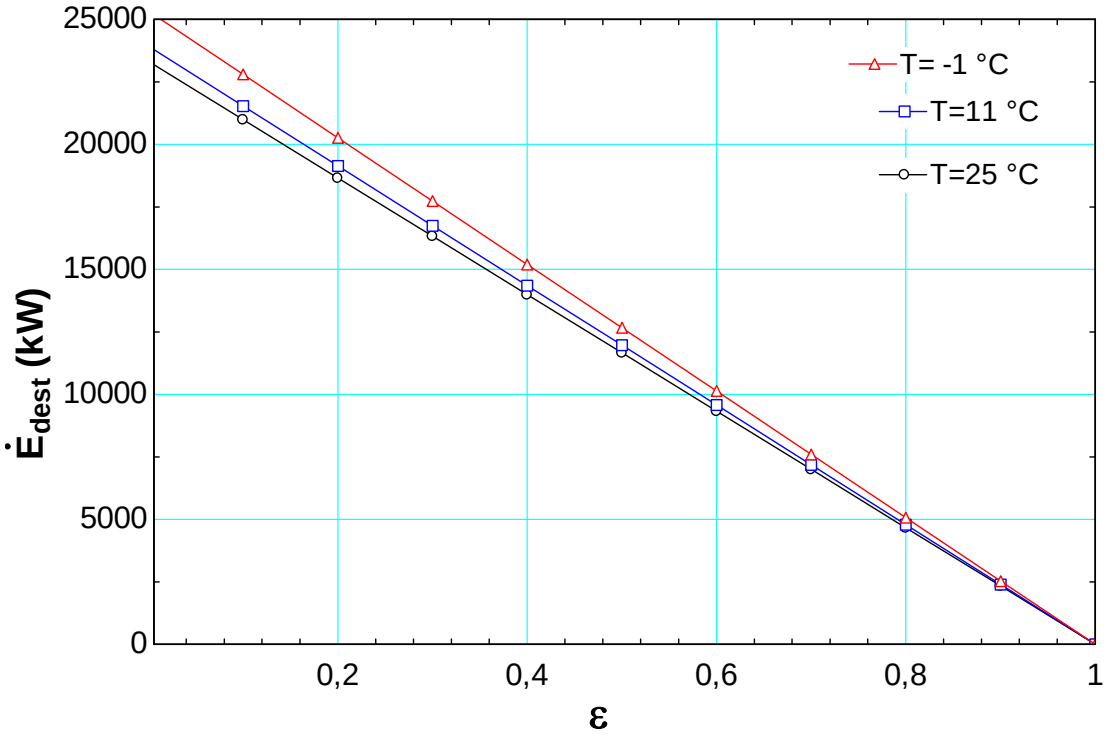

Figure 4.4 Exergy destructions as a function of second-law efficiency for three dead state temperatures in Low Temperature Heat Exchanger 1

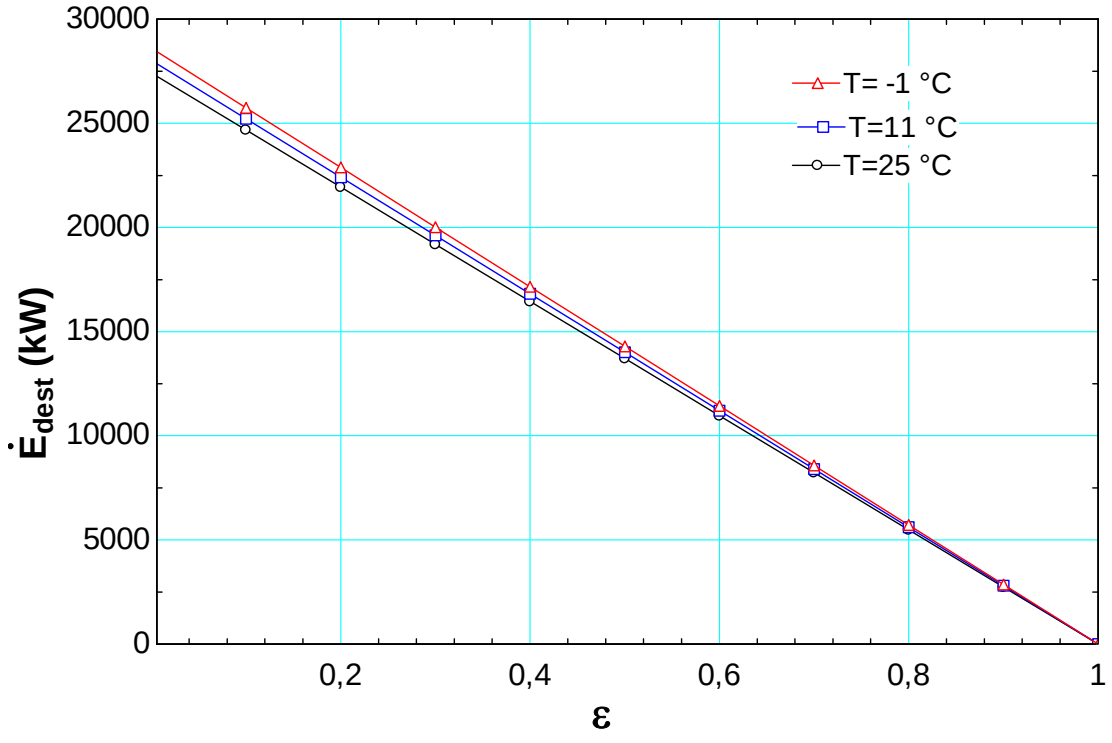

Figure 4.5 Exergy destructions as a function of second-law efficiency for three dead state temperatures in Medium Temperature Heat Exchanger 1

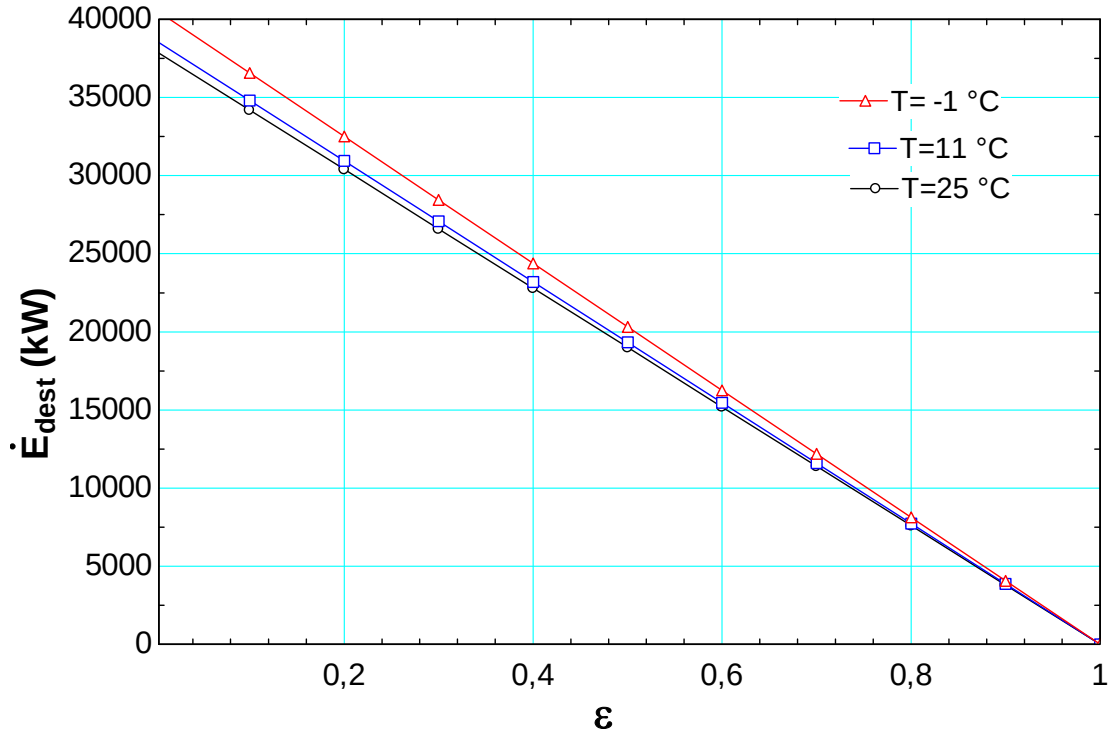

Figure 4.6 Exergy destructions as a function of second-law efficiency for three dead state temperatures in HighTemperature Heat Exchanger 1

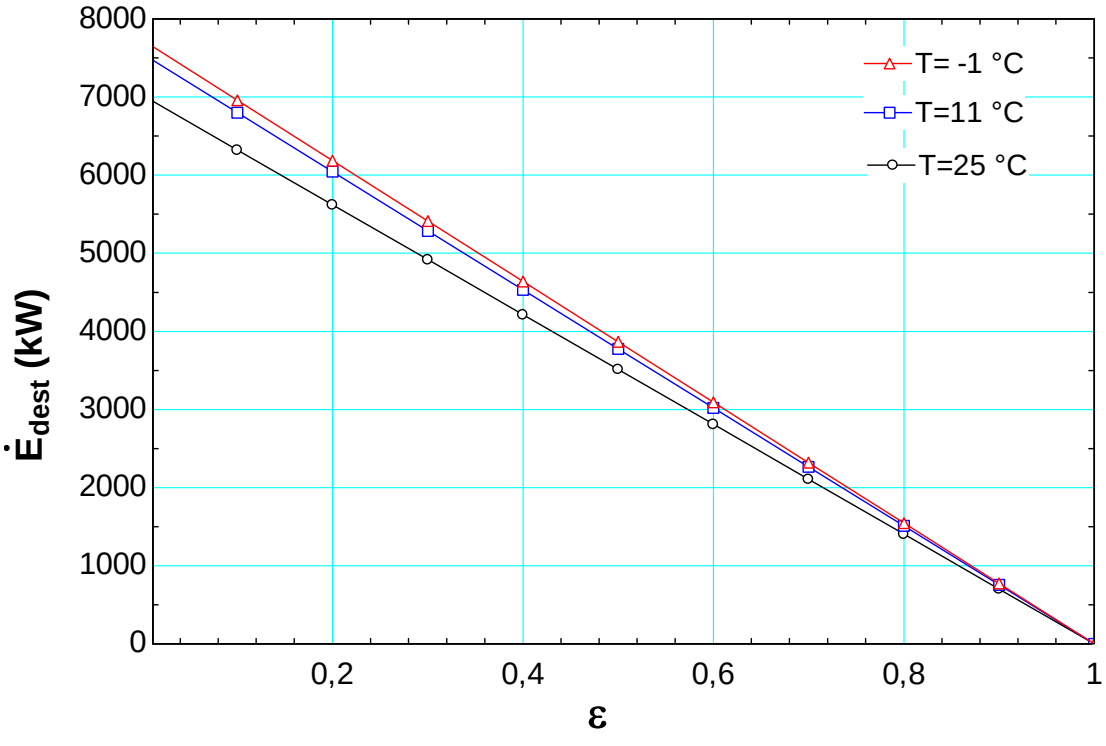

Figure 4.7 Exergy destructions as a function of second-law efficiency for three dead state temperatures in Low Temperature Heat Exchanger 2

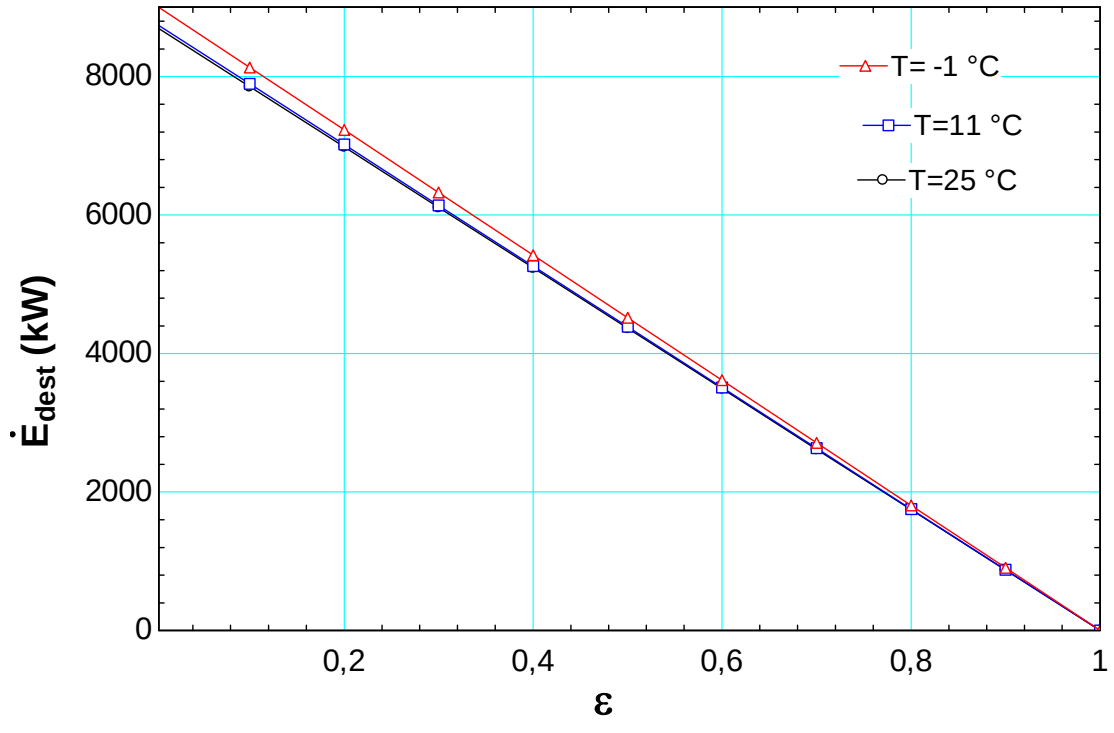

Figure 4.8 Exergy destructions as a function of second-law efficiency for three dead state temperatures in Medium Temperature Heat Exchanger 2

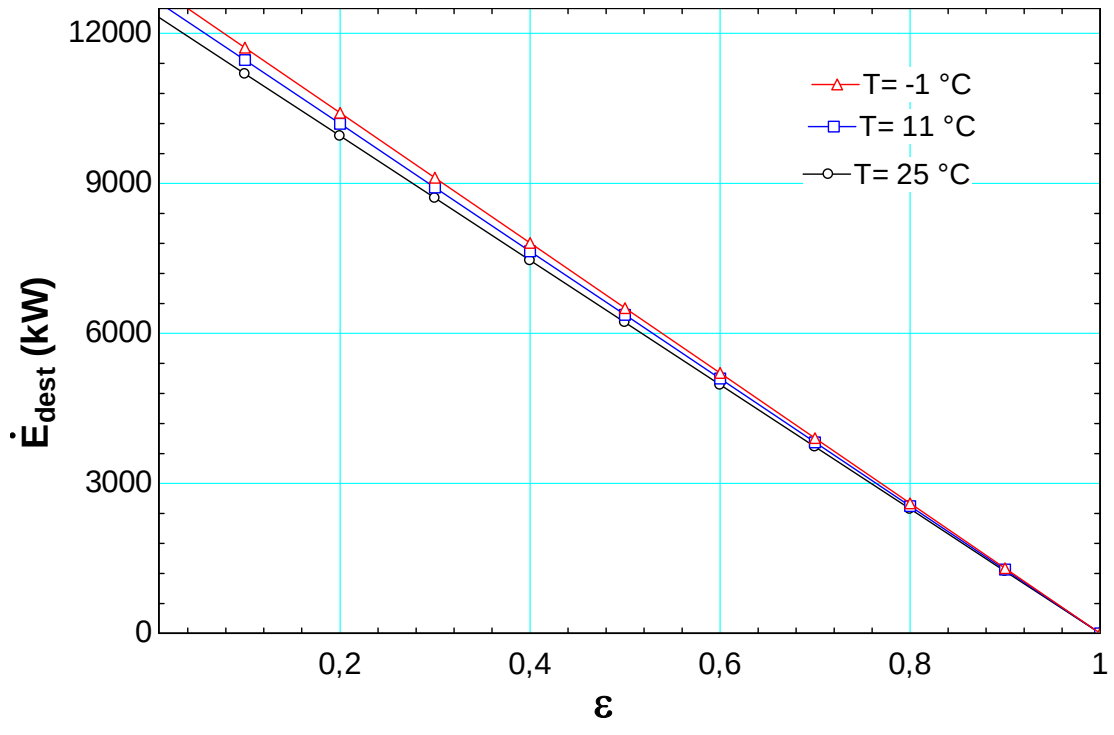

Figure 4.9 Exergy destructions as a function of second-law efficiency for three dead state temperatures in HighTemperature Heat Exchanger 2

4.6 Conclusions

In this chapter, thermodynamic analysis of the system is performed based on the first and second law of thermodynamics. Work and heat interactions, exergy destructions, and exergy efficiencies are determined for the main components of the system. The effect of exergy efficiency on exergy destructions are determined for three different dead state temperatures.

CHAPTER 5

EXERGOECONOMIC ANALYSIS

5.1 Introduction

The design of thermal systems requires the explicit consideration of engineering economics, as cost is always an important consideration. Thermoeconomics (also known as exergoeconomics) is the branch of engineering that combines exergy analysis and economic principles to provide information useful for designing a system and optimizing its operation and cost effectiveness, but not available through conventional energy analysis and economic evaluation. The objectives of thermoeconomic analysis include one or more of the following: (a) to calculate separately the costs of each product generated by a system having more than one product, (b) to understand the cost formation process and the flow of costs in the system, (c) to optimize specific variables in a single component, and (d) to optimize the overall system.

In this study, principles of thermoeconomics, as embodied in the specific exergy cost (SPECO) method, are used to determine changes in the design parameters of the each equipment that result in an improvement of the cost effectiveness of the geothermal assisted high temperature electrolysis system. SPECO method is based on specific exergies and costs per exergy unit, exergy efficiencies, and the auxiliary costing equations for system components. The method consists of the following three steps: (i) identification of exergy streams, (ii) definition of fuel and product for each system component and (iii) allocation of cost equations. For the exergoeconomic analysis, it is helpful to define a fuel and a product for the components of high temperature electrolysis system.

In this chapter, exergoeconomic analysis of geothermal assisted high temperature electrolysis system is conducted using the methodologies described in previous chapters. The results are obtained and discussed.

5.2 Economic Analysis

In order to calculate the cost rates of the plant, the economic data is obtained from Sigurvinsson's study [66]. This work was based on The Jules Verne project which marks the first stage of the collaboration between France and Iceland in 2003. In this work, the HTSE system is supplied as packaged system and cost allocation among its components (i.e. subsystems) is not separately quoted. However, to obtain more accurate results from thermoeconomic analysis, the subsystems are considered as separate and cost allocation of subsystems and the other expenditures are obtained by using economic relations given in Chapter 3.

The economic life of HTSE system is considered as 40 years that is from middle of 2005 to middle of 2045. The average capacity factor for the system is considered as 80% which means that the HTSE system will operate at full load 7008 hours of the total available 8760 hours per year. The cost accounting of the HTSE system is developed for the mass flowrate of 1.0 kg/s H_2 production, which means that the system's total annual H_2 production capacity is 34,800 tones. Electricity and steam costs are taken as 0.014 €/kWh and 2.73 €/kWh according to the Sigurvinsson's study [123]. Heat exchanger prices are varied according to their purpose and size in the HTSE system as follows: 400 €/m^2 for low temperature heat exchangers for the total surface area of 504 m^2, 800 €/m^2 for medium temperature heat exchangers for the total surface area of 995 m^2, and 4000 €/m^2 for high temperature heat exchangers for the total surface area of 189 m^2. In Table 5.1, the total capital investment and expenditures of geothermal assisted HTSE system is given with the corresponding economic data [66].

The average levelized hydrogen production cost per kg H_2 (HGC) is the average cost of producing hydrogen for the specific case developed for this study. The following equation can be utilized to calculate the levelized hydrogen production

$$HGC = \sum_t [(I_t + M_t + C_t)(1+r)^{-t} / \sum_t [H_t (1+r)^{-t}] \quad (5.1)$$

where *HGC* is the average lifetime levelized hydrogen generation cost per kg H_2, I_t is the capital expenditures, M_t is the operation and maintenance expenditures, C_t is the consumable expenditures, H_t is the hydrogen generation in the year *t* in kg, and *r* is the discount rate. Table 5.2 lists the results of the average levelized hydrogen generation cost for the mass flowrate of 1.0 kg/s H_2. The cost accounting of the HTSE system is calculated using a discount rate of 10% [66].

Table 5.1 The total capital investment and expenditures of geothermal assisted HTSE for the mass flowrate of 1.0 kg/s H_2 production

Fixed Capital Investment (FCI)	**Units**	**Unit Cost ($M)**	**Total Cost ($M)**
HTSE as packaged system	1	108.519	108.519
Freight and installation (5% of equipment)	---	5.426	5.426
Simple buildings	835 m^2	0.0012	0.983
Buildings for equipments	570 m^2	0.0015	0.839
Office buildings	300 m^2	0.0018	0.53
The total FCI			**116.297**
Variable and Operation & Maintenance Costs (VOMC)			
Maintenance and spare parts (2% of equipment)	---	2.17	2.17
Electrolysis equipment overhaul	23	0.3073	7.055
Contingency	---	0.092	0.092
The total VOMC			**9.317**
Offsite Costs			
Insurance of buildings	---	0.006	0.006
Insurance of equipment	---	0.358	0.358
Other duties	---	0.079	0.079
Wages of operators	10 persons	0.057	0.570
Wages of maintenance	2 persons	0.042	0.084
Contingency	---	0.033	0.033
The total offsite costs			**0.762**
The total annual cost			**10.079**
TOTAL INVESTMENT COST			**126.326**

It should also be kept in mind that the levelized costs are not directly comparable to actual costs at any given year of plant operation. In a conventional economic analysis of any production system, one may need to know the selling prices of all but one product in order to calculate the cost associated with this product. In other words, a conventional economic analysis does not provide criteria for apportioning the carrying charges, electricity and water costs, and O&M expenses to the various products generated in the same system.

Table 5.2 The average levelized hydrogen generation cost for the mass flowrate of 1.0 kg/s H_2

Levelized Costs	**Maintenance**	**Electricity**	**Capital**	**Total Cost**
Total cost (M€)	89.400	292.655	113.945	496.001
Cost per kg H_2 (€/kg)	0.287	0.941	0.366	1.595
Percentage (%)	18.0	59.0	23.0	100

HTSE systems with a higher production capacity than the mass flow rate of 1.0 kg/s H_2 will produce a lesser amount of production cost. By doubling the hydrogen production to 2.0 kg/s H_2, the relation forecasts a production cost of 1.56 €/kg H_2, and by doubling again to 4.0 kg/s the result will be 1.52 €/kg H_2. In Table 5.3, the results of the sensibility study are given. The results are calculated by changing each factor by ± 25% and calculating the effect on total production price [66].

Table 5.3 Sensibility of different factors to price

	- 25%	0%	25%
Discount rate	1.54	1.6	1.67
Maintenance cost	1.53	1.6	1.68
Electricity cost	1.36	1.6	1.84
Capital cost	1.53	1.6	1.68

5.3 Exergoeconomic Analysis

Thermoeconomics assess the cost of consumed resources, money and system irreversibilities in terms of the overall production process. It helps to point out how resources are used more effectively in order to save them. Monetary costs express the economic effect of inefficiencies and are used to improve the cost effectiveness of production processes. Assessing the cost of the flow streams and processes in a plant helps to understand the process of cost formation, from the input resources to final products [129].

In this study, specific exergy costing (SPECO) method is used to obtain and understand the cost formation structure of the HTSE system presented. Exergetic cost rates balances and corresponding auxiliary equations of the system are given in Chapter 3. The cost rates associated with first capital investment and O&M costs for the subcomponents of the HTSE system are given in Table 5.4. Since the level at which the cost balances are formulated (i.e. aggregation level) affects the results of the thermoeconomic analysis, the lowest possible aggregation level is set. Exergetic cost rate balances and corresponding auxiliary equations for each subsystem of geothermal assisted HTSE system is obtained by SPECO method and are given in the following equations (Eqs. 5.2 through 5.23) referred to the streams given in Fig 4.1. Solving the linear system consisting of related thermoeconomic equations given in these equations, we can obtain the cost flow rates and the unit exergetic costs associated with each stream of the HTSE system. These results are given in Tables 5.5, 5.6 and 5.7 for three environment (dead state) temperatures: standart environment temperature (25°C), summer temperature (11°C) and winter temperature (-1°C), respectively.

Low Temperature Heat Exchanger 1 (LT-1)

$$\dot{C}_1 - \dot{C}_2 + \dot{Z}_{LT-1} = \dot{C}_{15} - \dot{C}_{14} + \dot{C}_{15'} - \dot{C}_{14'} \tag{5.2}$$

$$\frac{\dot{C}_1 - \dot{C}_2}{E_1 - E_2} = \frac{\dot{C}_{15} - \dot{C}_{14}}{E_{15} - E_{14}} \tag{5.3}$$

$$\frac{\dot{C}_1 - \dot{C}_2}{E_1 - E_2} = \frac{\dot{C}_{15'} - \dot{C}_{14'}}{E_{15'} - E_{14'}} \tag{5.4}$$

$$c_{15'} = 0 \tag{5.5}$$

Medium Temperature Heat Exchanger 1 (MT-1)

$$\dot{C}_2 - \dot{C}_3 + \dot{Z}_{MT-1} = \dot{C}_{13} - \dot{C}_{12} + \dot{C}_{13'} - \dot{C}_{12'} \tag{5.6}$$

$$\frac{\dot{C}_2 - \dot{C}_3}{E_2 - E_3} = \frac{\dot{C}_{13} - \dot{C}_{12}}{E_{13} - E_{12}} \tag{5.7}$$

$$\frac{\dot{C}_1 - \dot{C}_2}{E_1 - E_2} = \frac{\dot{C}_{13'} - \dot{C}_{12'}}{E_{13'} - E_{12'}} \tag{5.8}$$

$$c_{13} = c_{14} \quad \text{and} \quad c_{13'} = c_{14'} \tag{5.9}$$

High Temperature Heat Exchanger 1 (HT-1)

$$\dot{C}_3 - \dot{C}_4 + \dot{Z}_{HT-1} = \dot{C}_{11} - \dot{C}_{10} + \dot{C}_{11'} - \dot{C}_{10'} \tag{5.10}$$

$$\frac{\dot{C}_3 - \dot{C}_4}{E_3 - E_4} = \frac{\dot{C}_{11} - \dot{C}_{10}}{E_{11} - E_{10}} \tag{5.11}$$

$$\frac{\dot{C}_3 - \dot{C}_4}{E_3 - E_4} = \frac{\dot{C}_{11'} - \dot{C}_{10'}}{E_{11'} - E_{10'}} \tag{5.12}$$

$$c_{11} = c_{12} \text{ and } c_{11'} = c_{12'} \tag{5.13}$$

Low Temperature Heat Exchanger 2 (LT-2)

$$\dot{C}_5 - \dot{C}_6 + \dot{Z}_{LT-2} = \dot{C}_{21} - \dot{C}_{20} \tag{5.14}$$

$$\frac{\dot{C}_5 - \dot{C}_6}{E_5 - E_6} = \frac{\dot{C}_{21} - \dot{C}_{20}}{E_{21} - E_{20}} \tag{5.15}$$

$$c_{21} = 0 \tag{5.16}$$

Medium Temperature Heat Exchanger 2 (MT-2)

$$\dot{C}_6 - \dot{C}_7 + \dot{Z}_{MT-2} = \dot{C}_{19} - \dot{C}_{18} \tag{5.17}$$

$$\frac{\dot{C}_6 - \dot{C}_7}{E_6 - E_7} = \frac{\dot{C}_{19} - \dot{C}_{18}}{E_{19} - E_{18}} \tag{5.18}$$

$$c_{19} = c_{20} \tag{5.19}$$

High Temperature Heat Exchanger 2 (HT-2)

$$\dot{C}_7 - \dot{C}_8 + \dot{Z}_{HT-2} = \dot{C}_{17} - \dot{C}_{16} \tag{5.20}$$

$$\frac{\dot{C}_7 - \dot{C}_8}{E_7 - E_8} = \frac{\dot{C}_{17} - \dot{C}_{16}}{E_{17} - E_{16}} \tag{5.21}$$

$$c_{18} = c_{17} \tag{5.22}$$

High Temperature Electrolysis (HTE)

$$\dot{C}_4 + \dot{C}_8 + \dot{C}_{W_{HTE}} + \dot{Z}_{HTE} = \dot{C}_{10} + \dot{C}_{10'} + \dot{C}_{16} \tag{5.23}$$

Table 5.4 The cost rates associated with first capital investment and O&M costs for the subcomponents of the HTSE system.

Component	Z_k^{CL} (€/h)	Z_k^{OM} (€/h)	Z_k^{T} (€/h)
LT-1	6.79	0.48	7.27
MT-1	90.64	0.47	91.11
HT-1	257.42	0.46	257.88
LT-2	3.02	0.12	3.14
MT-2	22.94	0.21	23.15
HT-2	39.95	0.16	40.11
HTE	1.45	0.14	1.59
Total Cost	422.21	2.04	424.25

Table 5.5 The exergy flow rates, cost flow rates and the unit exergy costs associated with each stream of HTSE system at 25 ºC.State numbers refer to Table 4.1.

State No	$\dot{E}(kW)$	$\dot{C}(€/h)$	C(€/kWh)
1	9035	24,666	2.73
2	11,886	24,575	2.068
3	15,163	24,580	1.621
4	18,685	23,658	1.266
5	3158	8621	2.73
6	3894	8644	2.22
7	5332	8533	1.6
8	6535	8179	1.25
9	-	-	-
10	13,144	9370	0.7129
11	10,527	10,054	0.9551
12	8548	8164	0.9551
13	6536	8255	1.263
14	8074	10,200	1.263
15	6408	10,253	1.6
10’	9688	448.4	0.0462
11’	7801	45.25	0.0058
12’	6982	40.52	0.0058
13’	5626	40.51	0.0072
14’	6211	45.05	0.0072
15’	4798	0	0
16	7104	250	0.0352
17	5760	142.3	0.0247
18	4832	119.7	0.0247
19	3096	15.17	0.0049
20	3864	19.08	0.0049
21	3132	0	0
$\dot{C}_{W_{HTE}}$	122,129	21,770	0.178

Table 5.6 The exergy flow rates, cost flow rates and the unit exergy costs associated with each stream of HTSE system at 11 ºC. State numbers refer to Table 4.2.

State No	$\dot{E}(kW)$	$\dot{C}(€/h)$	C(€/kWh)
1	9471	25,856	2.73
2	12,317	25,796	2.094
3	15,517	25,292	1.662
4	18,943	25,041	1.322
5	3469	9470	2.73
6	4237	9460	2.233
7	5713	9579	1.677
8	6939	9426	1.358
9	-	-	-
10	12,997	9181	0.7064
11	10,308	9769	0.9477
12	8243	7812	0.9477
13	6363	7903	1.242
14	7830	9729	1.242
15	6103	9765	1.6
10’	10,151	388.5	0.0382
11’	8234	30.47	0.0037
12’	7458	27.94	0.0037
13’	6070	27.92	0.0046
14’	6621	30.71	0.0046
15’	5155	0	0
16	7025	67.51	0.0096
17	5482	127.7	0.0233
18	4532	105.8	0.0233
19	3345	10.7	0.0032
20	4084	13.27	0.0032
21	3078	0	0
$\dot{C}_{W_{HTE}}$	122,129	24,832	0.203

Table 5.7 The exergy flow rates, cost flow rates and the unit exergy costs associated with each stream of HTSE system at -1 ºC. State numbers refer to Table 4.3.

State No	$\dot{E}(kW)$	$\dot{C}(€/h)$	C(€/kWh)
1	10,711	29,241	2.73
2	13,798	29,132	2.11
3	17,220	29,114	1.691
4	20,863	28,190	1.351
5	3746	10,227	2.73
6	4543	10,214	2.248
7	6052	10,330	1.707
8	7297	10,175	1.394
9	-	-	-
10	12,841	8425	0.6561
11	10,133	9116	0.8996
12	8328	7492	0.8996
13	6226	7583	1.218
14	7632	9298	1.218
15	5851	9362	1.6
10’	10,563	443	0.0419
11’	8617	53.43	0.0062
12’	7883	49.16	0.0062
13’	6467	49.15	0.0076
14’	6984	53.19	0.0076
15’	5473	0	0
16	6964	68.21	0.0097
17	5399	127.95	0.0273
18	4489	106.5	0.0273
19	3278	12.46	0.0038
20	3986	15.35	0.0038
21	2948	0	0
$\dot{C}_{W_{HTE}}$	122,129	29,431	0.24

The exergetic cost parameters of the plant components for three environment temperatures (25 ºC, 11 ºC and -1 ºC) are given in Tables 5.8, 5.9, and 5.10. These parameters indicate the performance of system components on a rational exergetic cost basis.

Table 5.8 The unit exergetic costs of fuels and products, relative exergetic cost difference, exergoeconomic factor, cost rate of exergy destruction, and total investment cost rate for the plant components at 25°C.

Componen	$c_{f,k}$ (€/kWh	$c_{p,k}$ (€/kWh	r (%)	f (%)	$\dot{D}_D$ (€/h	$\dot{Z}^T$ (€/h	ε
LT-1	1.2702	2.068	8.01	2.44	289.605	7.27	92.6
MT-1	0.9609	1.621	3.12	51.0	87.442	91.11	97.3
HT-1	0.7591	1.266	36.4	25.7	745.436	257.88	73.7
LT-2	0.0049	2.22	25.7	84.8	0.558	3.14	85.8
MT-2	0.0247	1.6	31.4	75.8	7.380	23.15	82.8
HT-2	0.0352	1.252	20.9	88.9	4.963	40.11	89.5
HTE	2.518	0.7942	68.4	0.2	770.508	1.59	-

Table 5.9 The unit exergetic costs of fuels and products, relative exergetic cost difference, exergoeconomic factor, cost rate of exergy destruction, and total investment cost rate for the plant components at 11 °C.

Componen	$c_{f,k}$ (€/kWh	$c_{p,k}$ (€/kWh	r (%)	f (%)	$\dot{D}_D$ (€/h	$\dot{Z}^T$ (€/h	ε
LT-1	1.246	2.094	12.2	1.65	432.362	7.27	89.1
MT-1	0.9514	1.662	5.27	58.4	64.695	91.11	95.3
HT-1	0.7446	1.322	35.8	22.6	878.628	257.88	74.1
LT-2	0.0032	2.233	44.3	83.6	0.614	3.14	76.3
MT-2	0.0233	1.677	36.0	77.4	6.733	23.15	80.4
HT-2	0.0096	1.358	59.5	92.9	3.043	40.11	79.4
HTE	2.68	0.7542	71.8	0.03	4363	1.59	-

Table 5.10 The unit exergetic costs of fuels and products, relative exergetic cost difference, exergoeconomic factor, cost rate of exergy destruction, and total investment cost rate for the plant components at -1°C.

Componen	$c_{f,k}$ (€/kWh	$c_{p,k}$ (€/kWh	r (%)	f (%)	$\dot{D}_D$ (€/h	$\dot{Z}^T$ (€/h	ε
LT-1	1.2256	2.11	6.66	2.81	251.248	7.27	93.7
MT-1	0.9058	1.691	3.15	51.1	86.95	91.11	97.2
HT-1	0.698	1.351	28.6	26.7	705.678	257.88	78.2
LT-2	0.0038	2.248	41.2	77.4	0.915	3.14	76.7
MT-2	0.0237	1.707	35.7	76.6	7.062	23.15	80.2
HT-2	0.0097	1.394	57.9	92.8	3.104	40.11	79.5
HTE	2.745	0.707	74.2	0.02	7719	1.59	-

We note the followings from the exergoeconomic results of this HTSE system as listed in Tables 5.8, 5.9 and 5.10:

• The steam input of the system is 1 kg/s at 230 °C and 1500 kPa. The exergetic cost rate of the steam entering the system are 8621 €/h, 9470 €/h, 10,227 €/h for state 5 and 24,666 €/h, 25,856 €/h, 29,241 €/h for state 1 at 25 °C, 11 °C and -1 °C respectively. The specific unit exergetic cost of steam is 2.73 €/kWh for each reference temperature.

• The capital investment cost, the operating and maintenance costs and the total cost of the HTSE system are found to be 422.21 €/kWh, 2.04 €/kWh and 424.25 €/kWh. We assume that the operating and maintenance costs are the same value for 25 °C, 11 °C and -1 °C reference temperatures.

• The net electrical power input of the system is 122,129 kW. The exergetic cost rate of the power input to the system is 21,770 €/h and the specific unit exergetic cost of the power input to the system is 0.17 €/kWh at 25 °C. The exergetic cost rate of the power input to the system is 24,832 €/h and the specific unit exergetic cost of the power input to the system is 0.20 €/kWh at 11 °C. The exergetic cost rate of the power input to the system is 29,430 €/h and the specific unit exergetic cost of the power input to the system is 0.24 €/kWh at -1 °C. As the reference temperature of the system increase, the exergetic cost rate of the power input to the system and the specific unit exergetic cost of the power input to the system decrease.

• Exergoeconomic factors for high temperature heat exchanger 2 is 92.94% at 11 °C. It is the highest exergoeconomic factor and has the lowest cost rate of exergy destruction among three reference temperatures.

• Exergoeconomic factors for high temperature electrolysis is 0.02% at -1 °C. It is the lowest exergoeconomic factor value and has the highest cost rate of exergy destruction among three reference temperatures.

• The relative cost difference for medium temperature heat exchanger 1 is 3.12% at 25 °C. It is lowest relative cost difference value. This is because of low investment, operation and maintance costs and high cost of effectiveness.

• The relative cost difference for medium temperature heat exchanger 1 is 59.50% at 11°C. It is highest relative cost difference value and it depends on high cost of effectiveness.

Cost rate of exergy destructions as a function of second-law efficiency (exergy efficiency) for three dead state temperatures are given in Figures 5.1 through 5.6 for the heat exchangers of the system. It is clear that as the exergy efficiency increases the cost rate of exergy destruction decreases. As the dead state temperature increases from -1°C to 11°C and 25°C, cost rate of exergy destructions decrease. This indicates that the system performs better at higher dead state temperatures.

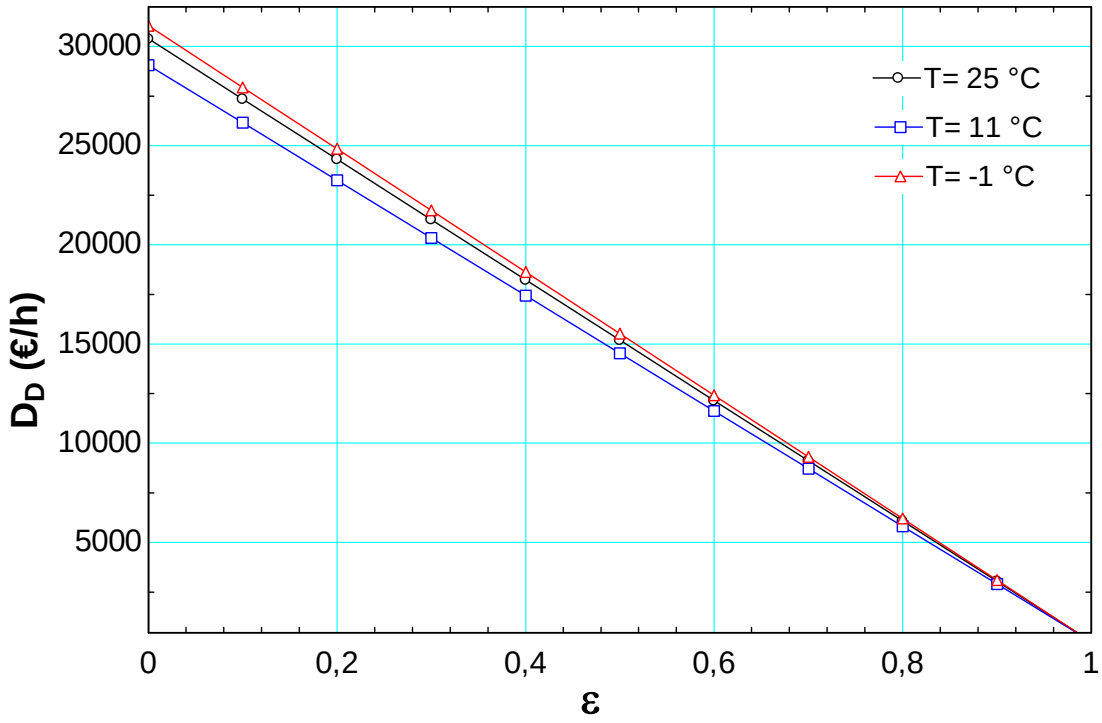

Figure 5.1 Cost rate of exergy destructions as a function of second-law efficiency for three dead state temperatures in Low Temperature Heat Exchanger 1

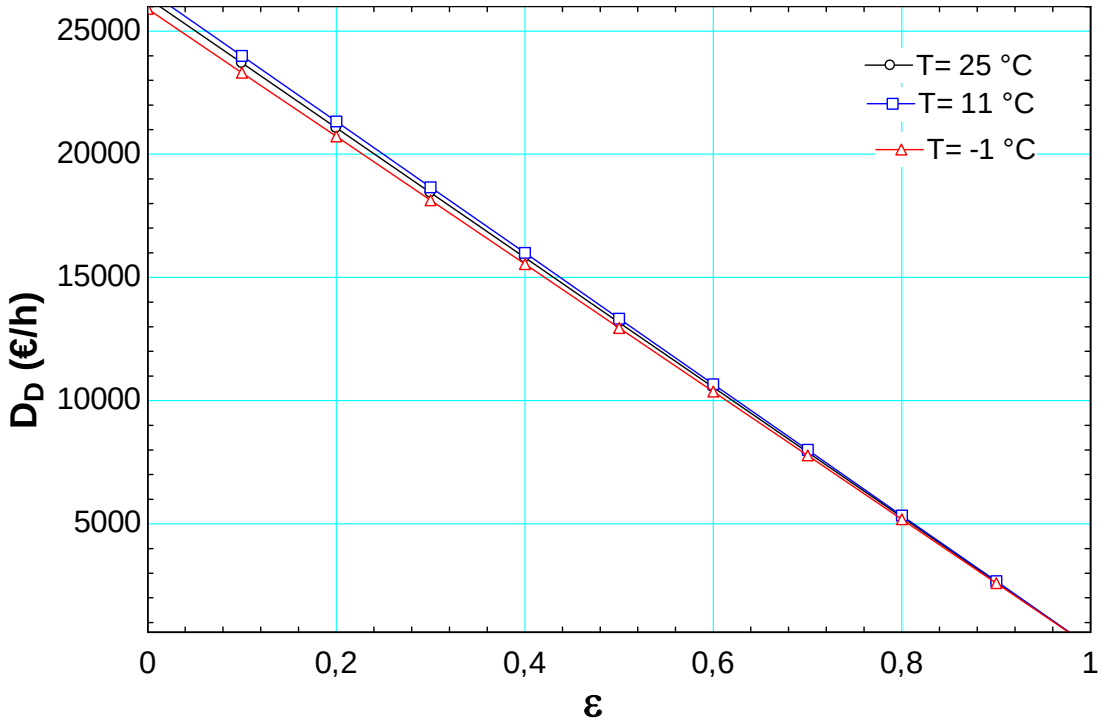

Figure 5.2 Cost rate of exergy destructions as a function of second-law efficiency for three dead state temperatures in Medium Temperature Heat Exchanger1

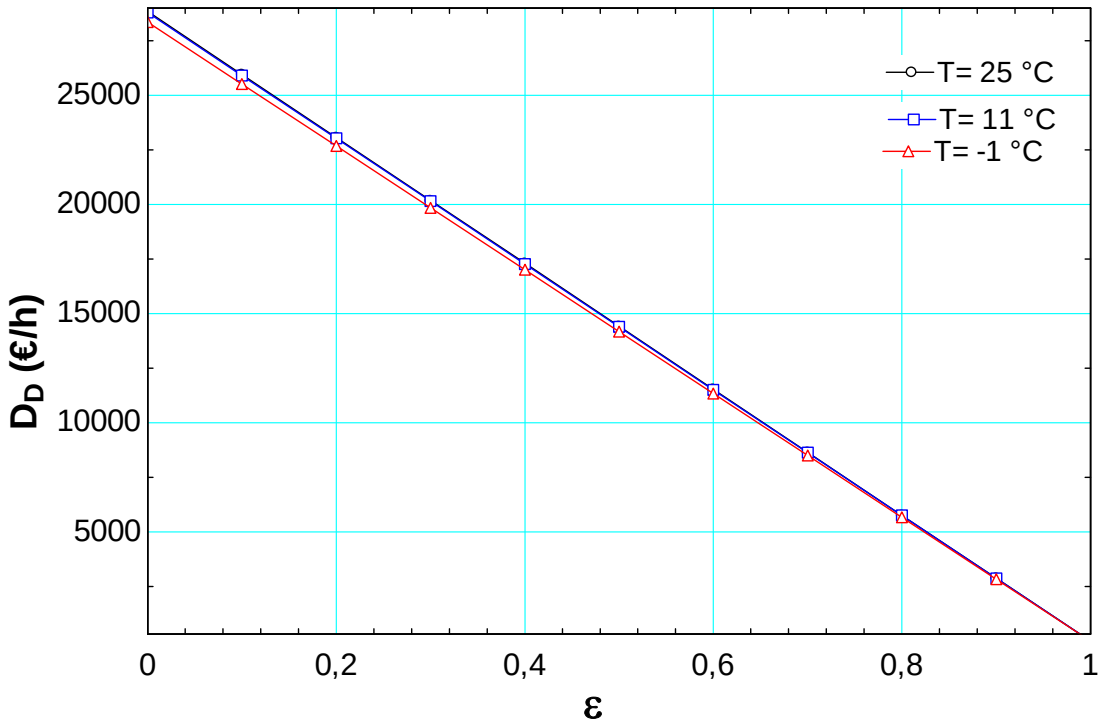

Figure 5.3 Cost rate of exergy destructions as a function of second-law efficiency for three dead state temperatures in High Temperature Heat Exchanger 1

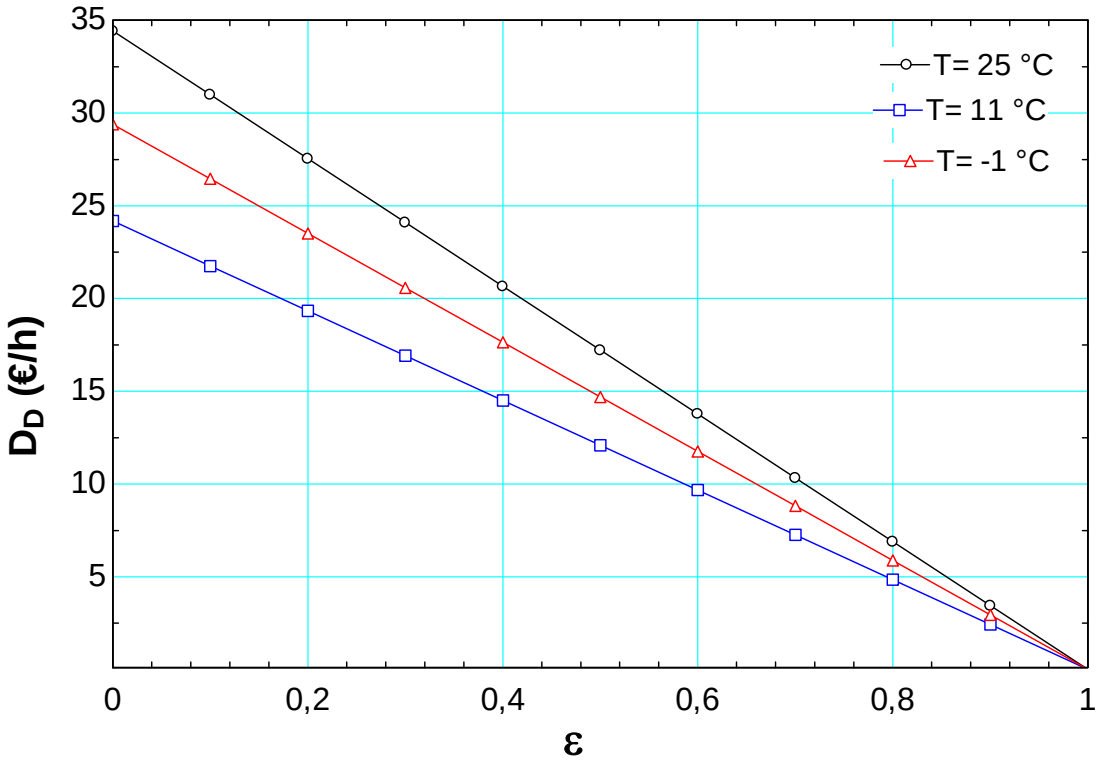

Figure 5.4 Cost rate of exergy destructions as a function of second-law efficiency for three dead state temperatures in Low Temperature Heat Exchanger 2

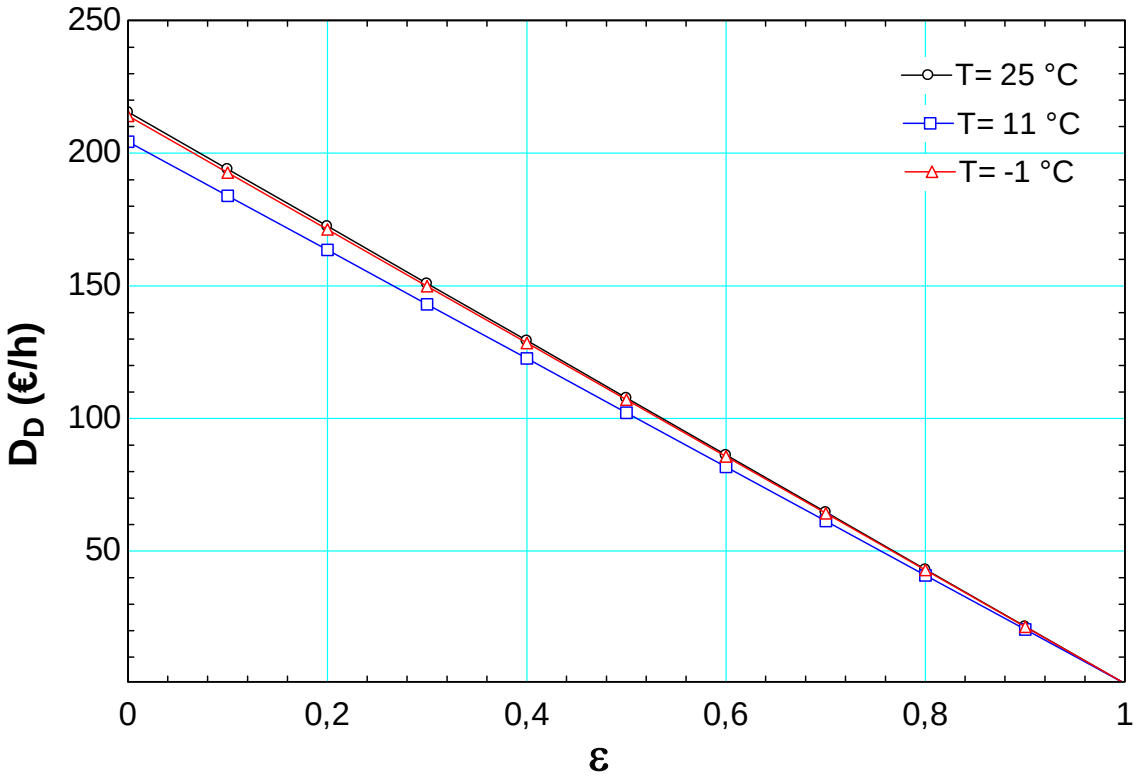

Figure 5.5 Cost rate of exergy destructions as a function of second-law efficiency for three dead state temperatures in Medium Temperature Heat Exchanger 2

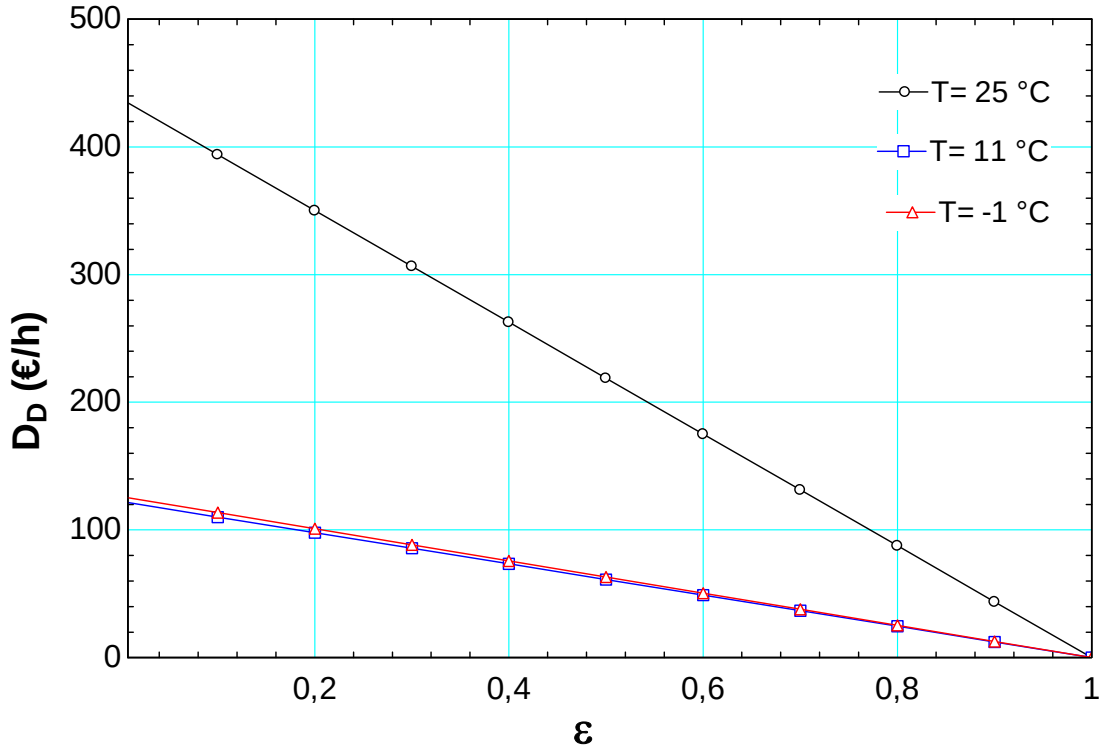

Figure 5.6 Cost rate of exergy destructions as a function of second-law efficiency for three dead state temperatures in High Temperature Heat Exchanger 2

Cost rate of exergy as a function of second-law efficiency (exergy efficiency) for three dead state temperatures are given in Figures 5.7 through 5.12 for the heat exchangers of the system. It is clear that as the exergy efficiency increases the cost rate of exergy increases. As the dead state temperature increases from -1°C to 11°C and 25°C, cost rate of exergy destructions decrease. This indicates that the system performs better at higher dead state temperatures.

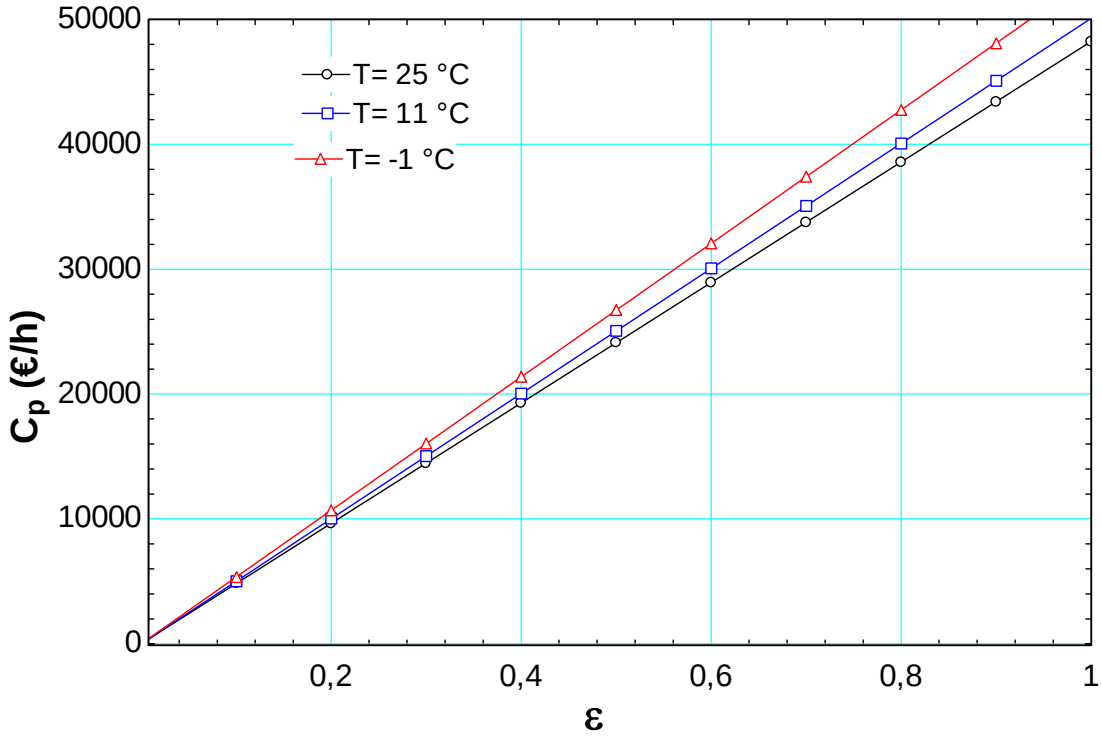

Figure 5.7 Cost rate of exergy as a function of second-law efficiency for three dead state temperatures in Low Temperature Heat Exchanger 1

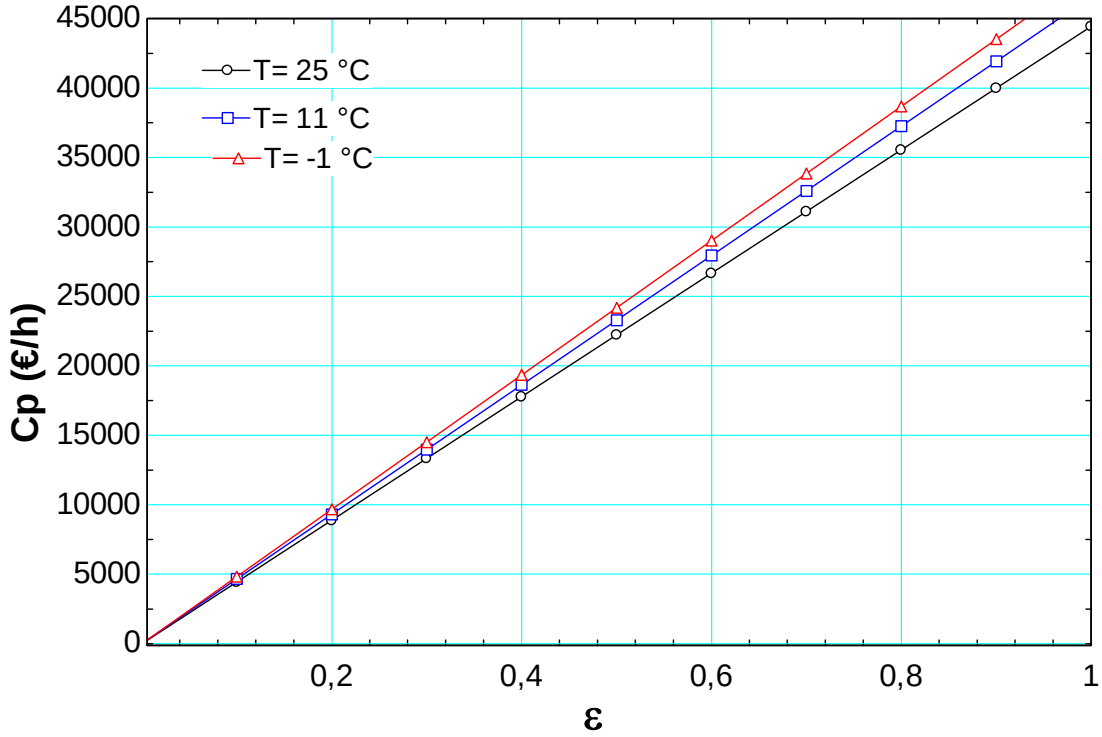

Figure 5.8 Cost rate of exergy as a function of second-law efficiency for three dead state temperatures in Medium Temperature Heat Exchanger 1

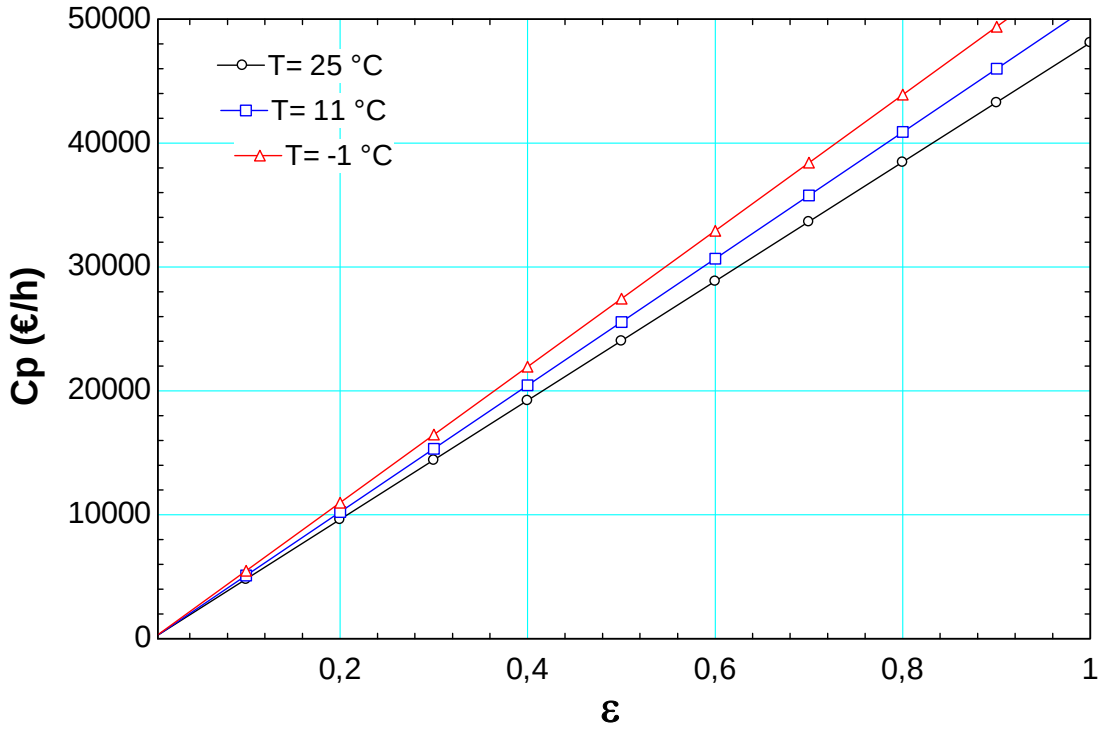

Figure 5.9 Cost rate of exergy as a function of second-law efficiency for three dead state temperatures in High Temperature Heat Exchanger 1

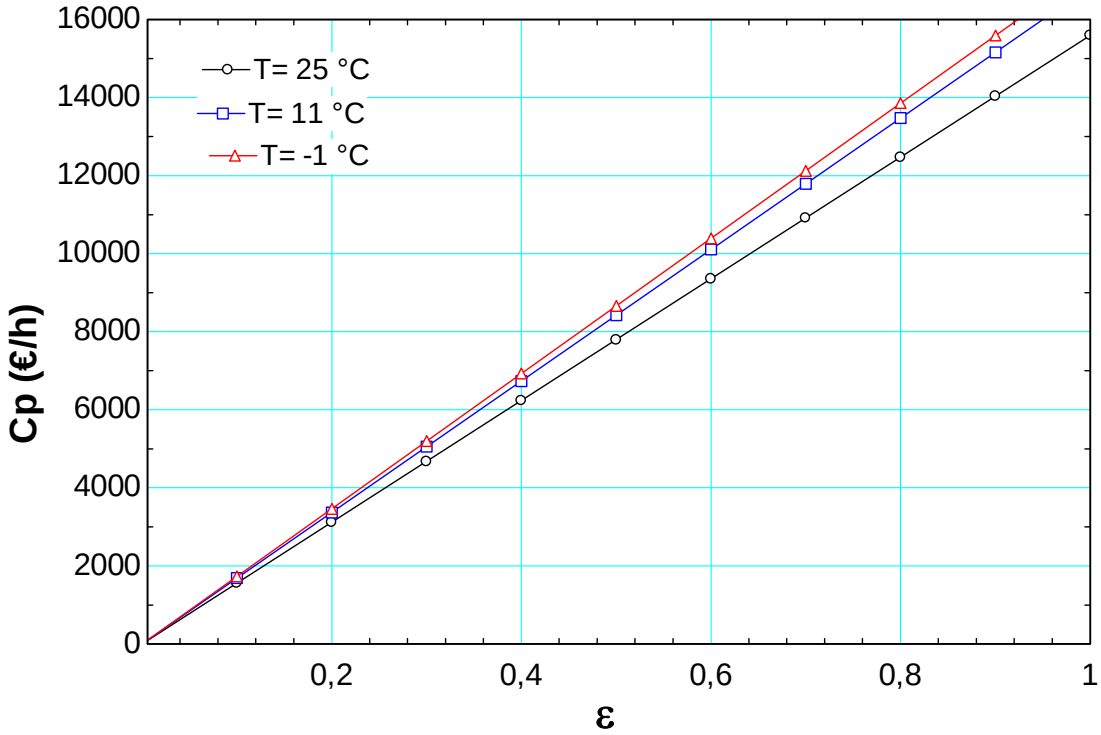

Figure 5.10 Cost rate of exergy as a function of second-law efficiency for three dead state temperatures in Low Temperature Heat Exchanger 2

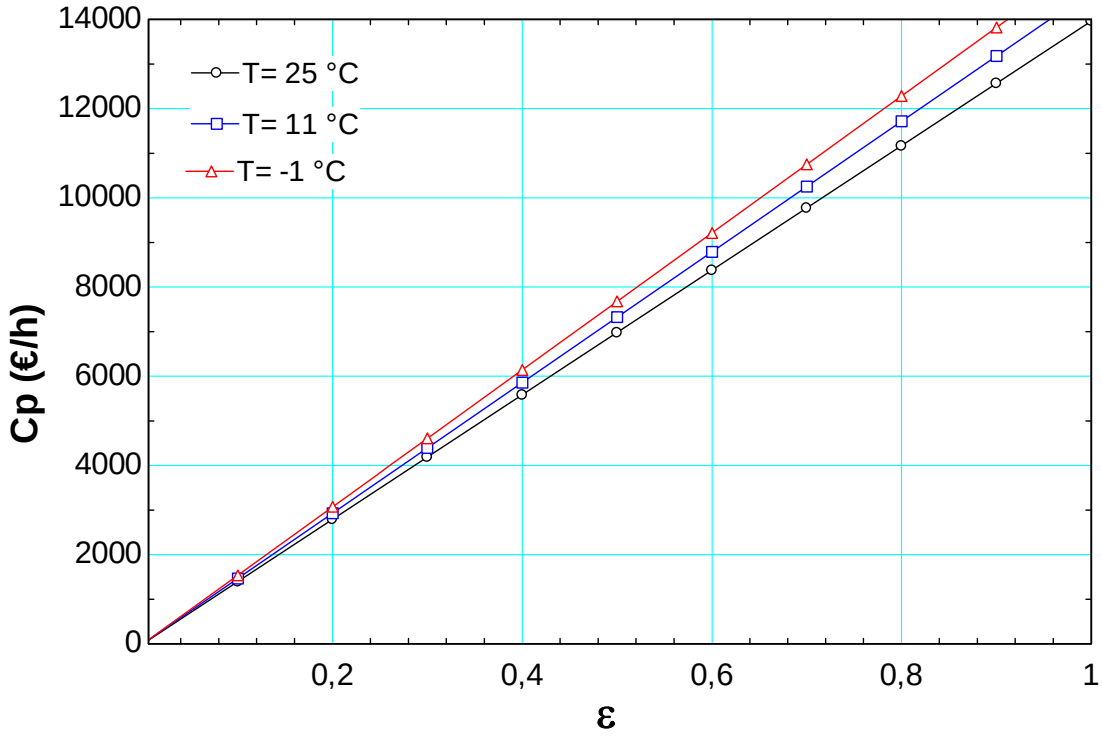

Figure 5.11 Cost rate of exergy as a function of second-law efficiency for three dead state temperatures in Medium Temperature Heat Exchanger 2

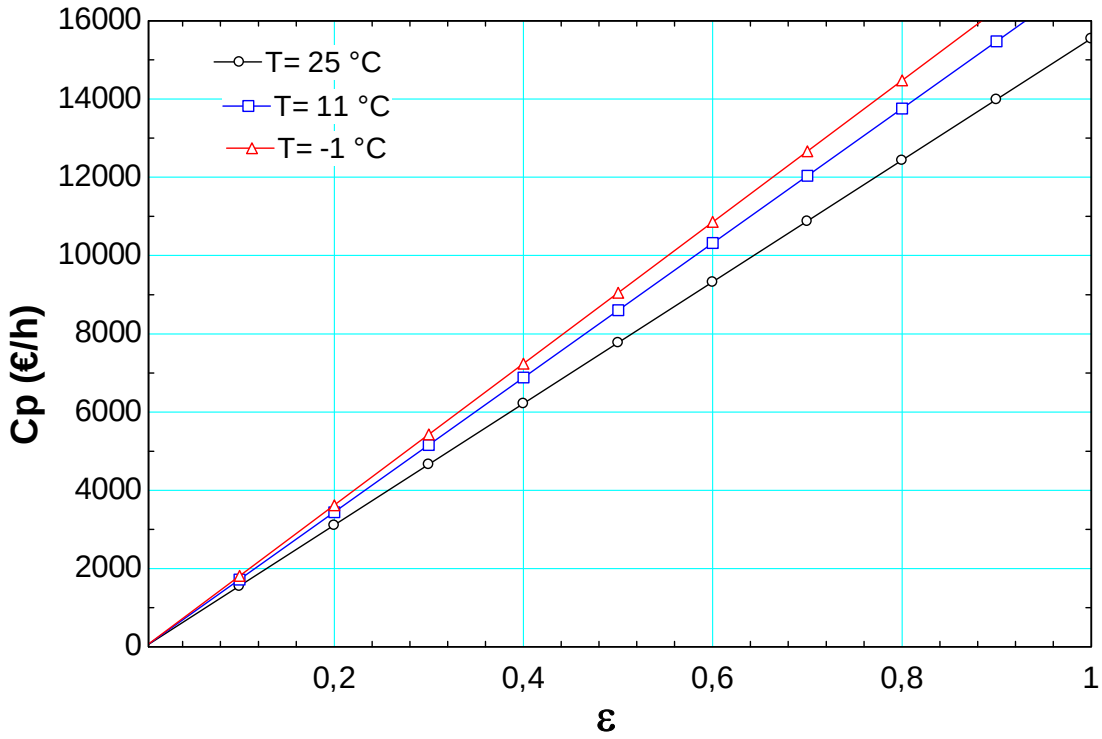

Figure 5.12 Cost rate of exergy as a function of second-law efficiency for three dead state temperatures in High Temperature Heat Exchanger 2

Exergoeconomic factor as a function of second-law efficiency (exergy efficiency) for three dead state temperatures are given in Figures 5.13 through 5.18 for the heat exchangers of the system. It is clear that as the exergy efficiency increases the exergoeconomic factor increases. As the dead state temperature increases from -1°C to 11°C and 25°C, cost rate of exergy destructions generally decrease but this decrease is minimal for some of the heat exchangers as shown in Figures 5.13 through 5.15. This indicates that the system performs better at higher dead state temperatures.

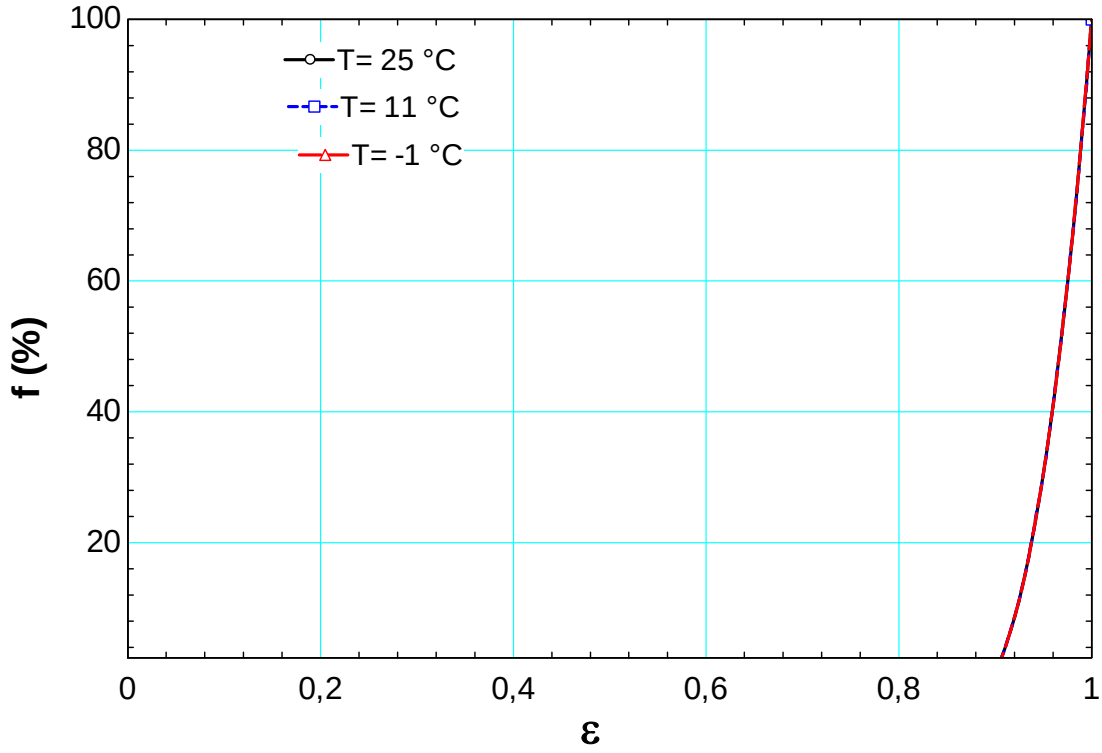

Figure 5.13 Exergoeconomic factor as a function of second-law efficiency for three dead state temperatures in Low Temperature Heat Exchanger 1

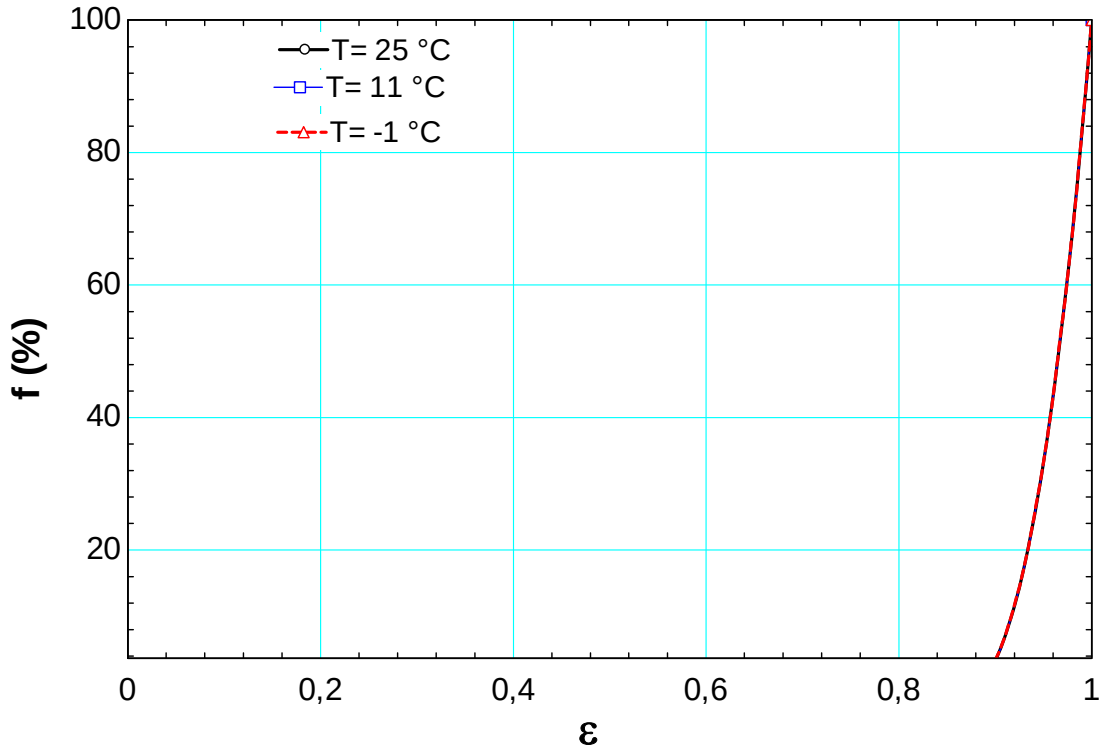

Figure 5.14 Exergoeconomic factor as a function of second-law efficiency for three dead state temperatures in Medium Temperature Heat Exchanger 1

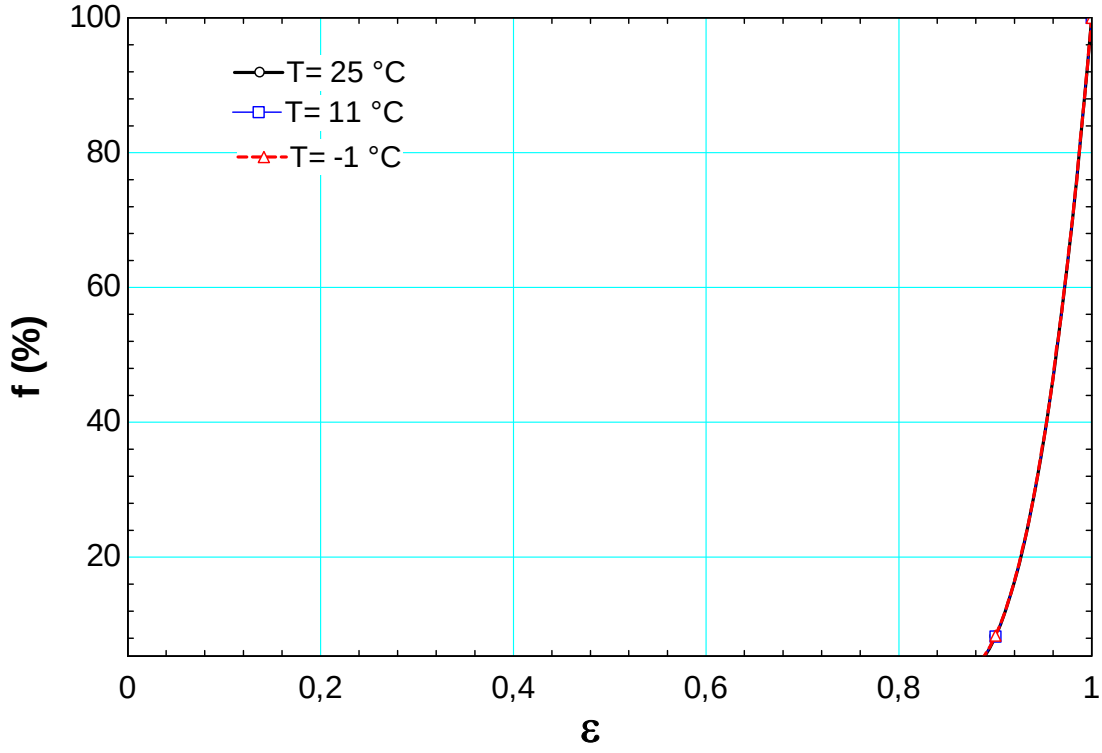

Figure 5.15 Exergoeconomic factor as a function of second-law efficiency for three dead state temperatures in High Temperature Heat Exchanger 1

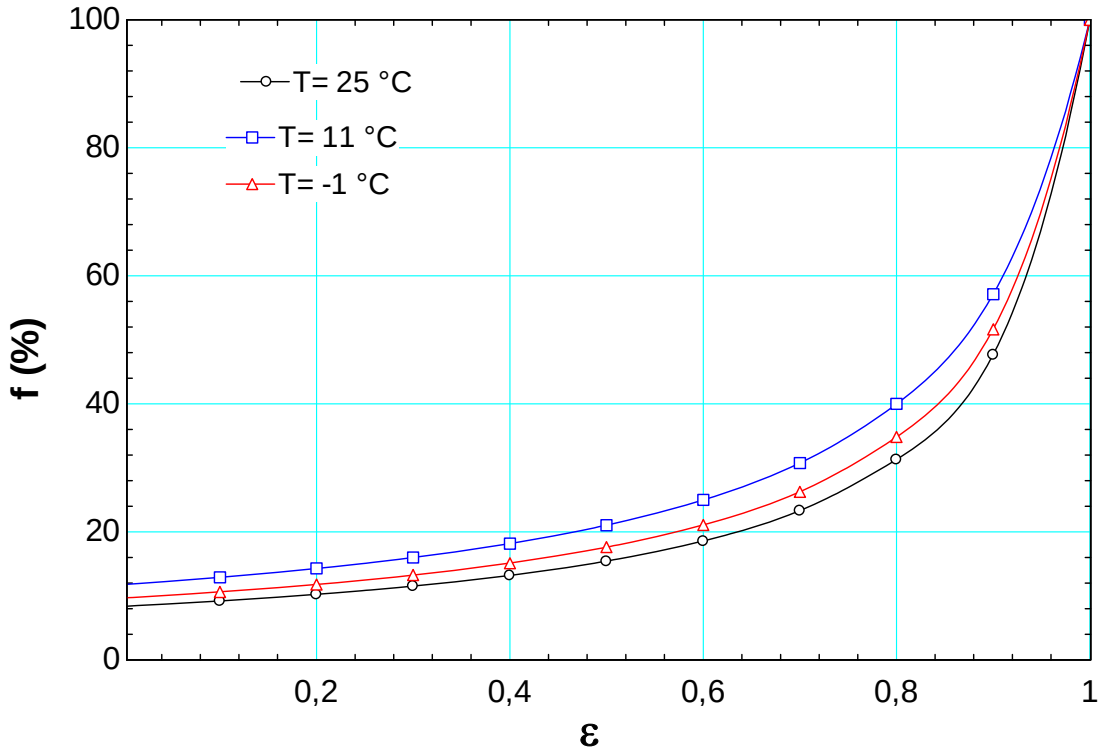

Figure 5.16 Exergoeconomic factor as a function of second-law efficiency for three dead state temperatures in Low Temperature Heat Exchanger 2

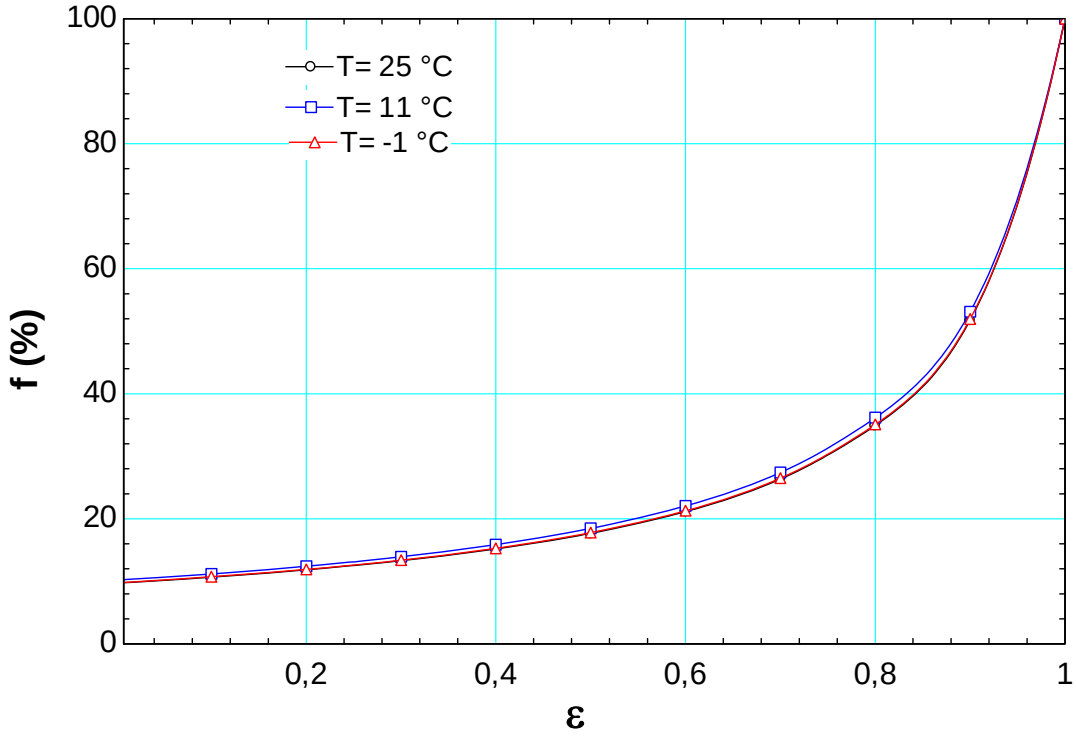

Figure 5.17 Exergoeconomic factor as a function of second-law efficiency for three dead state temperatures in Medium Temperature Heat Exchanger 2

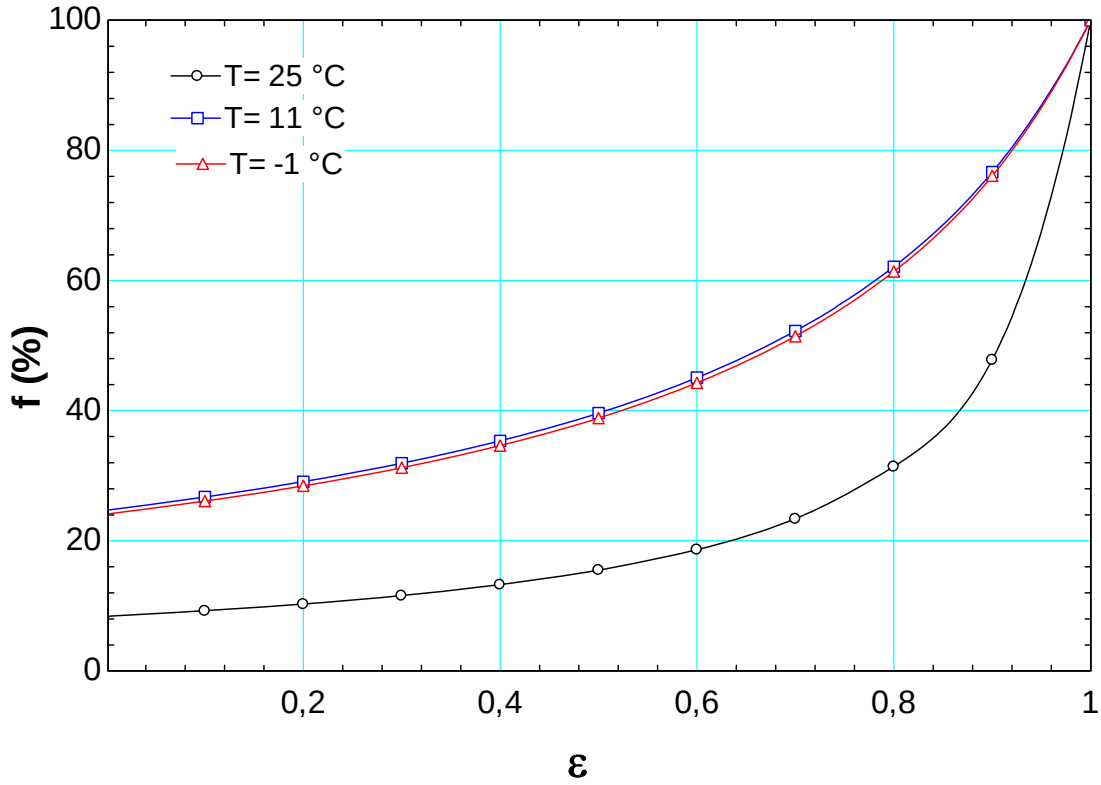

Figure 5.18 Exergoeconomic factor as a function of second-law efficiency for three dead state temperatures in High Temperature Heat Exchanger 2

Relative cost difference as a function of second-law efficiency (exergy efficiency) for three dead state temperatures are given in Figures 5.19 through 5.24 for the heat exchangers of the system. It is clear that as the exergy efficiency increases the relative cost differnce decreases. As the dead state temperature increases from -1°C to 11°C and 25°C, cost rate of exergy destructions decrease at a small rate. This indicates that the efffect of dead state temperature on relative cost difference is negligible.

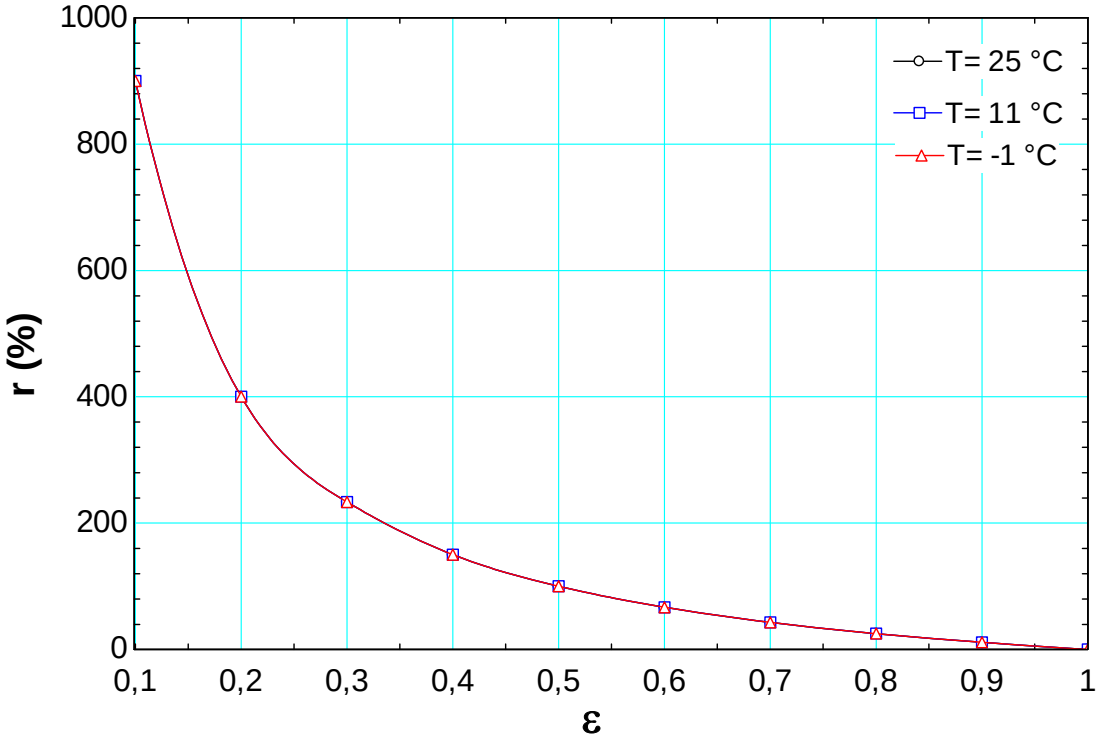

Figure 5.19 Relative cost differnce as a function of second-law efficiency for three dead state temperatures in Low Temperature Heat Exchanger 1

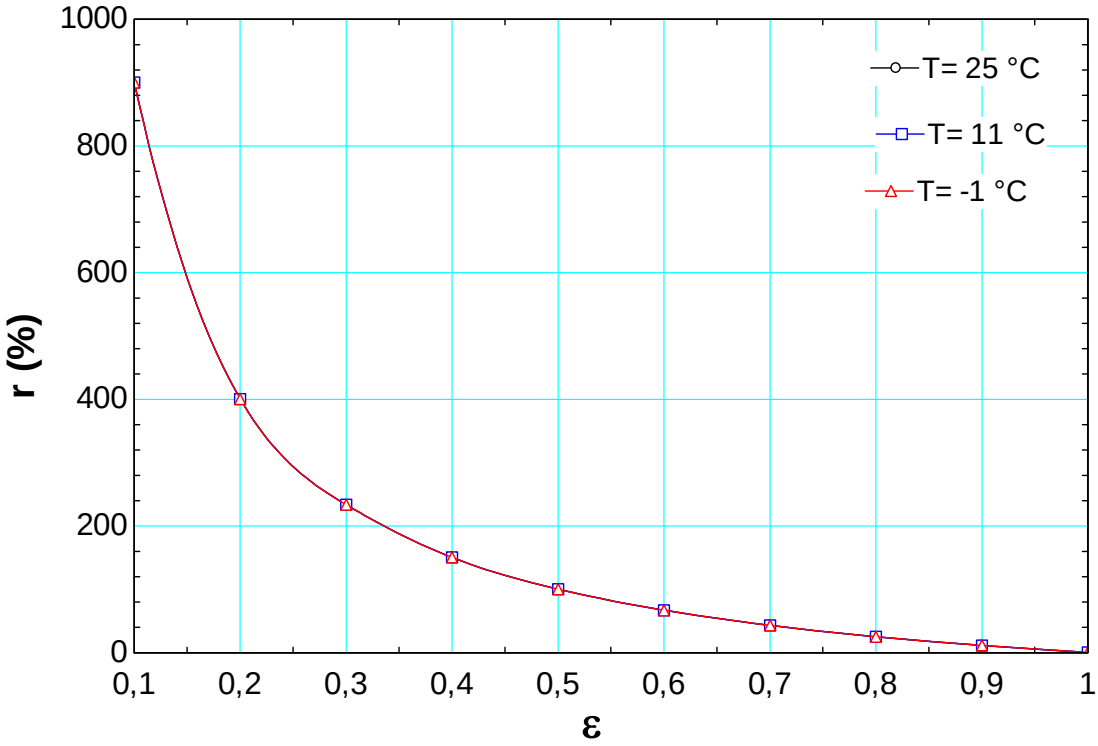

Figure 5.20 Relative cost differnce as a function of second-law efficiency for three dead state temperatures in Medium Temperature Heat Exchanger 1

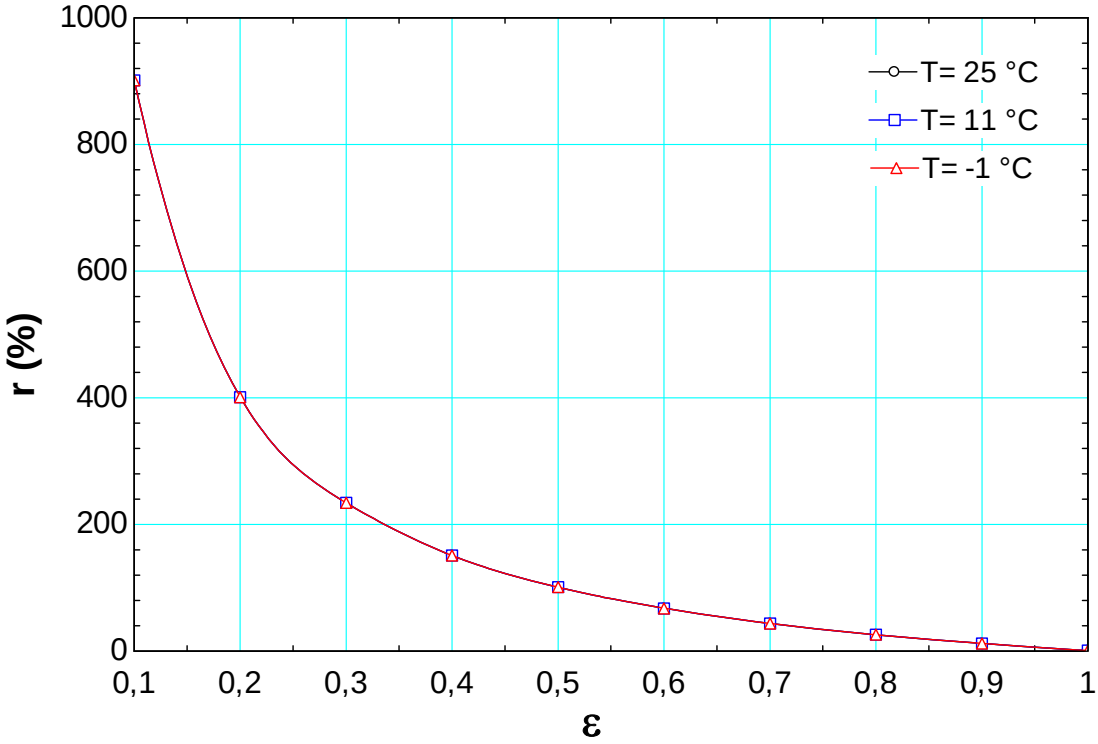

Figure 5.21 Relative cost differnce as a function of second-law efficiency for three dead state temperatures in for High Temperature Heat Exchanger 1

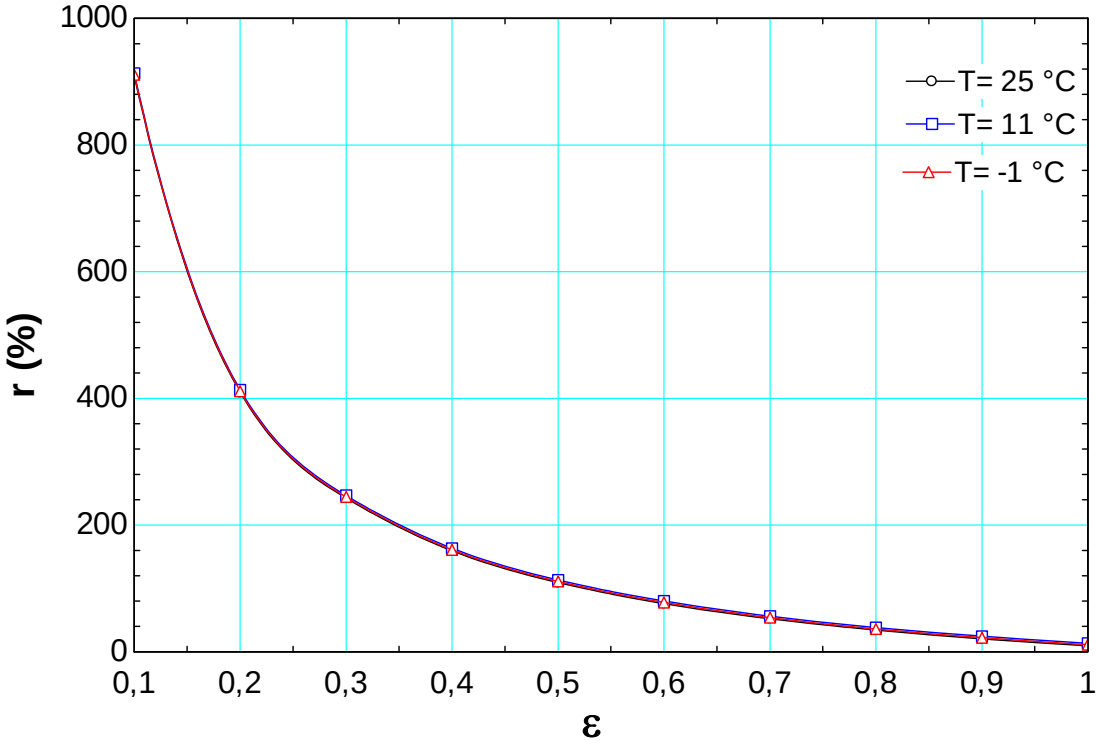

Figure 5.22 Relative cost differnce as a function of second-law efficiency for three dead state temperatures in Low Temperature Heat Exchanger 2

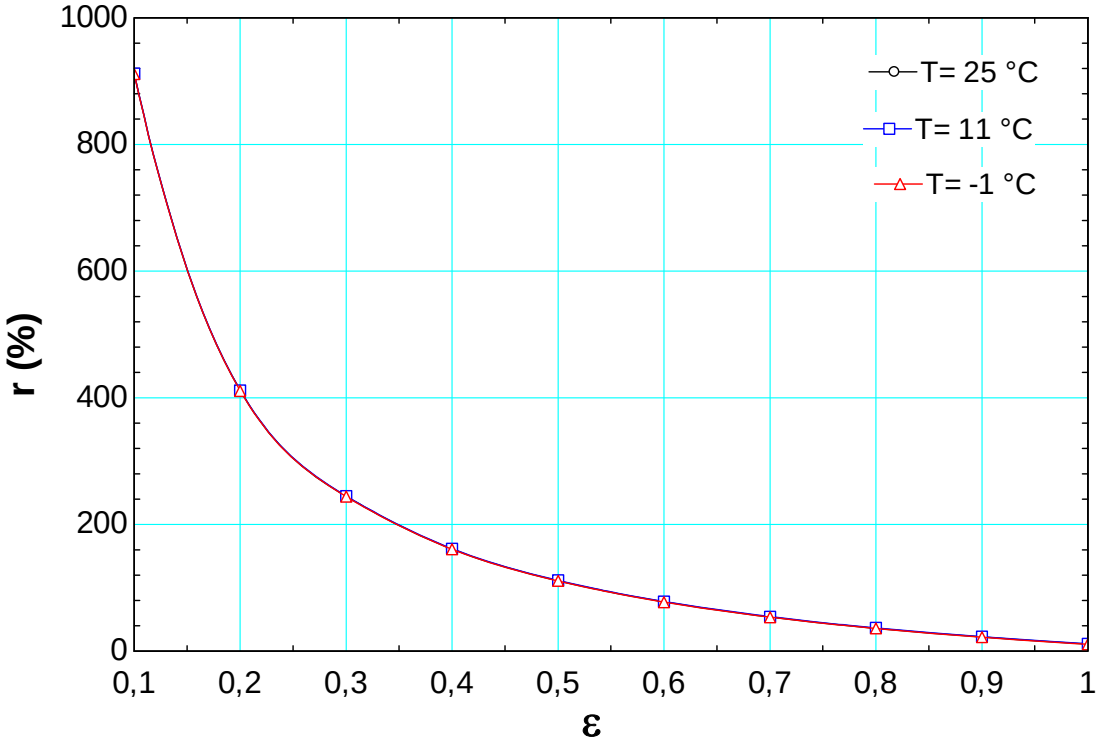

Figure 5.23 Relative cost differnce as a function of second-law efficiency for three dead state temperatures in for Medium Temperature Heat Exchanger 2

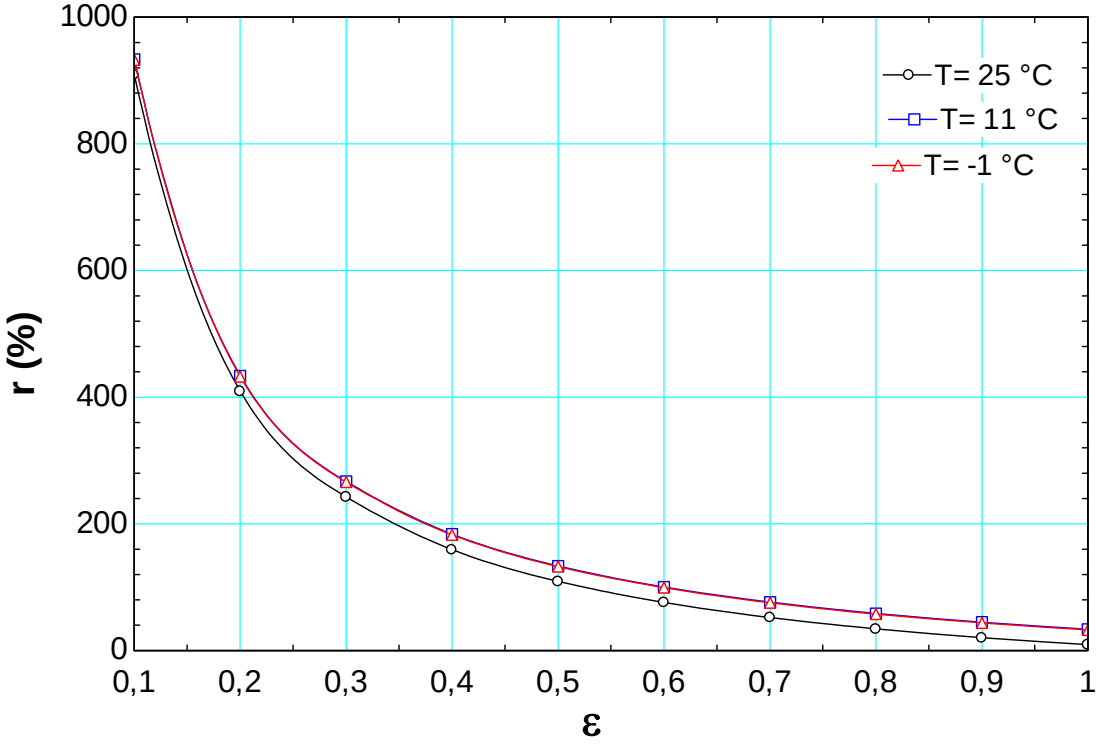

Figure 5.24 Relative cost differnce as a function of second-law efficiency for three dead state temperatures in High Temperature Heat Exchanger 2

5.4 Conclusions

Results are presented of the economic and exergoeconomic analyses of geothermal assisted high temperature electrolysis for hydrogen production, including estimates of hydrogen cost. The parameters studied include the exergy efficiency, rates of exergy destruction and exergy loss, the exergy destruction ratio, cost rates associated with exergy destruction, capital investment and operating and maintenance costs, the relative cost difference of unit costs, and exergoeconomic factor.

CHAPTER 6

CONCLUSIONS

This study is on thermodynamic and thermoeconomic analysis of geothermal assisted high temperature electrolysis system for hydrogen production. Thermodynamic performance parameters and required data are calculated. Economic data are taken from Sigurvinsson [123] and used for thermoeconomic analysis. The HTSE system produces 1 kg hydrogen per second and consumes 122,129 kW electricity.

The following is a summary of conclusions based on the the results of the study:

1. Thermodynamic relations of the system are given in Chapter 4 based on the general thermodynamic relations in Chapter 3. The temperature, pressure, and mass flow rate data and certain exergy evaluations of the plant are presented in Table 4.1, Table 4.2 and Table 4.3 for 25 °C, 11 °C and -1 °C reference temperatures, respectively. Energy and exergy calculations are done using a computer program with built in thermodynamic functions. Energy and exergy analyses results of the system are given in Table 4.4, Table 4.5 and Table 4.6 at 25 °C, 11 °C and -1 °C reference temperatures, respectively.

2. The economic life of HTSE system is 40 years. The length of operation is 7008 hours per year. Cost of hydrogen production is 1.6 €/kWh for 1 kg hydrogen production. The cost of steam entering the system is 2.73 €/kWh. The hourly levelized costs of capital investment, operating and maintance costs, and the total costs of the components of the system are given in Table 5.4.

3. In this study, specific exergy costing (SPECO) method is used to obtain the cost formation structure of the system. Exergetic cost rates balances and corresponding auxiliary equations of the plant are given in Chapter 3. Exergetic cost rate balances and corresponding auxiliary equations are formulated for each component of the system. Auxiliary equations are found by applying F and P principles. Results obtained are given in Table 5.5, Table 5.6, and Table 5.7 for 25 °C, 11 °C and -1 °C reference temperatures, respectively. The exergetic cost parameters of the system components are given in Table 5.8, Table 5.9, Table 5.10 at 25 °C, 11 °C and -1 °C reference temperatures, respectively. These parameters indicate the performance of system components on a rational exergetic cost basis. The steam input of the system is 1 kg/s at 230 °C and 1500 kPa. The exergetic cost rate of the steam entering the system are 8621 €/h, 9470 €/h, 10,227 €/h for state 5 and 24,666 €/h, 25,856 €/h, 29,241 €/h for state 1 at 25 °C, 11 °C and -1 °C, respectively. The specific unit exergetic cost of steam is 2.73 €/kWh for all three reference temperatures. The capital investment cost, the operating and maintenance costs and the total cost of the HTSE system are found to be 422.21 €/kWh, 2.04 €/kWh and 424.25 €/kWh. We assumed that the operating and maintenance costs are the same for 25 °C, 11 °C and -1 °C reference temperatures.

4. The net electrical power input to the system is 122,129 kW. The exergetic cost rate of the power input to the system is 21,770 €/h and the specific unit exergetic cost is 0.17 €/kWh at 25 °C. The corresponding parameters are 24,832 €/h and 0.20 €/kWh at 11 °C while they are 29,430 €/h and 0.24 €/kWh at -1 °C. When the reference temperature of the system increase, the exergetic cost rate and the specific unit exergetic cost of the power input to the system decrease.

5. Exergoeconomic factors for high temperature heat exchanger 2 is 92.94% at 11 °C. It is the highest exergoeconomic factor value and has the lowest cost rate of exergy destruction among the three reference temperatures. Exergoeconomic factor for high temperature electrolysis is 0.02% at -1 °C. This is the lowest exergoeconomic factor value and has the highest cost rate of exergy destruction among three reference temperatures. The relative cost difference for medium temperature heat exchanger 1 is 3.12% at 25 °C. This is because of low investment, operation and maintance costs and high cost of effectiveness. The relative cost

difference for medium temperature heat exchanger 1 is 59.50% at 11°C. This is due to high cost of effectiveness.

The results of the energy, exergy and exergoeconomic analyses provide valuable information on exergetic and cost performance of the system. These include exergy destructions and efficiencies and cost allocation among various components of the system. This information may be used to improve thermodynamic performance of the system. It may also be used for an exergoeconomic optimization to reduce the product costs.

REFERENCES

[1] Çengel, Y. A., Boles, M. A. (2008). Thermodynamics: An Engineering Approach. (6th edition). New York: Mc-Graw Hill.

[2] Celik MY, Sabah E. (2002).The geological and technical characterization of Omer-Gecek geothermal area and the environmental impact assessment of geothermal heating system. *Environmental Geology*, 41, 942–53.

[3] Fridleifsson IB. (2003). Status of geothermal energy amongst the world's energy sources. *Geothermics*, 32, 379–88.

[4] The Potential For The Production Of Hydrogen From Renewable Energy Sources In Austria ("Energy Markets - The Challenges of the New Millennium" 18th World Energy Congress Buenos Aires - Argentina. 21-25 October 2001

[5] Veziroglu T. Nejat,Sumer Sahın (2008).21st Century's energy: Hydrogen energy system. *Energy Conversion and Management*, 49 ,1820–1831

[6] Orhan M.F. (2008). *Energy, Exergy and Cost Analyses of Nuclear-Based Hydrogen Production via Thermochemical Water Decomposition Using a Copper-Chlorine (Cu-Cl) Cycle.* A master thesis,The Faculty of Engineering and Applied Science Mechanical Engineering Program,University of Ontario Institute of Technology,Canada.

[7] Energy Efficiency and Renewable Energy DOE/GO–102001–1102 FS175 March 2001.

[8] National Geothermal Collaborative "Geothermal Energy: Technologies and Costs"

[9] http://www.ren21.net/pdf/RE2007_Global_Status_Report.pdf

[10]http://www.renewableenergyfocus.com/view/3157/hydrogen-production-from-renewables/

[11] http://www.gas-plants.com/hydrogen-properties.html

[12] Konieczny A, Mondal K, Wiltowski T, Dydo P. (2008). Catalyst development for thermocatalytic decomposition of methane to hydrogen. , *International Journal of Hydrogen Energy*, **33**, 264.

[13] Yilanci A., Dincer I., Ozturk H.K. (2009). A review on solar-hydrogen/fuel cell hybrid energy systems for stationary applications. *Progress in Energy and Combustion Science*, **35**, 231–244.

[14] Veziroglu TN, Sahin S. (2008). 21st century's energy: hydrogen energy system. *Energy Conversion and Management*, **49**, 1820–1831.

[15] Dincer I. (2007). Environmental and sustainability aspects of hydrogen and fuel cell systems. *International Journal of Energy Research*, **31**, 29–55.

[16] Campen A, Mondal K, Wiltowski T. (2008). Separation of hydrogen from syngas using a regenerative system. *International Journal of Hydrogen Energy*, **33**, 33-332.

[17] Balat Mustafa, Balat Mehmet (2009). Political, economic and environmental impacts of biomass-based hydrogen. *International Journal of Hydrogen Energy*, **34**, 3589–3603.

[18] http://www1.eere.energy.gov/geothermal/powerplants.html

[19] Erdogdu Erkan (2009).A snapshot of geothermal energy potential and utilization in Turkey. *Renewable and Sustainable Energy Reviews*, **13**, 2535–2543.

[20] Celiktas Melih Soner, Sevgili Tarkan, Kocar Gunnur (2009). A snapshot of renewable energy research in Turkey. Renewable Energy, **34**,1479–1486.

[21] Fridleifsson Ingvar B. (2001). Geothermal energy for the benefit of the people. *Renewable and Sustainable Energy Reviews*, **5**, 299–312.

[22] Serpen Umran, Aksoy Niyazi, Öngür Tahir, Korkmaz E. Didem (2008). Geothermal energy in Turkey:2008 update. *Geothermics*, **38**, 227-237.

[23] Acar H.I. (2003). A review of geothermal energy in Turkey. *Energy Sources*, **25**,1083–1088.

[24] Serpen U. , Aksoy N. , Ongur T., Korkmaz E. D. (2009). Geothermal energy in Turkey: 2008 update. *Geothermics*,38,227–237.

[25] http://en.wikipedia.org/wiki/Solar_energy

[26] Pregger Thomas, Graf Daniel, Krewitt Wolfram, Sattler Christian, Roeb Martin, Möller Stephan (2009). Prospects of solar thermal hydrogen production processes. *International Journal of Hydrogen Energy*, **344**, 4256–4267.

[27] Nakamura T. (1977). Hydrogen production from water utilizing solar heat at high temperatures. *Energy*, **19**, 567-475.

[28] Shabani Bahman, Andrews John, Watkins Simon (2010). Energy and cost analysis of a solar-hydrogen combined heat and power system for remote power supply using a computer simulation. *Solar Energy*, **84**, 144–155.

[29] Steinfeld A. (2002). Solar hydrogen production via a two-step waters plitting thermochemical cycle based on Zn/ZnO redox reactions. *International Journal of Hydrogen Energy*, **27**, 611–619.

[30] Zedtwitz PV., Petrasch J., Trommer D., Steinfeld A. (2006). Hydrogen production via the solar thermal decarbonization of fossil fuels. *Solar Energy*, **80**, 1333–1337.

[31] Zini G., Tartarini P. (2009). Hybrid systems for solar hydrogen: A selection of case-studies. *Applied Thermal Engineering Review*, **29**, 2585–2595.

[32] Ford N.C., Kane J.W. (1971). Solar power. *Bull Ato Science*, **27,** 27.

[33] Zhixiang Liu, Zhanmou Qiu, Yao Luo, Zongqiang Mao, Cheng Wanga (2009). Operation of first solar-hydrogen system in China. *International Journal of Hydrogen Energy*, **34**, 1–5.

[34] Pregger Thomas, Graf Daniela, Krewitt Wolfram, Sattler Christian, Roeb Martin, Möller Stephan (2009). Prospects of solar thermal hydrogen production processes. *International Journal of Hydrogen Energy*, **344**, 4256–4267.

[35] Abanades S, Flamant G. (2006). Solar hydrogen production from the thermal splitting of methane in a high temperature solar chemical reactor. *Solar Energy*, **80**, 1321–1332.

[36] Abdel-Nasser Cherigui, Bouziane Mahmah, Farid Harouadi, Maiouf Belhamel, Samira Chader, Abdelhamid M.Raoui, Claude Etievant (2009). Solar hydrogen energy: The European–Maghreb connection. A new way of excellence for a sustainable energy development. International Journal of Hydrogen Energy, **34**, 4934–4940.

[37] Almogren Sulaiman, Veziroglu T. Nejat (2004). Solar-hydrogen energy system for Saudi Arabia. *International Journal of Hydrogen Energy*, **29**, 1181–1190.

[38] Padin J., Veziroglu T.N., Shahin A. (2000). Hybrid solar high-temperature hydrogen production system. *International Journal of Hydrogen Energy*, **25**, 295-317.

[39] Szyszka A. (1998). Ten years of solar hydrogen demonstration project at Neunburg Vorm Wald, Germany. *International Journal of Hydrogen Energy*, **23**, 23849–60.

[40] Zhixiang Liu, Zhanmou Qiu, Yao Luo, Zongqiang Mao, Cheng Wang (2010). Operation of first solar-hydrogen system in China. *International Journal of Hydrogen Energy*, **35**, 2762–2766.

[41] Bolton James R. (1996). Solar photo production of hydrogen: A review. *Solar Energy*, **57**, 37-50.

[42] Zini G., Tartarini P. (2009). Review Hybrid systems for solar hydrogen: A selection of case-studies. *Applied Thermal Engineering*, **29**, 2585-2595.

[43] Clarke R.E., Giddey S., Ciacchi F.T., Badwal S.P.S., Paul B., Andrews J. (2009). Direct coupling of an electrolyser to a solar PV system for generating hydrogen. *International Journal of Hydrogen Energy*, **34**, 2531–2542.

[44] Lehman PA, Chamberlin CE, Pauletto Rocheleau (1997). Operating experience with a photovoltaic hydrogen energy system. *International Journal of Hydrogen Energy*, **22**, 465–70.

[45] Hollmuller P, Joubert J.M., Lachal B, Yvon K. (2000). Evaluation of a 5 kWp photovoltaic hydrogen production and storage installation for a residential home in Switzerland. *International Journal of Hydrogen Energy*, **25**, 97–109.

[46] Bilgen E. (2004). Domestic hydrogen production using renewable energy. *Solar Energy*, **77**, 47–55.

[47] Thomas L. Gibson, Nelson A. Kelly (2008). Optimization of solar powered hydrogen production using photovoltaic electrolysis devices. *International Journal of Hydrogen Energy*, **33**, 5931–5940.

[48] Ahmad G.E., El Shenawy E.T. (2006). Technical Note Optimized photovoltiac system for hydrogen Production. *Renewable Energy*, **31**, 1043–1054.

[49] Valenciaga F., Evangelista C.A. (2010). Control design for an autonomous wind based hydrogen production system. *International Journal of Hydrogen Energy*, **35**, 1-9.

[50] Honnery Damon, Moriarty Patrick (2009). Estimating global hydrogen production from wind. *International Journal of Hydrogen Energy*, **34**, 727–736.

[51] Christopher J. Greiner, Magnus Korpas, Arne T. Holen (2007). A Norwegian case study on the production of hydrogen from wind power. *International Journal of Hydrogen Energy*, **32**, 1500–1507.

[52] Jose´ G. Garcı´a Clu´a,Herna´n De Battista,Ricardo J. Mantz (2010). Control of a grid-assisted wind-powered hydrogen production system. *International Journal of Hydrogen Energy*, **35**, 1 – 7.

[53] Kamaruzzaman Sopian, Mohd Zamri Ibrahim, Wan Ramli Wan Daud, Mohd Yusof Othman, Baharuddin Yatim, Nowshad Amin (2009). Performance of a PV–wind hybrid system for hydrogen production. *Renewable Energy*, **34**, 1973–1978.

[54] Jin Xuan, Michael K.H. Leung ,Dennis Y.C. Leung, Meng Ni (2009). A review of biomass-derived fuel processors for fuel cell systems. *Renewable and Sustainable Energy Reviews*, **13**, 1301–1313.

[55] Hulteberg P.C., Karlsson H.T. (2009). A study of combined biomass gasification and electrolysis for hydrogen production. *International Journal of Hydrogen Energy*, **34**, 772–782.

[56] Holladay J.D., J. Hu, D.L. King, Y. Wang (2009). An overview of hydrogen production Technologies. *Catalysis Today*, **139**, 244–260.

[57] Baofeng Zhao Baofeng Zhao, Xiaodong Zhang, Li Sun, Guangfan Meng, Lei Chen, Yi Xiaolu (2010). Hydrogen production from biomass combining pyrolysisand the secondary decomposition. *International Journal of Hydrogen Energy*, **35**, 2606–2611.

[58] Kalinci Yildiz, Hepbasli A., Dincer I. (2009). Biomass-based hydrogen production: A review and analysis. *International Journal of Hydrogen Energy*, **34**, 8799–8817.

[59] Cohce M.K., Dincer I., Rosen M.A. (2009). Thermodynamic analysis of hydrogen production from biomass gasification. *International Journal of Hydrogen Energy*, **34**, 1–11.

[60] Udagawa J., Aguiar P., Brandon N.P. (2007). Hydrogen production through steam electrolysis: Control strategies for a cathode-supported intermediate temperature solid oxide electrolysis cell. *Journal of Power Sources*, **166**, 127–136.

[61] Herring J.S., O'Brien J.E., Stoots C.M., Hawkes G.L., Hartvigsen J.J.,Shahnam M. (2007). Parametric study of large-scale production of syngas via high-temperature co-electrolysis. *International Journal of Hydrogen Energy*, **32**, 440–450.

[62] Shin Y., Park W., Chang J., Park J. (2007) . A novel process to fabricate membrane electrode assemblies for proton exchange membrane fuel cells. *International Journal of Hydrogen Energy* , **32**, 1486–1491.

[63] Youngjoon Shin, Wonseok Park, Jonghwa Chang, Jongkuen Park (2007). Evaluation of the high temperature electrolysis of steam to produce hydrogen. *International Journal of Hydrogen Energy*, **32**, 1486–1491

[64] Ozaki A., Kubota K., Yamada K., (2005). Nuclear hydrogen production systems. *Toshiba Review*, **60**, 27.

[65] Balta M. Tolga, Dincer Ibrahim, Hepbasli Arif (2009). Thermodynamic assessment of geothermal energy use in hydrogen production. *International Journal of Hydrogen Energy* , **34**, 2925–2939.

[66] Sigurvinsson J., C.Mansilla, P.Lovera, F.Werkoff (2007).Can high temperature steam electrolysis function with geothermal heat?.*International Journal of Hydrogen Energy*, **32**,1174–1182.

[67] SigurvinssonJ., Mansilla C., Arnason B., Bontemps A., Mare´chal A., Sigfusson T.I., Werkoff F. (2006). Heat transfer problems for the production of hydrogen from geothermal energy. *Energy Conversion and Management* , **47**, 3543–3551.

[68] Mansilla Christine, Sigurvinsson Jon, Bontemps Andre,Alain Marechal, Francois Werkoff (2007). Heat management for hydrogen production by high temperature steam electrolysis. *Energy*, **32**, 423–430.

[69] Theodore Wayne Han (2008). Hydrogen Production Using Geothermal Energy Graduate Theses and Dissertations, Utah State University, Utah Sate, USA.

[70] Masson J.P., Molina R., Roth E., Gaussens G., Lemaire F. (1982). Obtention and evaluation of polyethylene-based solid polymer electrolyte membrane for hydrogen production. *International Journal of Hydrogen Energy*, **7**, 167–71.

[71] Ulleberg Iystein (2003). Modeling of advanced alkaline electrolyzers: a system simulation approach. *International Journal of Hydrogen Energy*, **28**, 21 – 33.

[72] Perez-Herranz V., M. Perez-Page, R. Beneito (2010).Monitoring and control of a hydrogen production and storage system consisting of water electrolysis and metal hydrides. *International Journal of Hydrogen Energy*, **35**, 912–919.

[73] Kanoglu Mehmet, Dincer Ibrahim, Rosen Marc A. (2007). Understanding energy and exergy efficiencies for improved energy management in power plants. *Energy Policy*, **35**, 3967–3978.

[74] Ni Meng, Leung Michael K.H., Leung Dennis Y.C. (2007). Energy and exergy analysis of hydrogen production by solid oxide steam electrolyzer plant. *International Journal of Hydrogen Energy*, **32**, 4648 – 4660.

[75] Ni M, Leung M.K.H, Leung DYC (2008). Energy and exergy analysis of hydrogen production by a proton exchange membrane (PEM) electrolyzer plant. *Energy Conversion and Management*, **49**, 2748–56.

[76] Wall G. (1988). Exergy flows in industrial processes. *Energy*, **13**, 197–208.

[77] Tsatsaronis, G., Lin, L., Pisa, J. (1993). Exergy costing in Exergoeconomics. *Journal of Energy Resources Technology*, **115**, 9-16.

[78] Abusoglu Aysegul, Kanoglu Mehmet (2009). Refrence Exergetic and thermoeconomic analyses of diesel engine powered cogeneration : Part 2 – Application. *Applied Thermal Engineering*, **29**, 242–249.

[79] Abusoglu Aysegul, Kanoglu Mehmet (2009). Exergoeconomic analysis and optimization of combined heat and power production: A review. *Renewable and Sustainable Energy Reviews*, **13**, 2295–2308.

[80] Bejan, A., Tsatsaronis, G., Moran, M. (1996). *Thermal Design and Optimization*. (1st ed.). New York: Wiley.

[81] Van Wylen, G. J., Sonntag, R.E. (1985). Fundamentals of Classical Thermodynamics. (3rd edition). New York: John Wiley & Sons.

[82] Wark, K. Jr. (1995). Advanced Thermodynamics for Engineers. (1st edition).New York: Mc-Graw Hill.

[83] Tsatsaronis, G., Ho-Park, M. (2002). On avoidable and unavoidable exergy destructions and investment costs in thermal systems. *Energy Conversion and Management*, **43**, 1259-1270.

[84] Wall, G. (1986). *Exergy – A useful concept*. A doctorate thesis, Physical Resource Theory Group, Chalmers University of Technology and University of Goteborg. Goteborg, Sweden.

[85] Wall, G. (2003). Exergy tools. *Proceedings Institution of Mechanical Engineers,***217**, 125-136.

[86] Dunbar, W.R., Lior, N., Gaggioli, R.A. (1992). The components equations of energy and exergy. *Journal of Energy Resources Technology*, **114**, 75-83.

[87] Nikulshin, V., Wu, C., Nikulshina V. (2002). Exergy efficiency of energy intensive systems. *Exergy, An International Journal*, **2**, 78-86.

[88] Wall, G., Gong, M. (2001). On exergy and sustainable development – Part 1: Conditions and concepts. *Exergy, An International Journal*, **1**, 128-145.

[89] Wall, G., Gong, M. (2001). On exergy and sustainable development – Part 2: Indicators and methods. *Exergy, An International Journal*, **1**, 217-233.

[90] Vajpayee, S. K. (2001). Fundamentals of Economics for Enginering Technologists and Engineers. London: Prentice Hall.

[91] Park, C. S. (1990). Advanced Engineering Economics. New York: John Wiley& Sons.

[92] Gönen, T. (1990). Engineering Economy for Engineering Managers. NewYork: John Wiley & Sons.

[93] Tsatsaronis, G., Moran, M.J. (1997). Exergy-aided cost minimization. *Energy Conversion and Management*, **38**, 1535-1542.

[94] Lazzaretto A., Tsatsaronis G. (1997). On the quest for objective equations in exergy costing. In *Proceedings of the ASME Advanced Energy Systems Division*, **37**,197-209.

[95] Lozano, M.A., Valero A. (1993). Theory of the exergetic cost. *Energy*, **18**, 939-960.

[96] Reini, M., Lazzaretto A., Macor A. (1995). Average structural and marginal costs as a result of a unified formulation of the thermoeconomic problem. In *Proceedings of Second Law Analysis of Energy Systems: Towards the 21st Century*, Rome.

[97] Oh, S.D., Pang, H.S., Kim, S.M., Kwak, H.Y. (1996). Exergy analysis for a gas turbine cogeneration system. *Transactions of the ASME*, **118**, 782-791.

[98] Kwon, Y.H., Kwak, H.Y., Oh, S.D. (2001). Exergoeconomic analysis of gas turbine cogeneration systems. *Exergy, An International Journal*, **1**, 31-40.

[99] Lazzaretto, A., Tsatsaronis, G. (2001). Comparison Between SPECO-Based and Functional Exergoeconomic Approaches. In *Proceedings of the 2001 ASME International Mechanical Engineering Congress and Exposition in New York*, 1-16.

[100] Ahern, J. E. (1980). The Exergy Method of Energy System Analysis. (1st edition). New York: John Wiley & Sons.

[101] Gaggioli, R. A., Wepfer, W. J. (1980). Exergy economics. *Energy, The International Journal*, **5**, 823-837.

[102] Tsatsaronis, G., Lin, L., Pisa, J. (1993). Exergy costing in Exergoeconomics. *Journal of Energy Resources Technology,* **115**, 9-16.

[103] Tsatsaronis, G., Ho-Park, M. (2002). On avoidable and unavoidable exergy destructions and investment costs in thermal systems. *Energy Conversion and Management*, **43**, 1259-270.

[104] Sciubba, E. (2001). Beyond thermoeconomics? The concept of Extended Exergy Accounting and its application to the analysis and design of thermal systems. *Exergy,An International Journal*, **1**, 68-84.

[105] Kim, S.M., Oh, S.D., Kwon, Y.H., Kwak, H.Y. (1998). Exergoeconomic analysis of thermal systems. *Energy*, **23**, 393-406.

[106] Valero, A., Lozano, M.A., Serra, L., Torres, C. (1994). Application of the exergetic cost theory to the CGAM problem. *Energy*, **19**, 365-381.

[107] Kwon, Y.H., Kwak, H.Y., Oh, S.D. (2001). Exergoeconomic analysis of gas turbine cogeneration systems. *Exergy, An International Journal*, **1**, 31-40.

[108] Tsatsaronis, G., Ho-Park, M. (2002). On avoidable and unavoidable exergy destructions and investment costs in thermal systems. *Energy Conversion and Management*, **43**, 1259-270.

[109] Kwak, H. Y., Byun, G. T., Kwon, Y. H., Yang, H. (2004). Cost structure of CGAM cogeneration system. *International Journal of Energy Research*, **28**, 1145-1158.

[110] El-Sayed, Y., Evans, R. L. (1970). Thermoeconomics and the design of heat systems. *Journal of Engineering and Power*, **92**, 27-35.

[111] El-Sayed, Y.M., Gaggioli, R.A. (1989). A critical review of Second Law costing methods -1: Background and Algebraic Procedures. *Journal of Energy Resources Technology*, **111**, 1-7.

[112] Frangopoulos, C.A. (June 1991). Comparison of thermoeconomic and thermodynamic optimal designs of a combined-cycle plant. *International Conference on the Analysis of Thermal and Energy Systems, Athens, Greece*, 305-318.

[113] Frangopoulos, C.A. (1994). Application of the thermoeconomic functional approach to the CGAM problem. *Energy*, **19**, 323-342.

[114] Frangopoulos, C.A. (1991). Intelligent Functional Approach: A method for analysis and optimal synthesis – design – operation of complex systems. *International Journal of Energy, Environment, Economics*, **1**, 267-274.

[115] Frangopoulos, C.A. (1991). Optimization of synthesis – design – operation of a cogeneration system by The Intelligent Functional Approach. *International Journal of Energy, Environment, Economics*, **1**, 275-287.

[116] Frangopoulos, C.A. (1987). Thermoeconomic functional analysis and optimization. *Energy*, **12**, 563-571.

[117] Manolas, D.A., Frangopoulos, C.A., Gialamas, T.P., Tsahalis, D.T. (1997). Operation optimization of an industrial cogeneration system by a genetic algorithm. *Energy Conversion and Management*, **38**, 1625-1636.

[118] Von Spakovsky, M.R., Evans R.B. (1990). The design and performance optimization of thermal systems. *Journal of Engineering for Gas Turbines and Power*, **112**, 86-93.

[119] Tsatsaronis, G., Pisa, J., Valero, A., Lozano, M.A., Serra, L., Frangopoulos, C.,Von Spakovsky, M. (1994). CGAM problem: Definition and conventional solution.*Energy*, **19**, 279-286.

[120] Tsatsaronis, G., Pisa, J. (1994). Exergoeconomic evaluation and optimization of energy systems – Application to the CGAM problem. *Energy*, **19**, 287-321.

[121] Toffolo, A., Lazzaretto, A. (2002). Evolutionary algorithms for multi-objective energetic and economic optimization in thermal system design. *Energy*, **27**, 549-567.

[122] Marc A. Rosen, Ibrahim Dincer, Mehmet Kanoglu (2008). Role of exergy in increasing efficiency and sustainability and reducing environmental impact. *Energy Policy,* **36,** 128–137.

[123] http://theochem.org/bragastofa/CD/essen.pdf

[124] Orhan MF, Dincer I, Rosen MA (2009). The oxygen production step of a copper–chlorine thermochemical water decomposition cycle for hydrogen production: energy and exergy analyses, *Chemical Engineering Science,* **64**, 860–9.

[125] Orhan MF, Dincer I, Rosen MA(2008). Energy and exergy assessments of the hydrogen production step of a copper–chlorine thermochemical water splitting cycle driven by nuclear-based heat, International Journal of Hydrogen Energy, **33**, 6456–66.

[126] Orhan M.F., Dincer I., Naterer G.F. (2008). Cost analysis of a thermochemical Cu–Cl pilot plant for nuclear-based hydrogen production. International Journal of Hydrogen Energy, **33**, 6006–20.

[127]http://en.wikipedia.org/wiki/High_temperature_electrolysis

[128] Valero, A., Lozano, M.A., Serra, L., Torres, C. (1994). Application of the exergetic cost theory to the CGAM problem. *Energy*, **19**, 365-381.